BETA ARRESTIN 2 MEDIATES RENAL CELL CARCINOMA TUMOR GROWTH AND METASTASIS

By

JUDE N. MASANNAT

A DISSERTATION PRESENTED TO THE GRADUATE SCHOOL
OF THE UNIVERSITY OF FLORIDA IN PARTIAL FULFILLMENT
OF THE REQUIREMENTS FOR THE DEGREE OF
DOCTOR OF PHILOSOPHY

UNIVERSITY OF FLORIDA

2017

To my father, mother, brother and sister

ACKNOWLEDGMENTS

I would like to dedicate this work to my father, Naser and mother, Taghreed who sacrificed greatly for benefit of their children. And to my brother, Jawad and sister, Noor, who are my best friends, and to the entire Masannat family for loving me and having much faith in me. Also, to Jamison Joyce and his wonderful and loving family for their continuous encouragement and support. Their positive energy is inspirational and contagious.

I would also like to thank all the teachers and mentors at The Ahliyyah School for Girls; Amman-Jordan, and at the United World College of the Atlantic; Wales-UK, who had a huge impact on my academic and leadership success since I was a child and throughout high school. I would also like to specifically thank Dr. Jorg Bungert, Dr. Robert McKenna, Debra Anderson, Bill Kolb, and Regan Garner at the University of Florida, Gainesville-FL, for being the most wonderful mentors and advisors, and for pushing me towards pursuing a Ph.D.

I acknowledge and thank my Ph.D. mentor, Dr. Yehia Daaka for the opportunity to work in his lab, and for his guidance and motivation throughout the challenges that crossed my path during my graduate career. I am truly grateful for my committee members; Drs. Brian Law, Jeffrey Harrison, Christopher Cogle, and Edward Scott, for their time and efforts in mentoring and inspiring me to constantly improve my work and grow as a scientist. Moreover, I am very grateful for my lab mates; Dr. Hamsa Purayil, Dr. Yushan Zhang, Dr. WanJu Kim, Allyson Shea, and my undergraduate at the time, Michelle Russin, also, for Iqbal Mahmud who significantly contributed to the bioinformatics data in my work. And importantly, I thank my lifelong friends; Margaret White, Brian

Mahon, Miguel Zarate, and Jennifer Wiggins, for the scientific support, valuable discussions related to work and life, laughter, and encouragement during stressful times.

Finally, many thanks to Mr. Shelby Davis and the UWC Davis Foundation that made my education in the U.S. possible.

TABLE OF CONTENTS

page

LIST OF TABLES

LIST OF FIGURES

LIST OF ABBREVIATIONS

7TMRs	7-transmembrane receptors
AR	Androgen receptor
$AT_{1A}R$	Angiotensin II type A1 receptor
cAMP	Cyclic adenosine monophosphate
Cas9	CRISPR associated protein 9
ccRCC	Clear cell RCC
CK2	Casein kinase 2
CML	Chronic myeloid leukemia
CRISPR	Clustered regularly interspaced short palindromic repeats
CXCR4	Chemokine receptor 4
EGFR	Epidermal growth factor receptor
EMT	Epithelial to mesenchymal transition
ET-1	Endothelin-1
ET_AR	Endothelin-A receptor
FAK	Focal adhesion kinase
GPCRs	G protein-coupled receptors
GRKs	G protein-coupled receptor kinases
GSK3β	Glycogen synthase kinase 3β
HIF1α	Hypoxia induced factor 1α
HSCs	Hematopoietic stem cells
IGF-1	Insulin-like growth factor 1
IP3	Inositol-1,4,5-trisphosphate
JNK3	c-Jun N-terminal kinase 3
LPA	Lysophosphatidic acid

MAPKs	Mitogen-activated protein kinases
Mdm2	Mouse double minute 2 homolog
MEF	Mouse embryonic fibroblast
MET	Mesenchymal to epithelial transition
MMP9	Matrix metalloproteinase 9
mTOR	Mammalian target of rapamycin
nccRCC	Non-clear cell RCC
NK1R	Neurokinin-1 receptor
NSCLC	Non-small cell lung cancer
PAR2	Protease-activated receptor 2
PDGF	Platelet-derived growth factor
PGE2	Prostaglandin E2
PIPs	Phospoinositides
PTEN	Phosphatase and tensin homolog
Rb	Retinoblastoma protein
RCC	Renal Cell Carcinoma
RhoGAPs	RhoGTPase activating proteins
RhoGEFs	RhoGTPase exchange factors
RhoGEFs	RhoGTP exchange factors
RING	The really interesting new gene
RLNs	Renal lymph nodes
RTKs	Receptor tyrosine kinases
SDF-1	Stromal-derived factor 1
sgRNA	Short guide RNA
siRNA	Small interfering RNA

SP	Neuropeptide substance P
STRING	Search Tool for the Retrieval of Interacting Genes/Proteins
TCGA	The Cancer Genome Atlas
TGFβRs	Transforming growth factor β receptors
TNF-α	Tumor necrosis factor-α
ULNs	Urethral lymph nodes
VEGFR	Vascular endothelial growth factor receptor
β_2AR	β2 adrenergic receptor

Abstract of Dissertation Presented to the Graduate School
of the University of Florida in Partial Fulfillment of the
Requirements for the Degree of Doctor of Philosophy

BETA ARRESTIN 2 MEDIATES RENAL CELL CARCINOMA TUMOR GROWTH AND METASTASIS

By

Jude Masannat

August 2017

Chair: Yehia Daaka
Major: Medical Sciences – Physiology and Pharmacology

Renal Cell Carcinoma (RCC) is one of the most lethal urological cancers worldwide, with incidence and mortality rates increasing in the past two decades. The disease does not present early clinical symptoms and is commonly diagnosed at the metastatic stage, leaving the 5-year survival rate at ~10-20%. For a wide array of neoplasms, many key molecular determinants involved in mediating the process of tumor cell growth, invasion, and colonization at a secondary site (i.e. metastasis) have been reported. However, few molecular predictors have been identified for RCC, rendering the mechanism(s) underlying RCC metastases poorly understood. This results in the lack of effective treatment for patients with advanced RCC.

G protein-coupled receptors (GPCRs) and their effectors, such as the βArrestin proteins, have been implicated in tumor growth, metastasis, and angiogenesis. βArrestin are well known for their function in the desensitization and trafficking of GPCRs, but have also been implicated in unique signaling pathways to regulate fundamental cellular functions, including cell cycle progression, cell migration, and survival. Furthermore, βArrestin involvement has been identified in a number of breast, colorectal, lung, and

hematological malignancies. However, the role of βArrestin proteins in RCC is yet to be determined.

Our data show that βArrestin 2 protein levels correlate with growth and metastatic potential in several RCC cell lines, including ACHN and SN12C. We hypothesize that βArrestin 2 regulates RCC tumor progression, specifically through involvement in proliferation, invasion, and metastatic processes.

We used genetic-based loss of function approaches such as interfering RNA and CRISPR/Cas9. βArrestin 2 (*Arrb2* gene) knockdown results indicated a role in RCC malignancy as it significantly reduces the migration and invasion of RCC cell lines *in vitro. Arrb2* knockout (KO) induced morphological changes *in vitro* and impaired SN12C tumor growth *in vivo* compared to control cells. We identify βArrestin 2 a crucial mediator for tumor cell cycle progression and focal adhesion formation in RCC.

Our data implicates βArrestin 2 in RCC malignancy and present a diagnostic biomarker and a possible target in development of therapies for patients with advanced RCC.

CHAPTER 1
βARRESTINS: AN OVERVIEW ON THEIR ROLE IN CANCER

Introduction: Summary on βArrestin Function and Structure

Classical and Non-Classical βArrestin Functions

Originally, βArrestin proteins were the molecular determinants of the fate of activated G protein-coupled receptors (GPCRs). Upon ligand stimulation, GPCRs, the largest family of transmembrane receptors also called the 7-transmembrane receptors (7TMRs) superfamily with over 800 identified receptors; undergo a conformational change to elicit a signaling cascade (1, 2). GPCR signaling commences activating the alpha subunit of the heterotrimeric guanine-binding (G) proteins (Gα and Gβ/γ), through the exchange of a GDP to a GTP (3-5). Gα subunit activation then causes the generation of second messenger signaling molecules such as cyclic adenosine monophosphate (cAMP), inositol-1,4,5-trisphosphate (IP3), and diacylglycerol for further signal transduction (6). These second messengers then induce the activity of various effectors, including ion channels, serine/threonine kinases (PKA and PKC), Ca^{2+}/calmodulin-dependent kinases, and RhoGTPase exchange factors (RhoGEFs) (7). As such, the 7TMRs control an intricate web of intracellular cascades involved in the cellular response to outside cues, including cell survival, cell cycle control, metabolism, and cytoskeletal rearrangement (8). βArrestins exert an inhibitory function on GPCR signaling through two separate mechanisms; one, by creating a steric hindrance blocking further downstream activation of G protein signaling, or second, by facilitating the endocytosis of the activated GPCR. Once GPCRs are activated by binding agonists, G protein-coupled receptor kinases (GRKs) phosphorylate the ligand bound receptor on its C-terminal domain or “tail” and other intracellular serine/threonine sites (9-12). The

phosphorylation results in the recruitment of cytosolic βArrestins to the receptor, thereby blocking the access of Gα subunit to the guanine nucleotide exchange active site within specific transmembrane loops of the receptor (8, 12, 13). It has been shown that βArrestins can act as multifunctional adaptors or scaffolds capable of forming diverse complexes with over a hundred different proteins causing an induction of various cellular processes (Figure 1-2) (14). For example, βArrestins can recruit clathrin and adaptor protein AP-2 to assemble a clathrin coated pit around the stimulated GPCR causing its internalization for endosomal degradation or recycling (15). βArrestins also contain a domain that recruits E3 ligases, such as mouse double minute 2 homolog (Mdm2), that ubiquitinates βArrestins, resulting in the internalization of the GPCR (16-18). Therefore, βArrestins have been identified for their dual functions as the desensitizers and regulators of the intracellular trafficking of GPCRs.

The classical GPCR signaling entails an agonist binding the receptor leading it to a stable structural conformation, which triggers downstream G protein-dependent signaling (8, 19, 20). However, there has been a paradigm shift appreciating the notion that GPCRs can adapt a spectrum of conformations varying in stability and thus efficacy of downstream signaling (21-23). This occurs with regards to the type of ligand binding the receptor. Certain agonists may lead to an active receptor state favoring the G protein-dependent signaling cascade, where some may stabilize the receptor in a state allowing for non-G protein interactions with the GRKs and βArrestins (24, 25). Therefore, this non-classical GPCR signaling paradigm is often referred to as “biased agonism” (26-28). Receptor-βArrestin interactions, as a consequence, result in what is called the βArrestin-dependent signaling (24, 29, 30).βArrestin-dependent signalosome

involves major pathways such as the transforming growth factor β receptors (TGFβRs), epidermal growth factor receptor (EGFR), mitogen-activated protein kinases (MAPKs), and RhoGTPase signaling (31, 32). Through interactions with these diverse signaling proteins, βArrestins further integrate extracellular cues into a web of intracellular outcomes.

βArrestins Family and Structure

The arrestin protein family consists of four isoforms with closely related structures and molecular weights: arrestins are subdivided into visual (arrestins 1 and 4) and nonvisual arrestins (βArrestins 1 and 2). Arrestin 1, a 48kDa protein was originally described by Hermann Khun and discovered for its role in desensitizing the photo-rhodopsin receptors in the cone and rod cells (33, 34). Later, the other visual arrestin isoform; X-arrestin (or arrestin 4), which is more specific to the cone cells in the retina, was discovered by George Inana group (35, 36). βArrestins 1 and 2 constitute the nonvisual arrestins, which were identified and cloned through the works of the pioneers in the GPCR signaling field, such as Jeff Benovic and others in Robert Lefkowits laboratory (37, 38). Unlike arrestin 1 and 4, βArrestins 1 and 2 are shown to be ubiquitously expressed in all non-retinal tissues (39). Although expressed in different cell types, all arrestins share structural similarities; βArrestins 1 and 2 share up to 78% amino acids identity and 88% structural homology (40-43). The X-ray crystal structures of each βArrestin isoform show that they share an overall biconcave-like structure consisting of antiparallel β-sheets, an α-helix and a C-terminal tail (Figure 1-1). The overall structure can be divided into two main domains: N-domain, and C-domain that flank a polar core (41-44). The core domain can be described as a “phosphosensor”

domain that has high affinity to phosphorylated intracellular residues of the 7TMRs (45). The rapid recruitment of an arrestin molecule to the phosphorylated receptor is a necessary initial step in order for the arrestin to undergo a global conformational change necessary for its scaffolding or desensitizing functions (46). When the arrestin molecule comes in contact with the phosphorylated receptor, a finger loop within the N-domain of arrestins appears as a result of the sequential shift in the domain (46-48). The finger loop is observed to then get inserted in the transmembrane core of the activated receptor, hence hindering the Gα subunit access to the active site within the transmembrane, attenuating G protein-signaling through the steric interference (48). Moreover, the conformational change within the nonvisual βArrestins results in the exposure of a C-terminal tail which is usually tucked in by the N-domain β-sheets and polar core during the basal state of the βArrestin (49, 50). The tail and the C-domain are then capable of interacting with downstream proteins, for either promoting the internalization of the ligand-receptor-βArrestin complex and/or eliciting βArrestin-dependent signaling cascades (50).

The “phosphosensor” core allows βArrestin to not only be recruited to traditional GPCRs, but also to nontraditional 7TMRs including Frizzled and Smoothened, and to non-7TMRs like receptor tyrosine kinases (RTKs) (31, 32, 51, 52). Moreover, specific motifs in the N- and C-terminal domains have been identified as direct interaction points for βArrestin with cSrc, a non-receptor tyrosine kinase, and with the family of MAPKs (53). This supports the notion that βArrestins are involved in signaling pathways independent of G protein-signaling.

Despite the fact that βArrestins 1 and 2 are ubiquitously expressed throughout various tissues, when βArrestin 2 was first cloned from rat tissue in 1992, its mRNA level was found to be more concentrated in the central nervous system and the spleen (38). However, the general βArrestin mRNA tissue distribution shows over ten times the levels of βArrestin 1 to βArrestin 2 expression (40, 54, 55). As depicted from X-ray crystal structures and amino acid sequence alignments of arrestins, the nonvisual βArrestins in particular, share a great deal of structural similarities thus conserved in the way they bind phosphorylated receptors for desensitization and further trafficking. However, certain differences that lay within their sequences give rise to motifs that diversify some of their protein-protein interactions (56-58). The C-terminal domains of βArrestins 1 and 2 constitute less conserved regions between the two homologs (38). In fact, βArrestin 2 contains a leucine rich segment; a nuclear export signal, in its C-terminal that is absent from βArrestin 1 which constantly eliminates it from the nucleus (59). While βArrestin 2-interacting partners are confined to the cytoplasm, βArrestin 1 can interact with molecules in both the cytoplasm and nucleus (59, 60). Moreover, after the βArrestin 2 crystal structure resolution, which is the last structure resolved of the four arrestins, a striking difference in one of the C-domain beta sheets was observed between βArrestins 1 and 2 (13). A six to nine residues difference results in a looser βArrestin 2 interface with the receptor. This allows βArrestin 2 to obtain an increased selectivity with higher affinity towards phosphorylated and/or nonphosphorylated receptors over βArrestin 1 (13). Arrestins are potentially considered to be redundant in function, yet have been demonstrated to have distinct molecular interactions and subcellular localizations (61). Therefore, they could each regulate signal transduction in

physiological processes including disease progression such as with cancer in similar or unique means.

βArrestins in Cancer

Knockout mouse models have proven βArrestins to be crucial molecular regulators for various developmental and physiological processes such as cardiac output and central nervous system functions (61-63). In addition, βArrestins have been identified as important regulators of pathophysiological pathways leading to tumor initiation and progression (64).

βArrestins play an integral part in cell division and morphological changes through their direct interaction with cSrc upon GPCR activation. This ultimately activates the MEK-ERK1/2 cascade leading to the changes in cell division and morphology (31, 65, 66). Furthermore, βArrestins, βArrestin 2 in particular, can interact with c-Jun N-terminal kinase 3 (JNK3), modulating its spatial distribution and function as a pro-apoptosis kinase (59). βArrestins can also modulate apoptosis by binding and sequestering IκBα in the cytoplasm thereby changing gene expression. Sequestration of IκBα does not only deregulate apoptosis, but also influences the inflammatory and proliferative signals (67, 68). Additionally, βArrestins can mediate the internalization of phosphorylated RTKs independently of GPCR signaling such as with the TGFβRIII leading to increased epithelial cell migration (69, 70).

These studies are only a few examples demonstrating the versatile role for βArrestins signaling in various cellular functions all of which are implicated in disease progression. Current research is focused on better understanding the βArrestin-dependent mechanisms involved in tumors with the hope of developing more efficacious

cancer treatments. This chapter will focus on summarizing the findings on the role of βArrestin signaling in various hallmarks of cancers.

Sustained Proliferation and Replicative Immortality

One of the defining characteristics of cancer is uncontrolled cell division and proliferation and capacity for a replicative immortality (71). The first role of βArrestins described in cell proliferation was their involvement in regulating the MAPKs and PI3K-Akt pathways (72, 73). Later studies proved βArrestins to be involved in more cascades controlling cell cycle and replication. βArrestins were discovered to be recruited by phosphorylated tyrosine kinases like insulin-like growth factor 1 (IGF-1) receptor and trigger downstream Akt activation and anti-apoptotic signals (74). This was a βArrestin-dependent activation of Akt through linking IGF-1 to PI3K (74).

A key colorectal cancer study, gave important insight of βArrestin 1 role in the disease progression (75). In that study, βArrestins mediated the intracellular transactivation of EGFR by forming a scaffold with cSrc, leading to the downstream activation of Akt, inducing metastatic and proliferative signaling. Colorectal carcinoma cell lines were stimulated with prostaglandin E2 (PGE2), agonists to EP4. Upon ligand stimulation, the cytosolic βArrestins were recruited to the receptor, and with time, interactions with cSrc at the plasma membrane increased. PGE2-stimulated S412D-βArrestin 1 cells showed significantly less immunoprecipitation with cSrc and decreased Akt phosphorylation compared to wild type βArrestin 1 cells, hindering *in vitro* cell migration and proliferation as well as *in vivo* metastasis (75). Interestingly, a different system studying obestatin stimulation of a 7TMR called GPR39 in gastric cancer, revealed a βArrestin 1 mediated transactivation of EGFR-Akt through cSrc (76). Immunoprecipitation assay confirmed cSrc-βArrestin 1 complexes forming upon

obestatin stimulation. Small interfering RNA (siRNA) targeting βArrestin 1 significantly reduced Akt phosphorylation on both active sites, T308 and S473, in gastric cancer cell line KATO III compared to negative control scrambled siRNA transfected cells (76). These studies further confirmed the importance of βArrestin 1 mediated activation of kinases, such as Akt, which are involved in cellular activities such as cell cycle regulation, metabolism, and a number of downstream regulations of gene transcription.

In non-small cell lung cancer (NSCLC) cells, upon nicotine binding to the nicotine acetylcholine receptor, βArrestin 1 is recruited to the receptor and acts as a platform to recruit cSrc, which leads to the activation of the Raf1-MEK-ERK pathway (77). Raf1 then binds retinoblastoma protein (Rb) to dissociate it from E2F transcription factors on proliferative gene promoters. E2F regulates gene expression of important cell proliferation genes such as the cdc6 and thymidylate synthetase and cdc25A (77). A later study further demonstrated that with stable knockdown of the βArrestin 1 gene in NSCLC cell line, nicotine-induced cell proliferation was significantly lower than control cells (78). They also reported that βArrestin 1 not only facilitates the activation of E2F indirectly through the Raf1-MAPK pathway previously mentioned, but also by localizing and binding the E2F transcription factors within the nucleus (78). Thus, in smokers or nicotine consumers, βArrestin 1 is crucial in mediating the deregulated cell cycle and enhancement of proliferative and pro-survival promoters.

A study involving bladder cancer provided evidence that βArrestin 2, but not βArrestin 1, mediated malignant transformation and increased proliferation, migration and invasion of non-transformed urothelial cells (SV-HUC) and other transformed bladder cancer cell lines. Thromboxane synthase is described to be overexpressed in

bladder cancer patients' samples and correlates with poor prognosis (79). Results indicated that upon transfection of SV-HUC with plasmids expressing thromboxane receptor TPβ (a GPCR), cells grew faster than empty vector controls (79, 80). Additionally, SV-HUC stably overexpressing TPβ, subcutaneously injected in immunodeficient mice, were able to differentiate to a malignant phenotype versus control cells. Since βArrestins are downstream effectors of TPβ, RNAi targeting βArrestin 2, resulted in impairing the receptor signaling after agonist stimulation and negatively impacting the metastatic response (80, 81).

The roles of βArrestins in hematological malignancies were further shown in a study of chronic myeloid leukemia (CML) by Fereshteh *et al.* (82). This study investigated the proliferative capacities of T and B lymphocytes and induction of CML from wild type mice, βArrestin 1, or βArrestin 2 knockout bone marrow tissues. The results suggested that βArrestin 2 is crucial for the *ex-vivo* growth of hematopoietic stem cells (HSCs) from the bone marrow after determining their colony formation capacity. They further investigated the growth and differentiation of HSCs to induce the CML phenotype *in vivo*. This revealed that after infecting HSCs with the BCR-ABL fused gene followed by transplantation into βArrestin 2 knockout marrows, there was a significant reduction in CML development compared to wild type marrow. As suggested in the study, βArrestin 2 regulated βcatenin stability hence increased downstream pro-proliferation gene expression. The mechanism by which βArrestin 2 aids βcatenin stability in this system has not been delineated yet, but, the finding that βArrestins scaffold Dishevelled and Axin into a complex, thus protecting βcatenin from destruction is a possibility (83). This mechanism could implicate βArrestin 2 in CML sustained

growth and progression *in vivo*, or *in vitro* (82). A more recent study also supported this observation regarding βArrestin 2 involvement in CML tumorigenicity by applying the targeted RNA aptamer technology to specifically inhibit βArrestin 2 functions in lymphocytes. RNA aptamers apply a novel approach to selectively bind molecular structures or proteins such as βArrestins and intercept their future protein-protein interactions (84). The results suggest a potential therapeutic approach for cancer to target βArrestins in a tissue specific manner. Additionally, sequestering βArrestin 2 activity using RNA aptamers in CML, blocks the aberrant Hedgehog-Smoothened induced gene transcription of anti-apoptotic and angiogenic genes (85). These studies demonstrate a clear role for βArrestins in tumor cell proliferation in multiple cancer types through various pathways, possibly in a tissue specific manner. Hence, targeting βArrestins could provide a promising avenue for cancer therapeutics.

Evading Apoptosis and Growth Suppression

Characterization of βArrestins manipulation of the MAPK signaling cascade paved the way for a better understanding of the role of βArrestins in controlling apoptotic signaling in tumor cells. This led to the current understanding that βArrestins impose both a positive and a negative regulation on their associated kinases. Of these kinases, MAPK p38, ERK1/2 and JNK3 all interact with βArrestins but have opposing effects on cell survival with ERK1/2 promoting anti-apoptotic signaling, where as p38 and JNK3 activation can lead to apoptosis (32, 86-89). As such, βArrestin-dependent suppression of ERK1/2 apoptotic signaling is observed in Kirsten sarcoma virus-transformed rat kidney epithelial cells, and endothelial cells through the induction of neurokinin-1 receptor (NK1R) by neuropeptide substance P (SP). A study developed by DeFea *et al.*, showed that the SP-NK1R-βArrestin complex includes cSrc, which then

causes the subcellular localization and phosphorylation of ERK1/2. Activated ERK1/2 shuttles to the nucleus to further activate pro-survival and proliferative gene expression signature. To emphasize the role of βArrestin 1 in this particular signaling pathway, this complex formation was suppressed in cells expressing dominant negative βArrestin mutated at C-terminal residues 319-418, or a truncated NK1R that does not recruit βArrestin (65). In support to this observation, a study with mouse embryonic fibroblast (MEF) βArrestin 1 and/or 2 knockout cells, suggested βArrestin-dependent ERK1/2 activation upon lysophosphatidic acid (LPA) receptor stimulation. Gesty-Palmer *et al.*, concluded that there is an existence of a novel mechanism for βArrestins-ERK1/2 transcriptional regulation, different from the EGFR-dependent transactivation of downstream ERK1/2 transcription profile (90). The mechanism comprises of an agonist bound LPA receptor, βArrestin, and endogenous phosphorylated ERK1/2, all in a complex to induce downstream gene transcription.

βArrestins role in regulating apoptotic signals is not constrained to the MAPK pathway (72, 91). It has been demonstrated that there is a βArrestin-dependent convergent role between GPCR signaling and the apoptotic machinery. In one study, upon stimulation of the β_2AR, NF-κB activity relied on βArrestin 2 stabilization of the inhibitory protein IκBα and its protection from degradation by IκBα kinase, thus allowing IκBα to bind NF-κB in the cytoplasm and restricting its transcriptional activity away from the nucleus (68). However, immunoprecipitation assays suggest that both βArrestin 1 and 2 interact with IκBα. Although the overexpression of either βArrestin in tumor necrosis factor-α (TNF-α)-induced HeLa cells greatly reduced NF-κB activity, βArrestin 1 showed a much larger effect than βArrestin 2 in this case (67). In a different study, UV

radiation of MEF cells elicited a new mechanism for the regulation of UV-induced NF-κB activity to be under the control of casein kinase 2 (CK2), which phosphorylates βArrestin 2. Phosphorylated βArrestin 2 then dissociates from the inhibitory IκBα, ultimately leading to the upregulation of antiapoptotic signals, while dephosphorylated βArrestin 2, facilitated by ligand stimulation of the β_2AR promotes apoptosis in this system (92). This provides evidence that depending on the extrinsic apoptotic stimulus and the upstream receptor involved βArrestin 1 or 2 might regulate the stability and activity of NF-κB.

βArrestins have also shown the ability to rescue a cell from apoptosis by desensitizing and internalizing stimulated GPCRs that regulate apoptosis (51). A classic example is in the stimulation of the angiotensin II type A1 receptor ($AT_{1A}R$), where in double knockout of the βArrestin genes, *Arrb1* and *Arrb2*, mouse embryonic fibroblasts, apoptosis proceeded upon $AT_{1A}R$ activation. However, once either βArrestin 1 or 2 were rescued in the knockout cells, the apoptotic signal was hindered (72, 93). Later, it was shown that an intricate GPCR-mediated and βArrestin-dependent regulation of the serine/threonine phosphatase PP2A is crucial for a balanced activation of the Akt-glycogen synthase kinase 3β (GSK3β) signaling axis (72, 91). GSK3β plays an important role in the stability of the βcatenin molecule, and therefore impacting the βcatenin-dependent downstream transcriptional outcomes (94). In addition, it was discovered that βArrestin 2 is responsible for mitigating the resveratrol-induced apoptosis effect in endometrial cancer. It was elucidated through RNAi knockdown of βArrestin 2 in human endometrial cancer cell line (HEC1B) for example, that caspase-3 activity increased as well as apoptotic cells numbers in βArrestin 2 knockdown with resveratrol treatment compared to control HEC1B cells. Akt and GSK3β

phosphorylation was reduced significantly in the knock down cells after resveratrol treatment (95). This finding suggests a possible anti-apoptotic role of βArrestin 2 in endometrial cancer. Additionally, colon cancer studies found that βArrestin 1 scaffolds a complex consisting of Akt phosphatase PHLPP2 and the agonist-induced platelet-derived growth factor (PDGF) receptor, which dephosphorylates Akt at serine 473, thus in turn, induces the intrinsic apoptotic pathway (96, 97). A PHLPP1 orthologue on the other hand, has been identified as a prostate cancer suppressor as it triggers p53 activation in prostate tumor tissue of phosphatase and tensin homolog (PTEN) mutant mouse models; but whether it is also under the tight regulation of βArrestin scaffolding, is still unclear (98).

DNA damage through irradiation or chemotherapy can trigger the apoptotic activity of the tumor suppressor p53. The really interesting new gene (RING)-type ubiquitin E3 ligase Mdm2 is required for a balanced negative regulation of p53. However, there is a negative feedback loop as p53 also induces Mdm2 gene expression (99, 100). βArrestin 2 contains a motif specific for Mdm2 binding for its ubiquitination to facilitate downstream receptor modification and trafficking (16, 17). Therefore, it is not surprising that βArrestin 2 has been identified as a scaffold for the Mdm2-p53 complex in the cytoplasm, sequestering p53 away from the nucleus and dampening the expression of cell death genes such as NOXA, BAX, PUMA, and others (101, 102). Moreover, Mdm2 has been shown to also bind βArrestin 1 in the cytoplasm and in the nucleus, where in the nuclear localization case, the βArrestin-Mdm2-p53 complex formed could potentially promote p53 ubiquitination and degradation (103). Although, our understanding of the relationship between Mdm2, p53 and βArrestins is increasing,

there is still a lack of information regarding this relationship in cancer. More studies are needed to provide an insight to whether βArrestins up regulation in certain tumors is affecting therapy by blocking p53 activity.

Metastasis and Invasion

Tumor metastasis is defined as the migration of a cancer cell from the primary tumor site and invading and colonizing a secondary site (71). A number of events need to occur in order for the cancerous cells to successfully escape the primary tumor and establish metastasis (104-106). Although many of these migratory events are poorly understood in the tumor context, the importance of βArrestins involvement and regulation of these events is becoming clearer. In general, cell migration is triggered by migration-promoting agents such as chemokines. In βArrestin knockout mouse model studies, it was suggested that βArrestin 2 had a positive role in regulating cell migration (107). βArrestin 2 knockout T and B lymphocytes had decreased migration compared to wild type cells (108). Lymphocytes were treated with stromal-derived factor 1 (SDF-1) chemoattractant that acts on the GPCR chemokine receptor 4 (CXCR4). Although at the time it was considered counter intuitive for βArrestin knockout to attenuate CXCR4-mediated cell migration, later studies showed that βArrestins are indeed important for cell motility via the activity of p38 MAPK, ERK1/2 and other factors (109, 110). RNAi suppression of βArrestin 1 expression in HEK293 and HeLa cells significantly reduced SDF-1 induced chemotaxis (110). This observation is due to βArrestin 2 interaction with ASK1, a MAP3K upstream of p38 MAPK.

Cell morphology is a key indicator in predicting the capability for cell motility. Invasive and highly motile tumor cells tend to adapt polarized cell morphologies that enable them to invade and migrate through adjacent tissue and extracellular matrix

material (71). Rho subfamily proteins Rho, Rac, and Cdc42 of the small GTPases superfamily are recognized for their regulation of cytoskeletal rearrangements and cell polarity. The decreased TGFβRIII expression that is observed in a number of epithelial cancers has been associated with RhoGTPase Cdc42 activation, and is mediated by βArrestin 2 (69). In a non-tumorigenic context, the presence of TGFβRIII receptor can lead to the constitutive activation of Cdc42, promoting the formation of many small protrusions on the cell surface, rendering it to be non-polarized. However, when TGFβRIII receptor activity is depleted by βArrestin 2 sequestration, Cdc42 activity is attenuated to a level where protrusions are present on a part of the cell giving it a directional polarity (69). Reduced TGFβRIII along with the up regulation of the epithelial to mesenchymal transition (EMT) markers such as vimentin and N-cadherin, suggest an important role for βArrestin in EMT that is worth further investigation.

βArrestins have been shown to directly bind molecules that regulate the activity of RhoGTPases such as the RhoGEFs and the RhoGTPase activating proteins (RhoGAPs) (14, 66, 111). This scaffolding-mediated activation of RhoGTPases certainly has an impact on stress fibers formation and actin polymerization. Ma *et al*., observed that with carvedilol stimulation of the β_2AR in MEFs, cells adapted a more polarized conformation (112). Stress fibers and focal adhesions formation increased at the plasma membrane after receptor stimulation due to the activation of RhoA. βArrestin 2 and p115RhoGEF were also found to form a complex at the plasma membrane, potentially mediating the activation of RhoA. Distinctly, when Ma *et al.*, knocked down βArrestin 1 in MEFs in a different study, they observed a substantial increase in protrusion structures around the cell membrane, reducing cell polarity (113). It was

elucidated that βArrestin 1 has a gene repression regulation at the RasGRF2 promoter site. RasGRF2 is a known activator of small GTPase Rac1, which activates cofilin, an actin binding protein, by regulating its dephosphorylation. Aberrantly low expression levels of RasGRF2 have been reported in a number of adenomas and carcinomas, therefore βArrestin 1 can potentially impact cell migration and invasion through a RasGRF2-mediated mechanism in certain tumors. Detailed summary on βArrestins regulation of small GTPases and actin assembly have been summarized elsewhere (107, 114).

Interestingly, under hypoxic conditions in breast cancer tissue, βArrestin 1 colocalizes with hypoxia induced factor 1α (HIF1α) and stabilizes it within the nucleus (115). HIF1α transcriptional activity enhances metastatic growth via increased VEGF expression, promoting pro-survival and angiogenic signals (115, 116). Using invasive breast cancer MDA-MB-231 cells for tail vein metastasis assays, βArrestin 1 knockdown was associated with reduced colonization in the lungs. Likewise, βArrestin 1 knockdown MDA-MB-231 cells failed to survive under induced hypoxic conditions. Since cancerous cells undergo metabolic and genetic adaptations under hypoxic conditions, it was observed that βArrestin 1-HIF1α complex functions to drive the aerobic glycolysis metabolic shift in prostate cancer (117, 118).

Higher tumor progression could be correlated to elevated matrix metalloproteinase 9 (MMP9) levels (119, 120). MMP9 activity increases the release of angiogenic factors such as VEGF in the tumor microenvironment (119, 121). This was observed in a classical study using transgenic mice overexpressing HA-tagged βArrestin 1 where tumor xenografts grew faster and larger than those of HA-βArrestin 2

or wild type mice (122). Although, further analysis indicated a βArrestin-PI3K-MMP9 activation axis in this study, another possibility of enhanced MMP9 activity could be through the βArrestin/cSrc transactivation of the EGFR and MMP9 (75). Furthermore, when the effects of a recently FDA approved β_2AR agonist, indacaterol, were examined on fibrosarcoma cells metastasis and invasion, it was shown that NF-κB activity was inhibited in an βArrestin 2-dependent manner (123). Pretreatment of cells with indacaterol prevented TNF-α mediated activation of NF-κB and its nuclear translocation. Compared to untreated control cells, the stimulation of βArrestin 2 internalization of β_2AR after drug treatment significantly reduced the phosphorylation on IKK and IκBα ultimately attenuating MMP9 gene expression. This hindered tumor cell invasion and migration.

In breast cancer, elevated LPA expression is associated with increased metastasis in advanced stages of the disease via its activation of GPCRs receptors LPA1-3 (124). βArrestins bind LPA receptors and facilitate the interaction with RalGTPase, which leads to cytoskeletal rearrangement and migration (125, 126). Expression of mutant RalGDS (a GDP dissociation stimulator) lacking βArrestin binding domain, significantly hindered 3D invasion of tumor cells *in vitro*. Early observations of βArrestin 1 and 2 recruitment to the protease-activated receptor 2 (PAR2) in aggressive MDA-MB-231 cells, indicated the importance of βArrestin-regulated actin remodeling in invasive breast cancer (127, 128). The scaffolding of βArrestins to endothelin-A receptor (ET_AR) after stimulation by endothelin-1 (ET-1) ligand causes an EMT effect on ovarian cancer cells (129). In one way, downstream EGFR transactivation via the βArrestin-cSrc interaction stimulates Akt activation, increasing cell invasiveness independent of MMP9

activity in an ET-1 dose-dependent manner. In another cascade, tyrosine phosphorylation of βcatenin and increased nuclear interaction with TCF-4 potentiates pro-metastasis gene expression. βArrestin 1 further provided a βcatenin protective role by directly binding the intracellular molecule Axin, after ET_AR stimulation. βArrestin-mediated stabilization of βcatenin is critical for increased transcriptional activity of genes promoting EMT and increase cell invasiveness and metastasis (83, 130).

Collectively, it has become obvious that βArrestins control tumor cell migration and invasion in a cell, receptor, or interacting molecule-dependent manner. There are numerous studies nowadays that are focused on understanding the role of βArrestins in the different components of cytoskeletal and actin remodeling. Results thus far have clearly demonstrated the potential for novel therapies targeting migration-promoting βArrestin complexes. However, careful understanding of the spatial and temporal regulation of βArrestins to each of the steps that ultimately aid tumors to migrate and invade a secondary site will lead to more efficacious therapies.

Conclusion

Since both βArrestin 1 and 2 are engaged in multiple signaling circuits, it is no surprise that their function is prevalent in cancer initiation and progression. βArrestins share a high level of homology; yet have fundamental differences that allow them to manifest unique roles in cell signaling. For example, βArrestin 1 localizes to the nucleus and further stabilizes molecules like βcatenin and impact gene transcription (131). Purayil *et al.,* identified a regulatory role for βArrestin 1 on the androgen receptor (AR) activity and transcription in both castration and noncastration-resistant prostate cancer cells (132). As certain GPCRs stimulation leads to βArrestin 1 nuclear translocation, NF-κB-regulated transcription of apoptotic genes can be dependent on βArrestin activity in

certain tumor tissue (67). However, we have shown in this review, supporting evidence that under the control of either transmembrane receptors or intracellular kinases, βArrestin 1 nuclear function can directly or indirectly influence gene expression of pro-survival and metastasis genes.

βArrestin 2, unlike βArrestin 1, possesses a nuclear export signal in its C-terminus, thus confining its function to the cytoplasm and plasma membrane. Interestingly, while the consensus implies that βArrestin 1 is a pro-cancer protein, βArrestin 2 can have opposing effects in a context-dependent fashion. In prostate cancer, for instance, it has been shown that βArrestin 2 sequesters AR and targets it for ubiquitination through Mdm2 (133). βArrestin 2-mediated degradation of AR negatively regulates the expression of prostate specific antigen, which may lead to a tumor suppression effect. Meanwhile, cSrc/βArrestin 2 complex at the plasma membrane modulates EGFR activity or certain RhoGTPases leading to enhanced migratory and invasive phenotypes.

As scaffolds, βArrestins act as a platform to bring together protein molecular complexes and guide them spatially in and out of the nucleus or around the cytoplasm. This capacity to bind a repertoire of molecules is essential in regulating signaling networks resulting in a certain nuclear transcriptional or cytoskeletal structural outcome. βArrestins appear to be needed for the progression of many different cancers, as they act as signaling shuttles in what seems to be a tissue specific manner (summary Table 1-1). To better comprehend why and how the roles of βArrestins in tumor pathologies are context specific, we ought to map out the web of interactions that are deregulated

through the actions of βArrestins in tumors. Only then, we could potentially clarify which pathways are more suitable to be targeted for therapy.

Table 1-1. General summary of βArrestins role in cancer

Cancer Type	βArrestin	Reported interactions/mechanisms	Outcome	Reference
Breast	βArrestin 1	• HIF1α/VEGF expression	Survival, Angiogenesis	(115)
	βArrestin 2	• Akt-ERK1/2	Survival	(134)
		• RalGTPase activation	Migration, Invasion	(124)
	βArrestin 1/2	• ERK1/2 activation	Migration	(127), (128)
Colorectal and Gastric	βArrestin 1	• EP4-cSrc-EGFR transactivation	Migration	(76)
		• EP4-Akt phosphorylation	Proliferation	(75)
		• PDGF-PHLPP2-Akt dephosphorylation	Apoptosis	(96)
	βArrestin 2	• TGFβRIII/Ccd42	Migration	(69)
Ovarian	βArrestin 1/2	• ETAR-cSrc-EGFR-Akt activation	Invasion	(129)
		• ETAR-cSrc-EGFR-βcatenin-Tyr-phosphorylation	EMT induction, Metastasis and Invasion	(129), (130)
Endometrial	βArrestin 2	• Akt-GSK3β phosphorylation	Apoptosis	(95)
Lung	βArrestin 1	• Nicotine acetylcholine receptor-cSrc-Raf1-MEK-ERK	Survival, Proliferation	(77), (135)
	βArrestin 2	• E2F-p300 induced gene expression	Survival, Proliferation	(78)
		• CXCR4	Angiogenesis	(136)
Prostate	βArrestin 1	• HIF1α	Metabolic shift	(117)
		• AR	Gene expression	(132)
	βArrestin 2	• AR	Tumor suppression	(133)
Leukemia	βArrestin 2	• Wnt-Frizzled-βcatenin	Tumor initiation, Proliferation	(82)
		• Hedgehog-Smoothened		(85)
	βArrestin 1/2	• CXCR4	Survival Migration	(108), (109)
Bladder	βArrestin 2	• TPβ	Migration, Invasion, Proliferation	(80), (81)

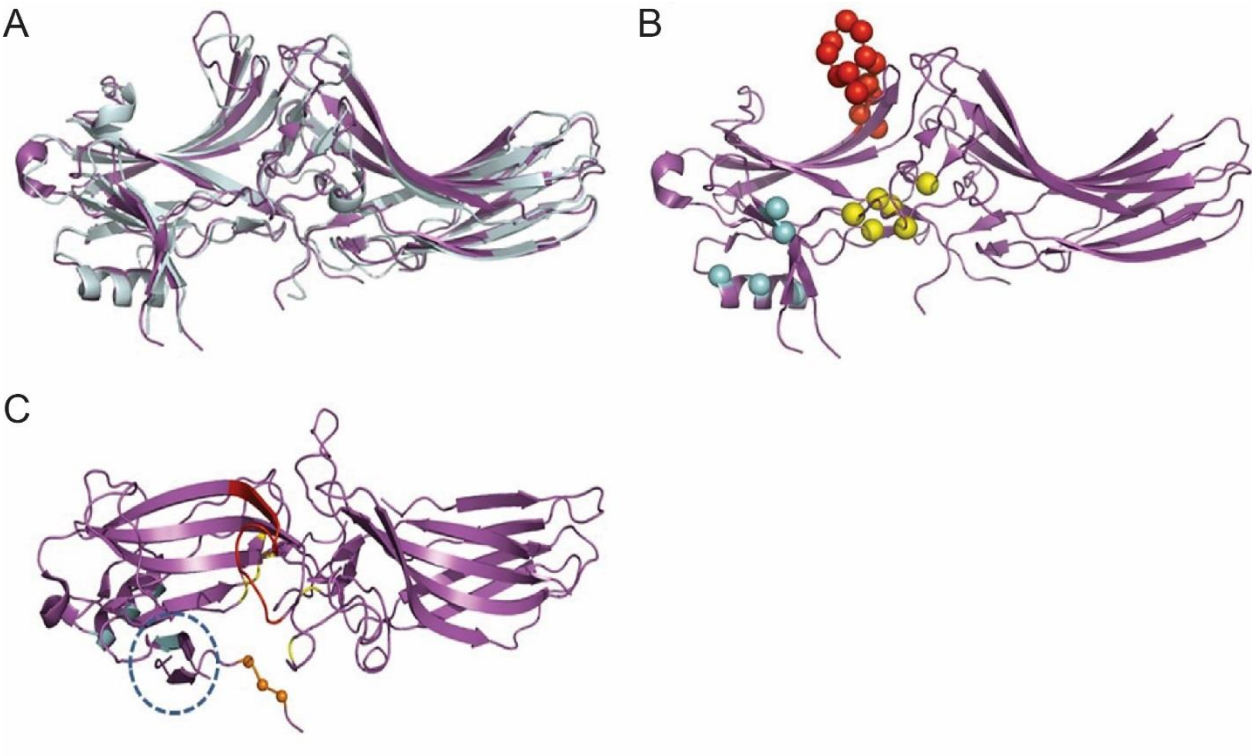

Figure 1-1. Schematic for the structure of βArrestin 1 and 2. A) Overlay of βArrestin 1 in magenta; PDB 2WTR crystal structure and βArrestin 2 in pale cyan; PDB 3P2D (13). Rmsd =1.305 angstroms. Figure was made using PyMol. B) βArrestin 1 crystal structure PDB 2WTR: highlighted are conserved functional elements. PDB 1ZSH: blue spheres; 3-element interaction domain: L100, L104, L108, K10, and K11. Yellow spheres; polar core and phosphosensor elements: D26, D29, R169, K170, D290, D297, and R393. Red spheres; finger loop region based on visual arrestin 1 crystal structure: residues 67-79. Predicted specific residues in βArrestin 1 finger loop are V70, L71, and L73 (137). Figure was generated using PyMol and PDB IDs 2WTR and 1ZSH (138). C) “Top view” of βArrestin 1 highlighting residues of the C-tail (Orange spheres: residues R393-R395) and dotted circle region (L376, I377, E378, L379, D380) responsible for clathrin and AP-2 interactions.

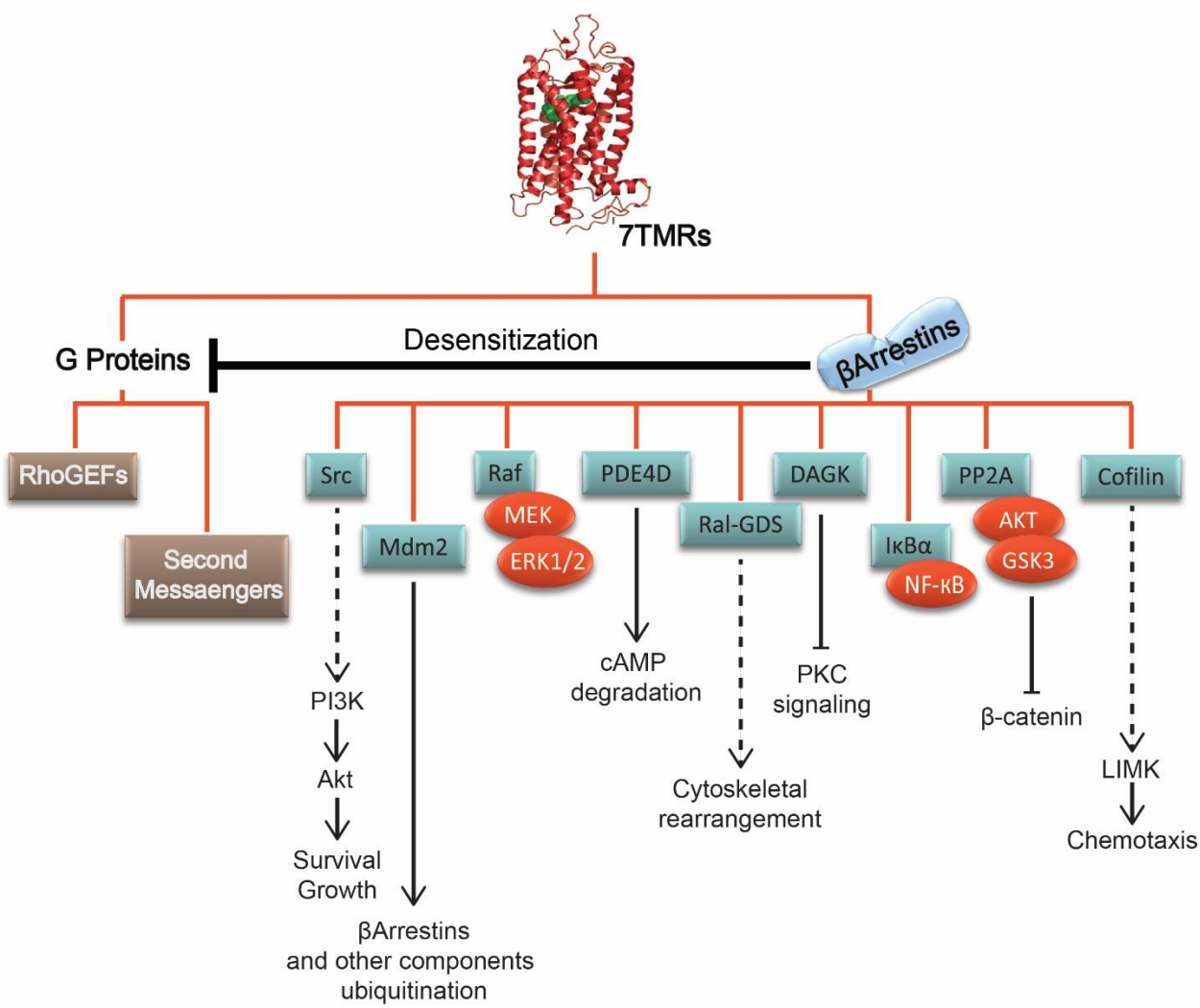

Figure 1-2. Schematic diagram summarizing some of the major interacting partners of βArrestins. Figure adapted from Luttrell *et al*. (139).

CHAPTER 2
βARRESTIN 2 MEDIATES RENAL CELL CARCINOMA PROGRESSION

Introduction

Kidney cancer is one of the top-ten leading cancers in the United States with low therapeutic rate and high lethal consequences. Kidney cancer incidence and mortality rate are on the rise. A decade ago, 31,900 cases of kidney cancer were diagnosed and 11,900 patients died from the disease (140). This year, the estimated new cases have doubled to 63,990 with around 14,400 estimated deaths (141). Hence, the identification of molecular culprits responsible for disease initiation and progression is urgently needed to address the ever-growing number of kidney cancer cases.

Majority (80-90%) of kidney cancer cases are histologically classified as renal cell carcinoma (RCC) that is subdivided into the clear cell RCC (ccRCC) and non-clear cell RCC (nccRCC) subtypes (142). The standard of care for patients diagnosed with organ-confined RCC is surgical resection of the tumor mass or whole kidney. However, this treatment may not be an option for patients with poor overall health or advanced stage of the disease, which decreases the overall 5-year life expectancy to around 10% (143). Also, about one third of all RCC cases are diagnosed at the metastatic stage where mortality rates are the highest among any adult urological cancers (144, 145). RCCs exhibit a spectrum of genetic mutations and often the available therapies which target receptor tyrosine kinases such as vascular endothelial growth factor receptor (VEGFR), and intracellular signaling hubs like mammalian target of rapamycin (mTOR) fail within a year of treatment (146).

GPCRs are the most widely expressed type of membrane receptors in mammalian cells (147). GPCRs are stimulated by a variety of extracellular molecules

and they transduce mitogenic signals through multiple effectors including heterotrimeric G proteins, GRKs, and βArrestins (148). The targeting of heterotrimeric G proteins and GRKs with drugs has proven difficult due, in part, to the expression of structurally-related and functionally-redundant isoforms (149). Moreover, despite the increased appreciation of the relationship between GPCRs and these downstream effectors in oncogenesis and tumor progression, only few drugs target GPCRs for cancer therapy (150-153). Emerging evidence shows that βArrestin proteins can serve as specific drug targets for the treatment of cancer (85).

There are two βArrestin proteins, namely βArrestin1 and βArrestin2 that are ubiquitously expressed. The βArrestins were originally identified and characterized based on their function to desensitize GPCRs with respect to G protein signaling and to mediate GPCR endocytosis (154). Work over the past decade has shown that βArrestins also function as scaffolds and transducers of mitogenic signals implicated in cell growth and survival (25, 27, 113). βArrestin 1 is expressed in the nucleus and cytosol whereas βArrestin2 is found strictly in the cytosol (155). Indeed, βArrestin1 has been shown to regulate androgen receptor and HIF1α transcription activity in prostate and breast cancer, respectively (115, 117, 156, 157).

βArrestin 2 is also reported to regulate mitogenic signals. For example, it forms complex with cSrc leading to cSrc activation and EGFR transactivation that, in turn, are well documented to regulate cell proliferation and migration (31). For example, in late-stage ovarian cancer, βArrestin 2 forms a complex with cSrc that transactivates EGFR to induce tumor cell invasion and metastasis (129). Also, invasive breast cancer cell lines express high levels of βArrestin 2, which was demonstrated to regulate cancer cell

proliferation, migration and invasion through Ral GTPase signaling (124). Here, we examined role of βArrestin 2 in RCC tumor growth and metastasis. Our results show that βArrestin 2 is indeed an important regulator of RCC tumor cell invasive cytoskeletal structure and increased proliferation. Therefore, βArrestin 2 presents as a potential prognostic biomarker and a possible target for the development of therapies for patients with advanced RCC.

Materials and Methods

Reagents

Antibodies: rabbit anti βArr1/2 (D24H9), rabbit anti-human LDHA (3582), rabbit anti-GAPDH (2118S), rabbit anti-Sin1 (D7G1A), rabbit anti-p-FOXO1 (9461), rabbit-anti active non-phospo-βcatenin (D13A1), rabbit anti-total βcatenin (9562S), rabbit anti-p-Akt T308 (9275S), rabbit anti-p-Akt S472 (9271L), rabbit anti-pGSK3α S21 (D1G2), rabbit anti-pGSK3β S9 (9336), and SignalStainBoost IHC detection reagent from Cell Signaling; rabbit anti-human Ki67 (92742), and mouse anti-actin (ab3280) from Abcam; mouse anti-HSP90 (610419) from Fischer; rabbit anti-Rictor (A300-458A) from Bethyl Laboratories; and HRP-coupled anti-rabbit or anti-mouse from Jackson ImmunoResearch Laboratories. Chemicals were obtained as follows: protease inhibitor cocktail, and puromycin from Sigma-Aldrich; polybrene from Millipore; collagen from Roche; matrigel from BD; SuperSignal West Pico chemiluminescent substrate from Thermo Scientific; and Target Retrieval Solution, Protein Block, AEC substrate and Faramount aqueous mounting medium from Dako. High pure RNA isolation kit was from Roche, and iScript™ reverse transcription supermix for RT-qPCR and iQ SYBR green supermix were from Bio-Rad. Control and targeted siRNAs were from Dharmacon.

Mission shRNA Bacterial Glycerol Stock clone ID: NM_004313.3-309s21c1 targeting *Arrb2* was from Sigma.

Mammalian Cell Culture

Human kidney cell lines were obtained as follows: HK2 (immortalized proximal tubule epithelial cells from normal adult kidney), CAKI-1 (metastatic clear cell RCC), 786O (primary clear cell RCC), and ACHN (pleural effusion metastatic RCC) from the American Type Culture Collection; and SN12C (primary unclassified RCC) from the National Cancer Institute. All cells were maintained in RPMI 1640 medium (Corning) supplemented with 10% FBS (Sigma), 100 units/ml penicillin and 100 mg/ml streptomycin. The SN12C Control (infected with lentiviral CRISPR/Cas9 vector containing no sgRNAs), Arrb2ex3-14, and Arrb2ex4-12.19 (infected with CRISPR/Cas9 lentiviral vector with sgRNA targeting exon 3 or exon 4 of *Arrb2* gene respectively) were engineered and maintained with 1 µg/ml puromycin.

CRISPR Reagents and sgRNA Design

LentiCRISPR-Cas9v2 plasmid was obtained from Addgene (Feng Zhang Lab; #52961). The sgRNA were designed using CrisprDirect online tool to specifically target *Arrb2* gene on either exon 3 or exon 4. Exons sequence were obtained from the USCS Genome Browser *(*https://genome.ucsc.edu*).* The sgRNAs were cloned in the CRISPR-Cas9 plasmid using NEBuilder HiFi DNA Assembly Master Mix (NEB #B7002). Lentivirus was packaged and produced in HEK293FT cells. Infected SN12C cells were selected with puromycin. Knockout of *Arrb2* was determined by Western blot. *Arrb2* sgRNA exon 3 sequence: (+) strand: 5’- GCG GGA CTT CGT AGA TCA CC -3’-TGG (PAM). *Arrb2* sgRNA exon 4 sequence: (+) strand: 5’-GAC TAC CTG AAG GAC CGC AA-3’-AGG (PAM).

RNA Extraction and Expression

Total RNA was extracted with High Pure RNA isolation kit, and 1 µg in a final volume of 20 µl was reverse-transcribed with iScript™ Reverse Transcription Supermix according to the manufacturer's instructions. Quantitative PCR reactions containing 400 ng of cDNA and 5 µl of iQ SYBR Green Supermix (Bio-Rad) in a total volume of 10 µl were performed in triplicate using Bio-Rad CFX detection system. Target gene expression was normalized to *18S* RNA (QT00199367) and primers to human *Arrb1* (QT00071197), *Arrb2* (QT00058051), and *Twist1* (QT00011956) were obtained from Qiagen. Fibronectin primers (H_FN1_1) were from sigma. Other EMT genes primers are as follows: N-cadherin (*Cdh2*): 5'-GTG CAT GAA GGA CAG CCT CT-3', 3'-CCA CCT TAA AAT CTG CAG GC-5', E-cadherin: 5'-TCA GAA TGA CAA CAA GCC C-3', 3'-ACA GAG GTT CCT GGA AGA G-5', Vimentin (*Vim*): 5'-CTT CAG AGA GAG GAA GCC GA-3', 3'-ATT CCA CTT TGC GTT CAA GG-5', *Zeb1*: 5'-GAT GAT GAA TGC GAG TCA GAT GC-3', 3'-CTG GTC CTC TTC AGG TGC C-5', *Snai1*: 5'-CCT TCT CTA GGC CCT GGC T-3', 3'-AGG TTG GAG CGG TCA GC-5', and *Twist2*: 5'-AGG CTC TCA GAA GAG GAC CC-3', 3'-AAG GAA AAG AAT AGC GGC GT-5'.

Immunoblotting

Cells were lysed with RIPA buffer (50 mM Tris-HCl pH 7.4, 150 mM NaCl, 2 mM EDTA, 1% NP-40, and 0.1% SDS) and fresh protease inhibitor cocktail. Total cell lysates (25 µg/lane) were separated on 8% SDS-PAGE and electrophoretically transferred to nitrocellulose membranes. The membranes were blocked in 4% BSA in PBS at room temperature for 1 hr, incubated with primary antibodies (1:1000) at 4°C for 16 hr, followed by washing and incubation with HRP-coupled secondary antibodies (1:30,000) for 1 hr. Specific bands were visualized with SuperSignal West Pico

Chemiluminescent Substrate, and blots were imaged with Kinoca Minilia SRX-101A processor. Band intensity was measured using imageJ software.

Immunofluorescence Imaging

Cell were seeded on fibronectin coated glass coverslips and incubated in complete medium (10% FBS RPMI) over night. Cell were then fixed with 4% formaldehyde. Rhodamine-conjugated phalloidin was used to visualize cells cytoskeletal structure. DAPI was sued to visual the nucleus. Primary antibodies were used at 1:200 concentration. Antibodies used were: rabbit anti-Paxillin Y113 (abcam; ab32084), rabbit-anti-active non-phospo-βcatenin (Cell Signaling; D13A1), and rabbit anti-p-FAK Y397 (Cell Signaling; 3283S). Slides were imaged with Nikon Eclipse Ti-E Inverted Confocal Microscopy System using 40x magnifying lens. Images were analyzed using NIS Elements confocal software version 4.50.

Migration and Invasion Assays

Cell migration assays were done using 8 μm pore transwell chambers (Fischer; 07-200-150). Cells were serum starved for 16 hr, detached, washed with PBS and resuspended in starvation medium, and added to the transwell chambers (2.5×10^4 cells/well for ACHN, and 3×10^4 cells/well for SN12C). Starvation medium containing 1% FBS was added to the lower chambers and cells were cultured at 37 °C for 8 hr for ACHN and 24 hr for SN12C. Invasion assay was done similarly to the migration assay. In this case, cells were seeded on pre-coated matrigel inserts (BD Biosciences; 08-774-122). For the invasion assay, 1×10^5 cells/well used for ACHN, and 5×10^4 cells/well for SN12C and incubated for 24 hours. Cells were fixed and stained with 0.1% crystal violet in 20% ethanol. Cells that remained at the top of filter were removed with a cotton swab

and migrated cells were counted through a 10x objective lens with an Axioskop microscope (Zeiss).

Tumor Implantation and Measurement

All experiments involving mice were done according to a protocol reviewed and approved by the Institutional Animal Care and Use Committee at the University of Florida. Subrenal capsule implantation protocol is well established and detailed in Zhang *et al.* (158). In summary, we used n=7 male hsd:athymic nude-Fox^{1nu} mice (Envigo), 6 weeks old, and grouped them according to body weight. Soft collagen pellets containing 1 x 10^6 cells were placed under the capsules of the left kidneys. Tumor growth was monitored by palpation and ultrasound imaging (GE Medical System InSiteExC), and, at the end of the experiment, the kidneys, draining lymph nodes (DLN), spleen, liver, intestine, and lung were harvested, weighed, and fixed in 10% buffered formalin phosphate.

Immunohistochemistry

Subrenal tumor grafts or mouse tissues were embedded in paraffin and sectioned (5 μm), deparaffinized in xylene, rehydrated in graded alcohol, subjected to heat-induced antigen retrieval with Target Retrieval Solution, and blocked with Protein Block. Sections were probed with rabbit anti-human LDHA (1:200) or rabbit anti-human Ki67 (1:100) antibody at 4°C overnight, washed, and then incubated with SignalStainBoost. Samples were developed with AEC substrate, counterstained with hematoxylin, and mounted with Faramount. Microscopic images were taken at 10 or 40x using Nikon Eclipse 50i microscope equipped with a DS-Fi1 camera and NIS-Elements BR3.1 software.

Cell Cycle Analysis

All cell cycle analysis was performed following the DAPI nucleic acid stain protocol from Invitrogen. 0.5-1.0 x 10^6 cells were collected, pelleted, and resuspended with 0.5-1 mL DAPI solution. Cells in solution were incubated for 10-20 minutes and analyzed using the LSR II flow cytometry machine. Data was analyzed using the FCS Express 6 Flow Research software.

Statistics

Data are expressed as means ± SEMs or SDs. Statistical analysis was performed with either One-way ANOVA with Tukey's post-test or by using two-tailed paired Student's *t* test, and a $P < 0.05$ was considered statistically significant. Graphs were generated using GraphPad Prism 6 software and axis labels were generated using Adobe Illustrator CS5.1.

Results

Arrb2 is a Clinically Relevant and Possible Therapeutic Target for Select RCC

To investigate whether gene expression levels of βArrestins are differentially expressed in RCC patients tumor tissue compared to normal kidney tissue, we first analyzed *Arrb1* and *Arrb2* gene expression levels from an available dataset of a cohort of 606 ccRCC patients. We found that *Arrb2,* but not *Arrb1,* is highly expressed in tumor samples relative to normal tissue (Figure 2-1 A). *Arrb1* gene expression was not significantly differentially expressed in tumors compared to normal tissue. These observations were consistent with various samples of kidney cancer types from different datasets, such as papillary RCC, chromophobe RCC and other nccRCC (Figure 2-1 D and Figure 2-2 A-D). We also found that *Arrb2* gene expression correlates with the progressive stage of the disease in the ccRCC ATCG dataset (Figure 2-1 B). Patients

with high *Arrb2* gene expression had a significant reduction in patient survival outcomes compared to patients with low expression levels (Figure 2-1 C). These data suggest that *Arrb2,* but not *Arrb1,* is important for tumor progression and metastasis in RCC disease. Therefore, we hypothesize that βArrestin 2 is involved in tumor growth, invasion, and metastasis in this disease.

βArrestin 2 Expression is Upregulated in Metastatic RCC Cell Lines

To test our hypothesis, we first examined gene and protein expression levels of both βArrestins in commonly used RCC cell lines such as 786O, CAKI-1, SN12C, and ACHN compared to normal adult kidney epithelial cell line, HK2. SN12C and ACHN cell lines showed increase in gene expression levels of *Arrb2* relative to HK2 and CAKI-1 cells, and significant βArrestin 2 (referred to as βArr2 in figures) protein levels increase of 6 to 8 folds respectively, compared to HK2, 786O, and CAKI-1 cells (Figure 2-3 A and B). βArrestin 1 (referred to as βArr1 in figures) protein and gene levels were not significantly differentially expressed between these cell lines (Figure 2-3 A and B). Our lab has characterized the growth and metastatic potential of these cell lines *in vitro* and *in vivo* experiments (Figure 2-4 A-D) and ranked ACHN and SN12C to have higher tumor growth, metastatic and invasive potentials than CAKI-1 and 786O after taking into consideration the incubation time, and size/ weight of the tumors at endpoint. Therefore, we conclude that increased βArrestin 2 levels correlate with the increased metastatic and proliferative capacities of RCC cell lines and with advanced stages of the disease. Next, we wanted to examine the effect of βArrestin 2 on cell migration. We knocked down gene expression using siRNA in ACHN cells and shRNA in SN12C cells (Figure 2-5 A and Figure 2-6 A) and allowed cells to migrate through a Boyden Chamber membrane over time. We observed a substantial decrease in cell migration of around

50% for both cell lines compared to their respective controls (Figure 2-5 B and 2-6 B). In addition, we tested whether βArrestin 2 knockdown will affect ACHN cells invasion through a matrigel coated membrane of the Boyden chamber. ACHN cells invasion was hindered as well compared to control (Figure 2-5 C). Taken together these results indicate that βArrestin 2 is involved in RCC cells migration and invasion *in vitro*.

βArrestin 2 Knockout Induces Cell Morphology Changes and Hinders Proliferation

To further test the function of βArrestin 2 in RCC cell lines, we established a stable *Arrb2* knockout (KO) in SN12C cells using the CRISPR/Cas9 system. Cells were infected using a single lentiviral CRISPR/Cas9 plasmid with a specific sgRNA cloned into it, which targets either exon 3 or 4 of the *Arrb2* gene (Figure 2-7 A and B). Since initial CRISPR infection yielded a mixed population of cells with various KO degrees (Figure 2-8 A), we used single cell clonal expansion to produce purer SN12C *Arrb2* KO clones (Figure 2-8 B). Control cells were also infected with the same CRISPR/Cas9 plasmid, however, it lacked any sgRNAs. The primary round of single cell clonal expansion yielded clone Arrb2ex3-14 and the secondary round of clonal expansion yielded clone Arrb2ex4-12.19 with no detectable βArrestin 2 protein band, while having no effect on βArrestin 1 expression as observed in a western blot (Figure 2-9 A). Cell morphology was observed for the KO clones and compared with control SN12C cells under phase contract and confocal microscopy (Figure 2-9 B and C, respectively). It was clear that KO cells resemble a more epithelial-like morphology with a less spindle-like shape than control cells. Under confocal imaging, it was obvious that KO cells lack cytoskeletal extensions that the control cells have (Figure 2-9 C). Because of such morphological changes, we further tested the ability of Arrb2ex3-14 cells to form

spheres in a 3D matrigel system in comparison to control cells (Figure 2-10 A). As previously determined, SN12C cells can form large spheres from single cells in the 3D matrigel assay (Figure 2-5 D). In this assay, images were captured at days 6, 9, 12, 15 and 20. Here, we are showing start (day 6), midpoint (day 12) and end point (day 20) images, but spheres volumes were measured for the largest 15 spheres selected at day 6 and tracked throughout each of the time points. Control cells invaded through the matrigel as observed from the day 12, day 12 (10x), and day 20 panels, and formed numerous spheres by day 20 (Figure 2-10 A and B). On the other hand, Arrb2ex3-14 cells formed very few spheres that were significantly smaller in size and lacked any cellular extensions or invasion in the surrounding matrigel. In fact, Arrb2ex3-14 spheres resembled the shape of HK2 spheres that were grown previously (Figure 2-10 C). In support to the hindered tumor cell sphere development and growth phenotype, a prestoblue experiment confirmed that KO cells are capable of proliferating however at much slower rates than control cells (Figure 2-10 D). Furthermore, it was striking to us, that not only are the KO cells incapable of proliferating compared to control cells, they are also unable to attach to the surface of the plastic culture plate as well as control cells do (Figure 2-11 A and B). This was also the case when cells were seeded on fibronectin coated plates (Figure 2-12). Taken together, these *in vitro* results give strong indications that βArrestin 2 is required for tumor cell proliferation and invasion through extracellular space.

βArrestin 2 Knockout Tumors Fail to Grow and Metastasize *in Vivo*

In order to further characterize whether *Arrb2* KO is important for tumor growth *in vivo*, we used the subrenal capsule implantation model to compare control and *Arrb2* KO SN12C cells capacities to grow in nude mice. Control, Arrb2ex3-14, and Arrb2ex4-

12.19 cells were implanted orthotopically in the subrenal capsule space. Tumors were allowed to grow for 5 weeks before animals were sacrificed and then kidneys as well as distant organs such as lymph nodes, lungs, spleen, liver, and intestine were collected and analyzed. Tumor size was monitored every week by palpitation and ultrasound imaging (Figure 2-13 A), and compared to the contralateral normal kidney where no tumor was implanted. At the end point, we observed many visible metastatic lesions throughout the control mice bodies, while no visible lesions were seen in KO mice (Figure 2-13 B and C). Tumor weights were determined for each mouse (Figure 2-14 A) and results show that SN12C *Arrb2* KO tumors grew significantly smaller than control SN12C tumors. Anti-human LDHA staining revealed that *Arrb2* KO tumors were not able to invade through the cortex (arrow heads) of the kidney in contrast to control tumors where majority of the kidney cortex was infiltrated (arrows) with SN12C cells (Figure 2-14 B). Lymph nodes are the primary sites for tumor cell dissemination to distant organs, therefore, we collected adjacent renal lymph nodes (RLNs) of the tumor sides (T) and normal sides (N) of all mice. As expected, mice with control tumors, have significant metastasis as observed by weight and LDHA staining compared to RLNs tumor side of *Arrb2* KO mice (Figure 2-15 A and B). RLNs normal side from control mice also had metastasis, while no metastasis was detected in *Arrb2* KO mice. Interestingly, we observed in all control animals that RLNs tumor side had an interesting tumor invasion pattern where cells were invading around germinal centers (40x panel Figure 2-15 B) as they infiltrated throughout the lymph node. This could lead to a new tumor invasion pattern understanding if investigated further in future studies. Urethral lymph nodes (ULNs) showed no visible differences in size between groups, but LDHA staining

revealed metastasis in tumor side nodes (Figure 2-16 A and B). Moreover, metastasis in the lungs was detected in 6 out 7 control mice, but none in *Arrb2* KO mice (Figure 2-16 C). Since *Arrb2* KO cells proliferated at a much slower rate than control cells, we stained the tumor tissue for anti-human Ki67, a proliferation marker that is only present during active cell cycle progression. *Arrb2* KO tumor sections showed less cells with Ki67 staining compared to control tumors (Figure 2-17 A). *Arrb2* KO tumors were significantly smaller than control and we were unable to directly extract proteins from the KO tumor tissue. Therefore, we used cell lysates to examine Ki67 expression, and found that indeed, control cells express higher levels of Ki67 compared to KO cells (Figure 2-17 B). This suggests that *Arrb2* KO can lead to cell cycle arrest in the G_0 phase. All together these data indicate that βArrestin 2 is necessary for tumor growth and invasion *in vivo*, which ultimately leads to metastasis to distant organs.

We then performed a second subrenal implantation experiment to observe whether KO tumors would eventually grow larger over an extended period of time and if so, would they metastasize to nearby lymph nodes or certain organs such as lungs, liver, and spleen as control tumors did. We decided to allow KO tumors to grow for 9 weeks which is almost twice as long as the initial experiment. Since control tumors reached a large size at 5 weeks, it would not be feasible to grow them for 9 weeks, therefore, were not included in this experiment. To our surprise, even with almost doubling the incubation time, *Arrb2* KO cells did not grow and tumor weights remained very similar to 5 weeks tumors (Figure 2-18 A). Moreover, mice had no visible metastasis (Figure 2-18 B and C). This data is remarkable and demonstrates that βArrestin 2 is necessary mainly for RCC cells growth and proliferation.

βArrestin 2 Regulates RCC Progression Through Multiple Mechanisms

Cell cycle progression and proliferation

Our results thus far indicate that *Arrb2* KO caused a couple of major phenotypic changes in SN12C cells. One major change is the reduced tumor cell proliferation. Another important change is a mesenchymal to epithelial-like switch. To further investigate the cell cycle status of the *Arrb2* KO cells, we looked for cyclin D1 and cyclin A protein expression (Figure 2-17 C and D). Cyclin A but not cyclin D levels were reduced in the KO cells. This confirms a cell cycle arrest caused by *Arrb2* KO. To investigate further into our findings, we performed a cell cycle analysis on control vs. *Arrb2* KO cells 48 hours after seeding. Cells were stained with DAPI, which detects the nucleic acid content, and cells were analyzed. 5×10^4 cells were counted and according to the FSC measure were gated to count for live cells versus "other" which is potentially cell debris (Figure 2-19 A and B). We noticed that majority of the *Arrb2* KO cells were outside the range of what was considered live for the control cells population (Figure 2-19 C). Majority of the *Arrb2* KO cells counted were likely apoptotic or fragmented. Of the live cells, we then calculated the cells that were in G1, S, and G2 phase for each of the populations (Figure 2-19 D). It was very clear that both *Arrb2* KO cell lines had less cells in the G2 phase. In fact, Arrb2ex3-14 cell line consistently had 0% cells in G2. This data is consistent with the reduced expression of cyclin A.

As cells prepare for a mitotic division, cell size increases during the S phase until the cell divides into two daughter cells. During cell culture, we observed under the microscope that KO cells seem larger in size. From the cell cycle analysis, we performed and FCS data, it became clearer that it is possible that since *Arrb2* KO cells are halted at the S phase and thus are not progressing efficiently into the G2 phase to

ultimately divide as control cells do. The FSC medians and geometric means are increased for KO cells especially Arrb2ex3-14 clone (Figure 2-20 A-C).

Cell morphology

The second main phenotypic alteration observed with *Arrb2* KO cells is that they have become rounder and less spindle-like in structure compared to control SN12C cells (Figure 2-9 B and C). Control SN12C cells are elongated and have numerous long cytoskeletal extensions. On the other hand, KO cells show a cobble stone shape with few to no cytoskeletal extensions. Moreover, knocking down and knocking out βArrestin 2 caused a marked reduction in migration and invasion (Figures 2-5 and 2-6 and *in vivo* results). To further understand cell morphology changes, we aimed to check for differences in focal adhesion numbers and cytoskeletal remodeling for both control and KO cells. Focal adhesions formation/ turnover and distribution are necessary for cell polarity that lead to cell migration by forming a leading edge in migrating cells (159). Key molecular determinants involved in the assembly of focal adhesions and the lamellipodia structure are the focal adhesion kinase (FAK), Paxillin, Rho small GTPases members, Src, integrins and many others (160-164). Total FAK protein and phosphorylated Paxillin Y118 levels were down regulated in KO cells (Figure 2-21 A) which indicate a reduced focal adhesion turnover, potentially reducing cell migration. Src tyrosine kinase which takes part in phosphorylating Paxillin, can be generally stimulated by the mechanical forces applied through the focal adhesion as they form and promote cell growth and adhesion (161, 165, 166). Activated levels of p-Src Y416 were significantly reduced in the absence of βArrestin 2 (Figure 2-21 A). Furthermore, confocal imaging show confirm that control cells have numerous distinct focal adhesion structures (white arrow heads) as seen from the amount of Paxillin staining (green).

Conversely, both KO clones have far fewer focal adhesions and less Paxillin staining (Figure 2-21 B). This could also explain the increased cell detachment that was observed earlier (Figures 2-11 and 2-12).

Other altered interactions

Aberrant Akt activation is often observed in cancers, as it an important regulator of cell migration, growth and survival. Therefore, we aimed to examine Akt activity in control versus *Arrb2* KO cells. We first looked at Akt phosphorylation on S473 and T308 (Figure 2-22 A). Interestingly, p-Akt-S473 unlike p-Akt-T308 was significantly reduced in *Arrb2* KO cells compared to control. Then we evaluated the activation of downstream targets of Akt; GSK3α/β and βcatenin. Surprisingly, GSK3α and β phosphorylation were not significantly altered, yet active non-phosphorylated-βcatenin and total βcatenin protein levels were significantly elevated (Figure 2-22 B and C). As mentioned above, *Arrb2* KO induced what seems to be a mesenchymal to epithelial (MET) morphology switch in SN12C cells. Gene expression analysis of hallmark EMT genes revealed a significant increase in E-cadherin (*Cdh1*), and decrease in *Zeb1*, *Twist1*, and *Twist2* genes, but no significant change with N-cadherin (*Cdh2*), Vimentin (*Vim*), Snail (*Snai1*) or Fibronectin (*Fn1*) gene expression (Figure 2-23 A). Since βcatenin is known to stabilize the E-cadherin complex (167, 168), we sought to determine the localization of the active βcatenin protein (Figure 2-23 B and C). Nuclear versus cytoplasmic fractionation showed that βcatenin was present in all the cell lines in the cytoplasm but with much higher concentrations in the *Arrb2* KO cells. Confocal imaging (Figure 2-23 B) show that there are many active-βcatenin puncta localized in the nucleus of control cells, but in KO clones, active-βcatenin is now mostly present at the plasma membrane (white arrow heads). Although this explains our predictions for increased E-cadherin

levels or stability in the KO cells, it is still unclear how eliminating βArrestin 2 is increasing the levels of active βcatenin in SN12C. The data suggest that βArrestin 2 is mediating βcatenin upregulation independently from GSK3 regulation, indicating that perhaps and according to p-Src downregulation results shown thus far, it is dependent on a βArrestin 2-Src-βcatenin/E-cadherin axis in SN12C cells.

mTORC2 is an upstream regulator of Akt and it phosphorylates Akt on the S473 residue which is needed to prime Akt for full activation by further PDK1 phosphorylation on T308 (169, 170). mTORC2 is also involved in the activation of PKC which leads to cell migration and cytoskeletal rearrangements, and of SGK which phosphorylates FOXO1/3a which blocks apoptosis. Therefore, based on increasing literature evidence, mTORC2 exerts a regulatory effect on cell growth, survival, and cytoskeletal dynamics. Recent evidence also suggests that Sin1 is an important regulator of mTORC2 activity. Through PIP_3-PH domain binding to Sin1 and pulling it away from the kinase domain of mTOR, Akt is then phosphorylated on Ser473. Arrestins have been identified to have a strong binding affinity towards phospoinositides (PIPs) especially PIP_2 and PIP_3 (171). Based on this and FAK results shown above, we were curious to check if the mTORC2 complex integrity is altered by deleting βArrestin 2. We performed a co-immunoprecipitation assay to determine whether Sin1 is bound to the mTORC2 complex in the presence or absence of βArrestin 2. We immunoprecipitated using anti-Rictor, a protein specific for mTORC2, and blotted for Sin1 in control and *Arrb2* KO cells. To our surprise, there was no hindering of Sin1 binding Rictor in KO cells (Figure 2-24). Therefore, any attenuation in mTORC2 activity is not through Sin1-mTORC2 interactions.

In summary, our results indicated that ACHN and SN12C cells need βArrestin 2 activity for migration and invasion as well as induced cell proliferation. ACHN and SN12C cells migration and invasion are greatly inhibited with reduced βArrestin 2 levels. SN12C tumors are incapable of proliferating *in vivo* in the absence of βArrestin 2, thus do not metastasize to other organs. Furthermore, cells have become more prone to detachment from the extracellular matrix or fibronectin upon seeding. We observe two main phenotypes in the context of cell cycle progression and proliferation, and a mesenchymal to epithelial transition. Since βArrestin 2 is a scaffolding molecule, we confirm here that multiple proteins and genes are altered with regards to expression levels or spatial localization and phosphorylation thus, triggering multiple mechanisms to be deregulated in RCC.

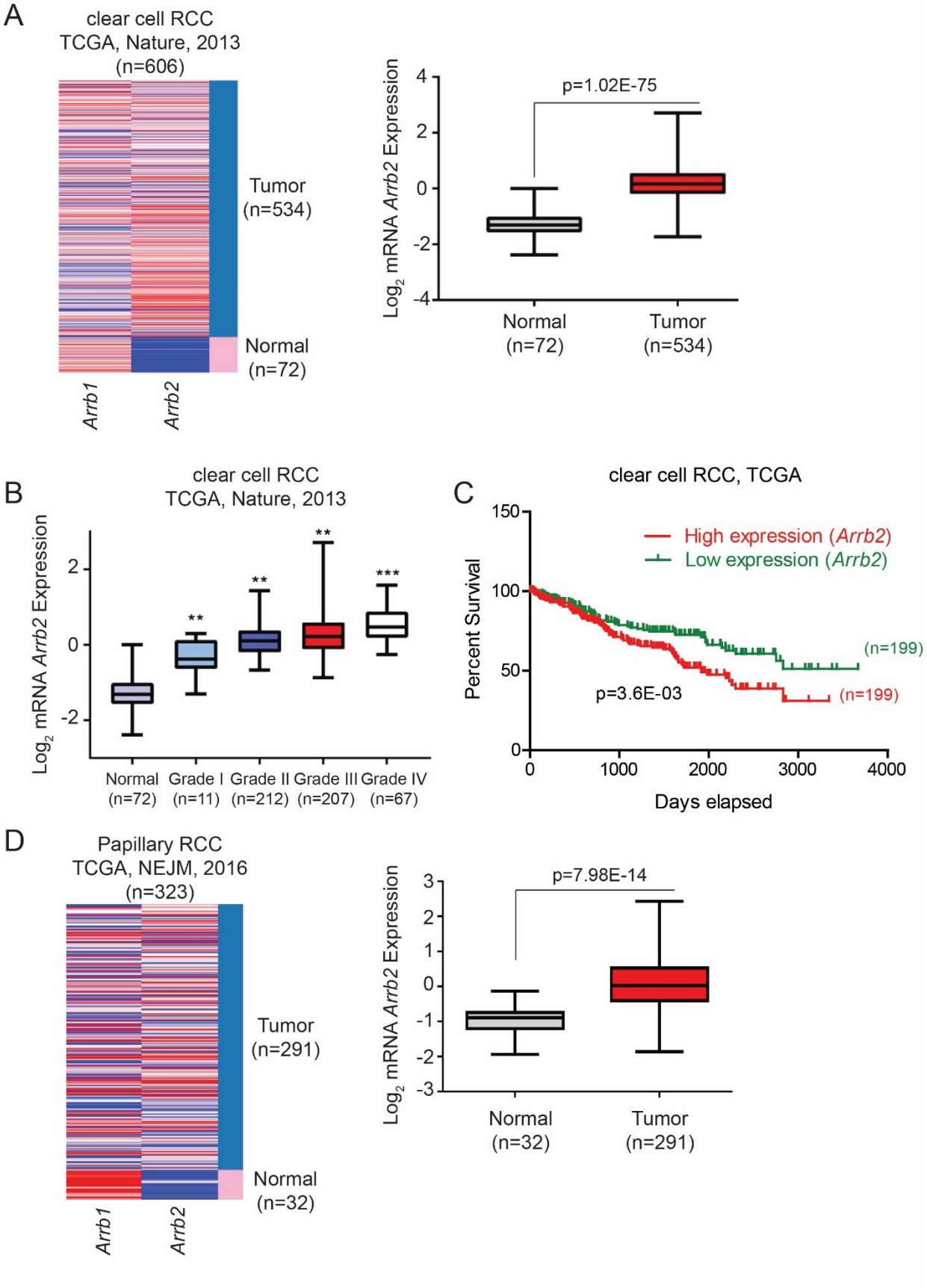
A
clear cell RCC
TCGA, Nature, 2013
(n=606)
Tumor
(n=534)
Normal
(n=72)
Arrb1
Arrb2
p=1.02E-75
Log2 mRNA Arrb2 Expression
Normal
(n=72)
Tumor
(n=534)
B
clear cell RCC
TCGA, Nature, 2013
Log2 mRNA Arrb2 Expression
Normal
(n=72)
Grade I
(n=11)
Grade II
(n=212)
Grade III
(n=207)
Grade IV
(n=67)
C
clear cell RCC, TCGA
High expression (Arrb2)
Low expression (Arrb2)
Percent Survival
p=3.6E-03
(n=199)
(n=199)
Days elapsed
D
Papillary RCC
TCGA, NEJM, 2016
(n=323)
Tumor
(n=291)
Normal
(n=32)
Arrb1
Arrb2
p=7.98E-14
Log2 mRNA Arrb2 Expression
Normal
(n=32)
Tumor
(n=291)

Figure 2-1. *Arrb2* is a clinically relevant and possible therapeutic target for select (RCC). A) Left panel: heat map generated from The Cancer Genome Atlas (TCGA) database showing relative mRNA expression of *Arrb1* and *Arrb2* gene in normal and renal clear cell carcinoma patients. Right panel: box plots showing gene expression data for *Arrb2* in RCC patient compared to normal patient data from TCGA. Log2-normalized read count [RNA-seq by expectation-maximization (RSEM)] is shown. B) Box plots represent *Arrb2* gene expression for tumor samples stratified according to histologic grade. C) Kaplan–Meier plots represent overall survival of RCC patients in whole datasets for RCC patients categorized according to *Arrb2* gene expression (high versus low). The *P* value was calculated using a log-rank test. Box plot line (from top to bottom): maximum; Q3, third quartile; median; Q1, first quartile; and minimum. D) Left panel: heat map generated from the TCGA database showing relative mRNA expression of *Arrb1* and *Arrb2* gene in normal and papillary carcinoma patients. Right panel: box plots showing gene expression data for *Arrb2* in RCC patient compared to normal patient data from TCGA. Log2-normalized read count [RNA-seq by expectation-maximization (RSEM)] is shown. *P* values were calculated by using two-tailed paired Student's *t* test. Data shown are mean ± SEM, $^{**}P < 0.001$,$^{***}P < 0.0001$.

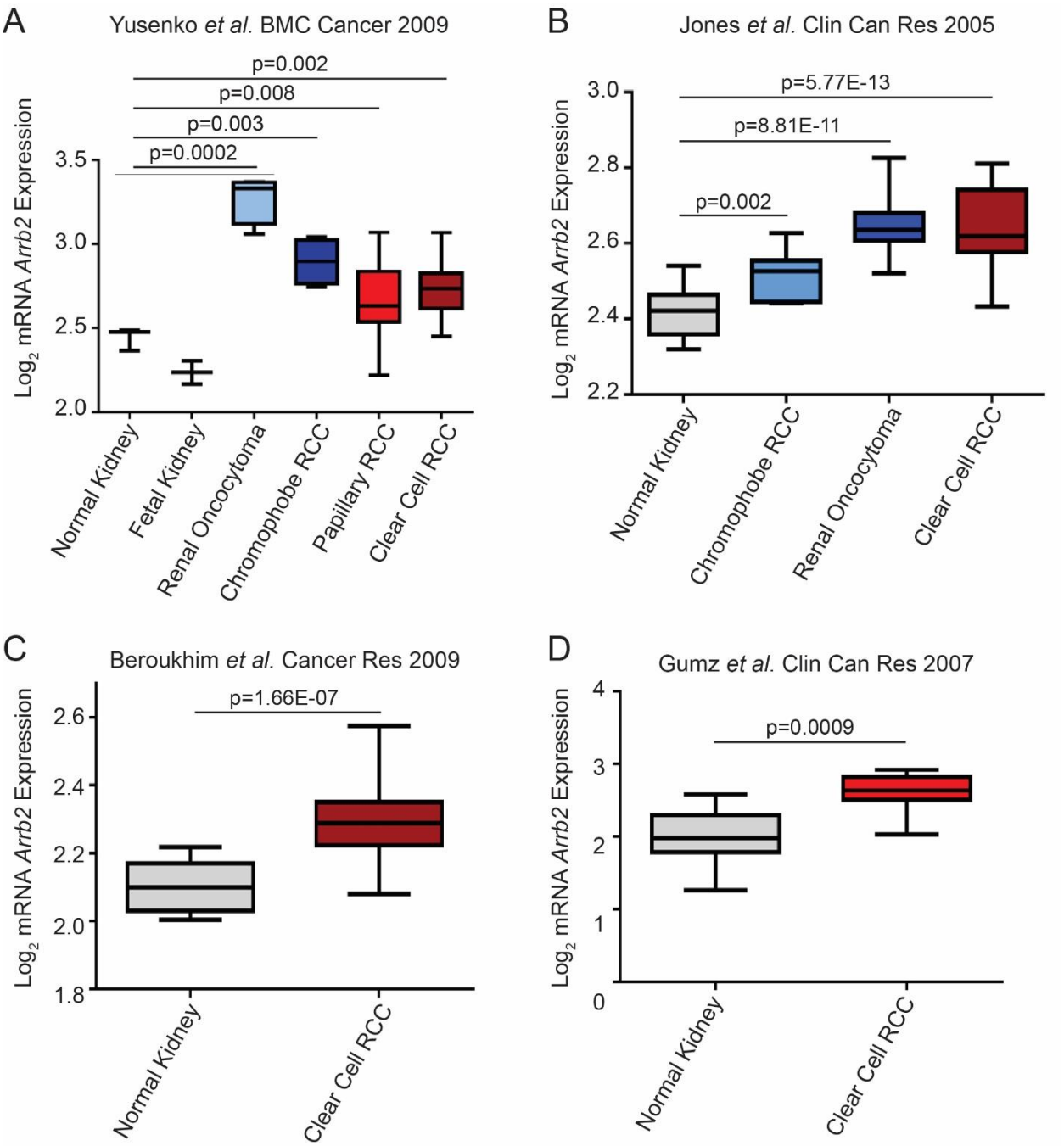

Figure 2-2. *Arrb2* is amplified and/or overexpressed in large number kidney cancer patient datasets. *Arrb2* transcript levels from four Gene Expression Omnibus (GEO) datasets of A) Yusenko *et al*., B) Jones *et al.*, C) Beroukhim *et al.*, and D) Gumz *et al*., were queried for association with disease status. *P* values were calculated by using two-tailed Student's *t* test. Box plot line (from top to bottom): maximum; Q3, third quartile; median; Q1, first quartile; and minimum.

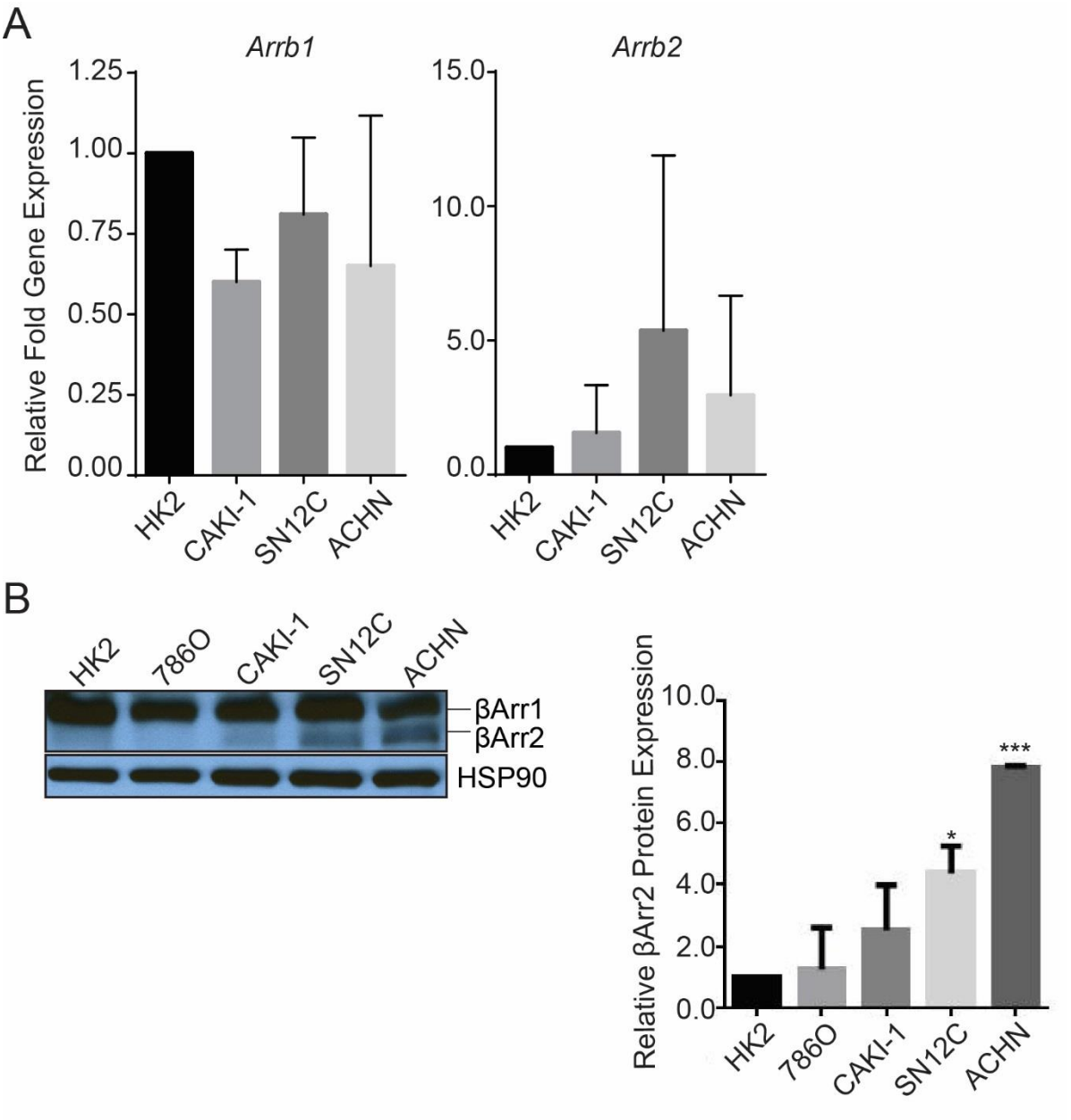

Figure 2-3. βArrestin 2 expression is upregulated in metastatic RCC cell lines. A) Relative expressions of *Arrb1* and *Arrb2* mRNA in CAKI-1, SN12C, and ACHN to HK2 cells were measured by real-time PCR. Gene expression is represented as a fold change in mRNA levels relative to HK2 cells. B) Relative protein expression levels for βArr1 and βArr2 in HK2, 786O, CAKI-1, SN12C, and ACHN cells. βArrestin 2 protein levels were quantified as show in right panel. Protein levels in the RCC cells are shown as a relative fold change to HK2 cells. Data shown are mean ± SD for three trials, $*P < 0.05$, $**P < 0.001$, $***P < 0.0001$.

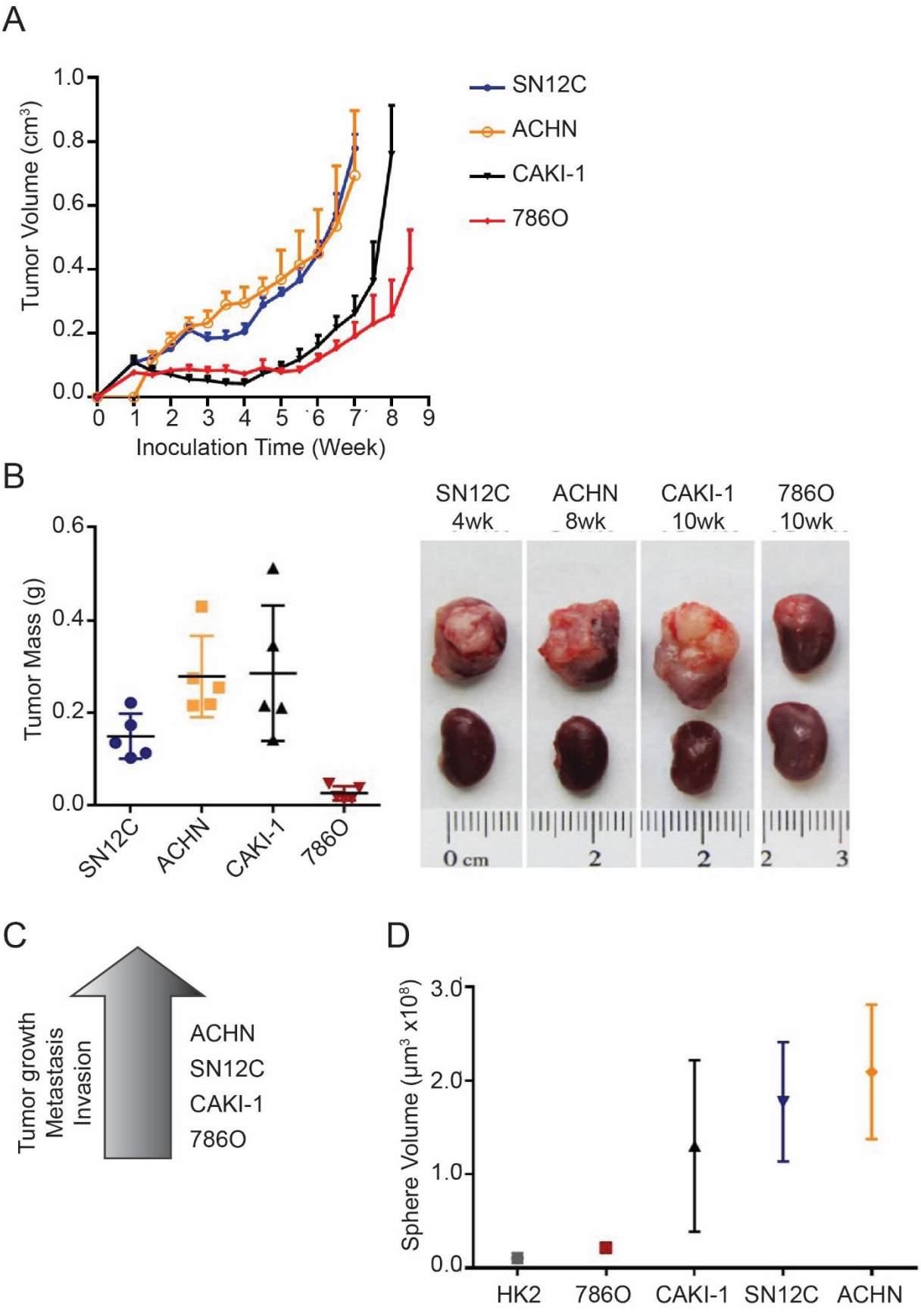
A
Tumor Volume (cm³)
1.0
0.8
0.6
0.4
0.2
0.0
0 1 2 3 4 5 6 7 8 9
Inoculation Time (Week)
SN12C
ACHN
CAKI-1
786O
B
Tumor Mass (g)
0.6
0.4
0.2
0.0
SN12C
ACHN
CAKI-1
786O
SN12C 4wk
ACHN 8wk
CAKI-1 10wk
786O 10wk
0 cm
2
2
2
3
C
Tumor growth
Metastasis
Invasion
ACHN
SN12C
CAKI-1
786O
D
Sphere Volume (μm³ x10⁸)
3.0
2.0
1.0
0.0
HK2
786O
CAKI-1
SN12C
ACHN

Figure 2-4[1]. RCC cell lines tumor growth. A) Subcutaneous tumor growth. 1 x 10^7 cells were inoculated in the flank of athymic nude mice. Tumor growth was monitored by measuring the length and width of the tumors, and tumor volume was calculated using the formula: V= 0.524 x length x $width^2$ (n=6 animals per cell line). B) Subrenal tumor growth. 1 x 10^6 cells were embedded in collagen pellet and implanted under the renal capsule of athymic nude mice. Tumors were harvested at 4 to 10 weeks after implantation (n=5 animals per cell line). Weight of tumors from experiment calculated by subtracting weight of the contralateral normal kidney from the weight of kidney bearing tumor. Tumor growth experiments were repeated twice with similar results. C) Cell lines ranked for their tumor growth, metastatic, and invasive capacities based on data in A and B, taking into consideration the duration of tumor growth for each cell line. D) Average volume of the largest 10 spheres for each cell line at endpoint. 200 cells for each cell line were seeded in 3D matrigel sandwich; matrigel mixed with plain media in a 1:1 ratio, in 24-well inserts and allowed to grow for 22 days. Media containing serum was added to the top of the matrigel and changed every three days.

[1] Figure 2-4 subsections A and B data are the work of Dr. Yushan Zhang and is unpublished data.

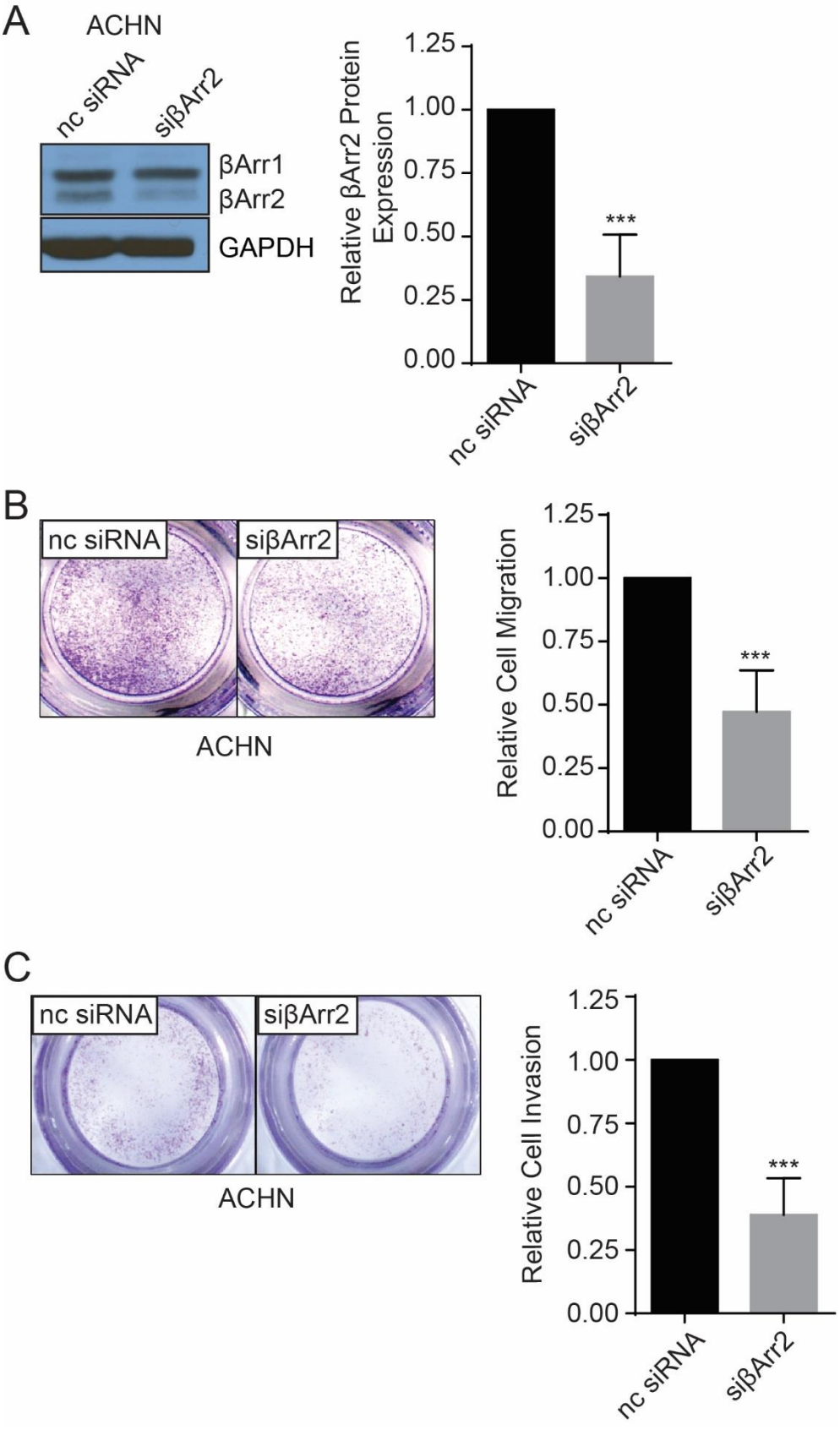
A
ACHN
nc siRNA
siβArr2
βArr1
βArr2
GAPDH
Relative βArr2 Protein Expression
1.25
1.00
0.75
0.50
0.25
0.00
***
nc siRNA
siβArr2
B
nc siRNA
siβArr2
ACHN
Relative Cell Migration
1.25
1.00
0.75
0.50
0.25
0.00
***
nc siRNA
siβArr2
C
nc siRNA
siβArr2
ACHN
Relative Cell Invasion
1.25
1.00
0.75
0.50
0.25
0.00
***
nc siRNA
siβArr2

Figure 2-5. βArrestin 2 knockdown in ACHN cells. A) βArrestin 2 knockdown in ACHN cells reduced cell migration. ACHN cells were transfected with 50nM siRNA targeting βArrestin 2 which effectively reduced βArr2 protein levels to more than 50%. Control cells were transfected with scramble negative control siRNA (nc siRNA). B) Migration assay. ACHN control and siβArr2 cells were starved overnight in 0.1%BSA containing RPMI media without serum. 2.5 x 10^4 cells were seeded into transwell migration inserts and stimulated with 1%FBS containing media added to the outside of the insert for 8 hours. Cells in five 100x fields were counted and siβArr2 cells migration was plotted as a ratio to control cells. Images shown are representative of three independent trials. C) Invasion assay. Done similarly as the migration assay with the differences of using matrigel coated inserts, 1.0 x 10^5 cells, and a 24 hours incubation time. Data shown are mean ± SD for three trials, $*P < 0.05$, $**P < 0.001$, $***P < 0.0001$.

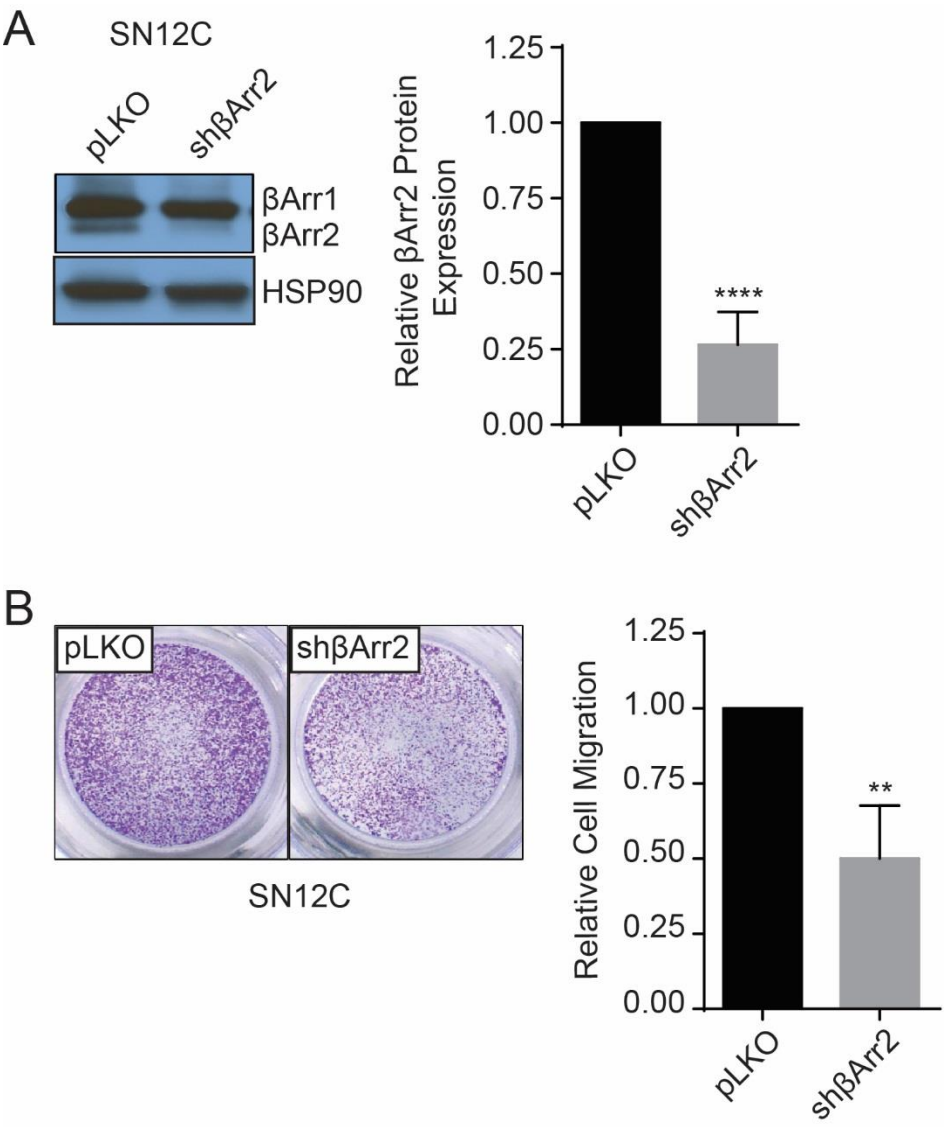

Figure 2-6. βArrestin 2 knockdown in SN12C cells. A) shRNA targeting βArr2 in SN12C knocked down expression by around 75%. Control cells were infected with empty pLKO plasmid. B) Migration assay. shβArr2 and pLKO cells were starved overnight in 0.1%BSA containing RPMI media without serum. 3 x 10^4 cells were seeded into transwell migration inserts and stimulated with 1%FBS containing media added to the outside of the insert for 24 hours. Cells in five 100x fields were counted and shβArr2 cells migration was plotted as a ratio to control cells. Images shown are representative of three independent trials. Data shown are mean ± SD for three trials, *$P < 0.05$, **$P < 0.001$, ***$P < 0.0001$.

A Exon 3

5’…CTCACCGTGTACTTGGGCAAGCGGGACTTCGTAGATCACCTGGACAAAGTGGACCCTGTAGGT… 3’
3’…ACCTACAGGGTCCACTTTGTCCAGGTGATCTACGAAGTCCCGCTTGCCCAAGTACACGGTGAG… 5’

sgRNA oligo sequence:
(+) strand: 5’ GCGGGACTTCGTAGATCACC 3’ - TGG (PAM)

position		target sequence	sequence information			number of target sites		
start - end	+ −	20mer+PAM (total 23mer)	GC% of 20mer	Tm of 20mer	TTTT in 20mer	20mer +PAM	12mer +PAM	8mer +PAM
3 - 25	+	TCACCGTGTACTTGGGCAAGCGG [gRNA]	55.00 %	75.13 °C	-	1 [detail]	16 [detail]	7748 [detail]
4 - 26	+	CACCGTGTACTTGGGCAAGCGGG [gRNA]	60.00 %	77.27 °C	-	1 [detail]	12 [detail]	4654 [detail]
6 - 28	-	CCGTGTACTTGGGCAAGCGGGAC [gRNA]	60.00 %	78.55 °C	-	1 [detail]	18 [detail]	4035 [detail]
22 - 44	+	GCGGGACTTCGTAGATCACCTGG [gRNA]	60.00 %	75.89 °C	-	1 [detail]	1 [detail]	5128 [detail]
31 - 53	+	CGTAGATCACCTGGACAAAGTGG [gRNA]	50.00 %	70.26 °C	-	1 [detail]	28 [detail]	6672 [detail]
40 - 62	-	CCTGGACAAAGTGGACCCTGTAG [gRNA]	55.00 %	74.30 °C	-	1 [detail]	28 [detail]	5337 [detail]

B Exon 4

5’…ATGGCGTGGTGCTTGTGGACCCTGACTACCTGAAGGACCGCAAAGG…3’
3’…CCTTTGCGGTCCTTCAGGTAGTCAGGGTCCACAAGCACCACGCCAT…5’

sgRNA oligo sequence:
(+) strand: 5’ GACTACCTGAAGGACCGCAA 3’ - AGG (PAM)

position		target sequence	sequence information			number of target sites		
start - end	+ −	20mer+PAM (total 23mer)	GC% of 20mer	Tm of 20mer	TTTT in 20mer	20mer +PAM	12mer +PAM	8mer +PAM
15 - 37	+	TGTGGACCCTGACTACCTGAAGG [gRNA]	55.00 %	76.02 °C	-	1 [detail]	11 [detail]	4180 [detail]
21 - 43	-	CCCTGACTACCTGAAGGACCGCA [gRNA]	55.00 %	75.88 °C	-	1 [detail]	9 [detail]	2900 [detail]
22 - 44	-	CCTGACTACCTGAAGGACCGCAA [gRNA]	55.00 %	75.01 °C	-	1 [detail]	10 [detail]	2774 [detail]
25 - 47	+	GACTACCTGAAGGACCGCAAAGG [gRNA]	55.00 %	75.01 °C	-	1 [detail]	3 [detail]	482 [detail]

Figure 2-7. Designing sgRNAs for targeting *Arrb2* gene on exons 3 and 4. A-B) *Arrb2* exon 3 and exon 4 sequences that were targeted for Cas9 double strand break. Oligo sgRNAs design for both exons was based on CrisprDirect design tool algorithm. (http://crispr.dbcls.jp/). Screenshot images of the results tables with best fit sgRNA sequences. Red arrows indicate the selected oligo sequence, and the selected PAM region is highlighted in yellow for each of the exons.

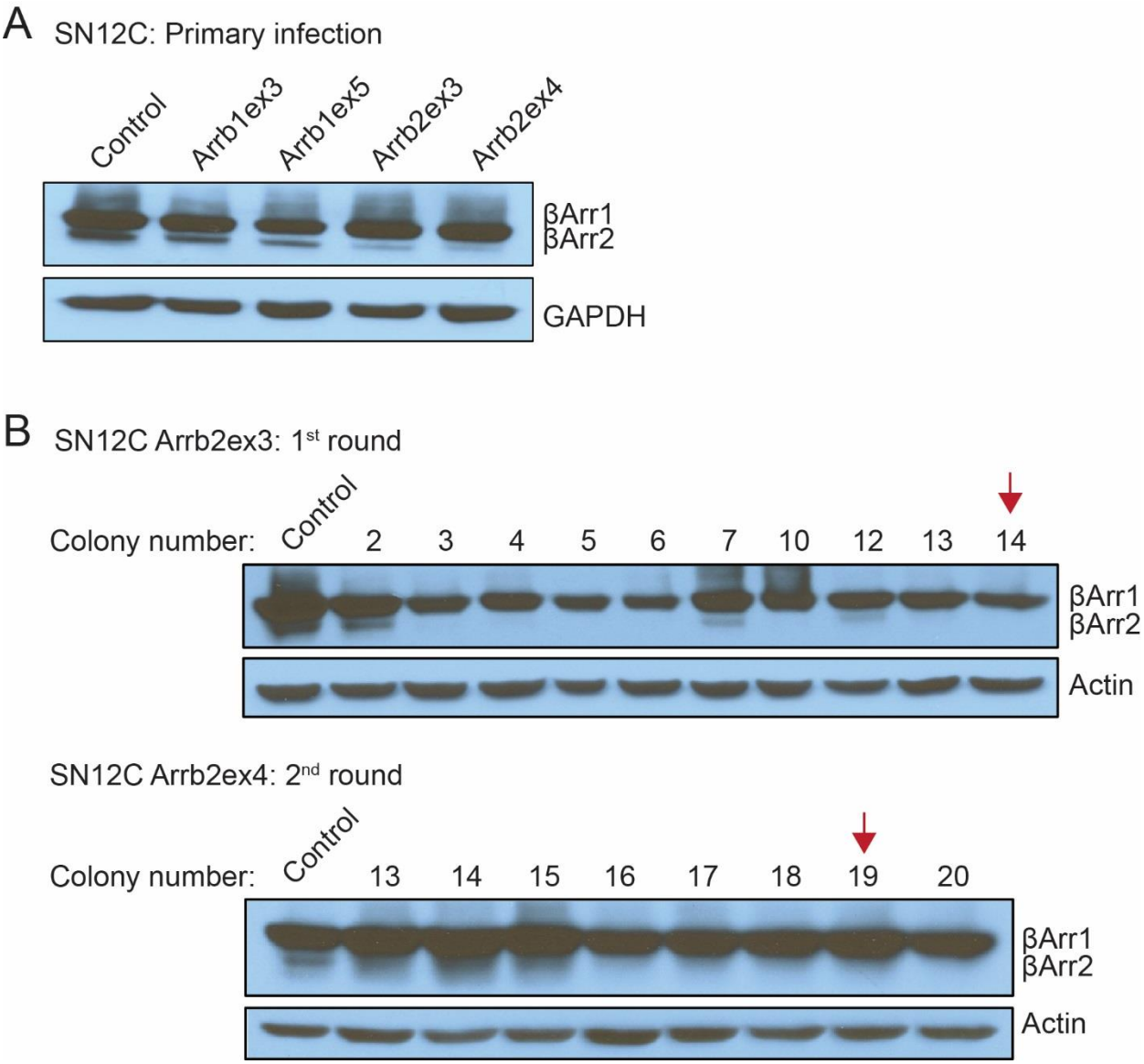

Figure 2-8. Selecting SN12C *Arrb2* KO clones. A) Protein expression levels for βArr1 and βArr2 proteins after initial infection with lentiviral plasmids containing the specific sgRNA for each exon. Upper band is βArr1 protein and lower band is βArr2. B) Western blots analyzing βArr2 protein levels after first and second rounds of single cell clonal expansion. Arrows indicate clones Arrb2ex3-14, and Arrb2ex4-12.19 that were used for further experimenting.

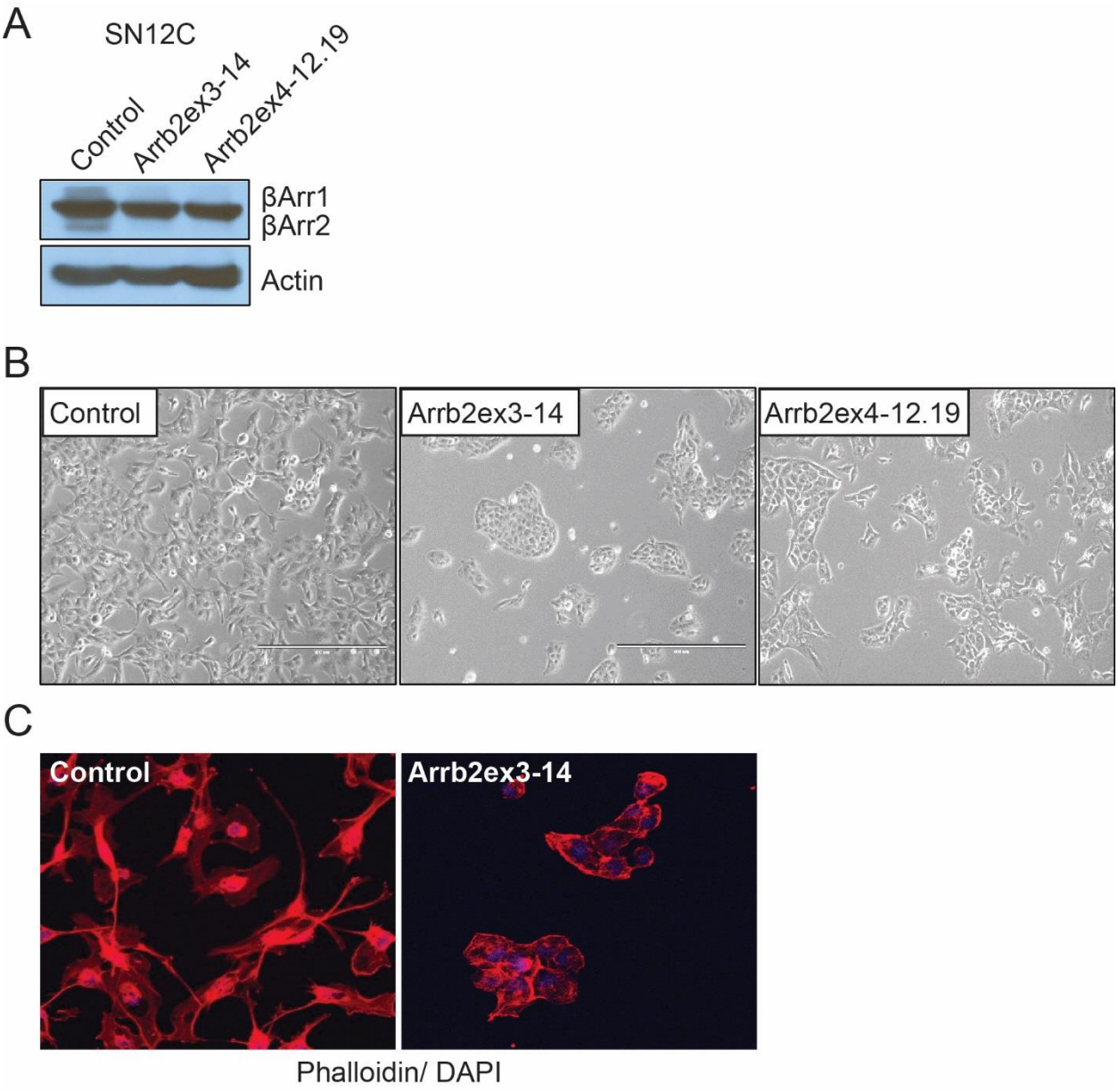

Figure 2-9. βArrestin 2 knockout induces cell morphology changes. A) Western blot confirming *Arrb2* KO in two SN12C clones; Arrb2ex3-14 and Arrb2ex4-12.19, compared to control SN12C. Arrb2ex3-14 and Arrb2ex4-12.19 cell lines denote SN12C infected with lentivirus CRISPR/Cas9 containing sgRNA targeting exon 3 or exon 4 respectively. Control SN12C cells were infected with lentivirus CRISPR/Cas9 that contains no sgRNAs. Upper band is βArr1 protein and lower band is βArr2. Actin was used as a loading control. B) 10x phase contrast images of *Arrb2* KO clones compared to control cells. C) 40x confocal images of Arrb2ex3-14 and control cells stained with phalloidin (red) and DAPI (blue).

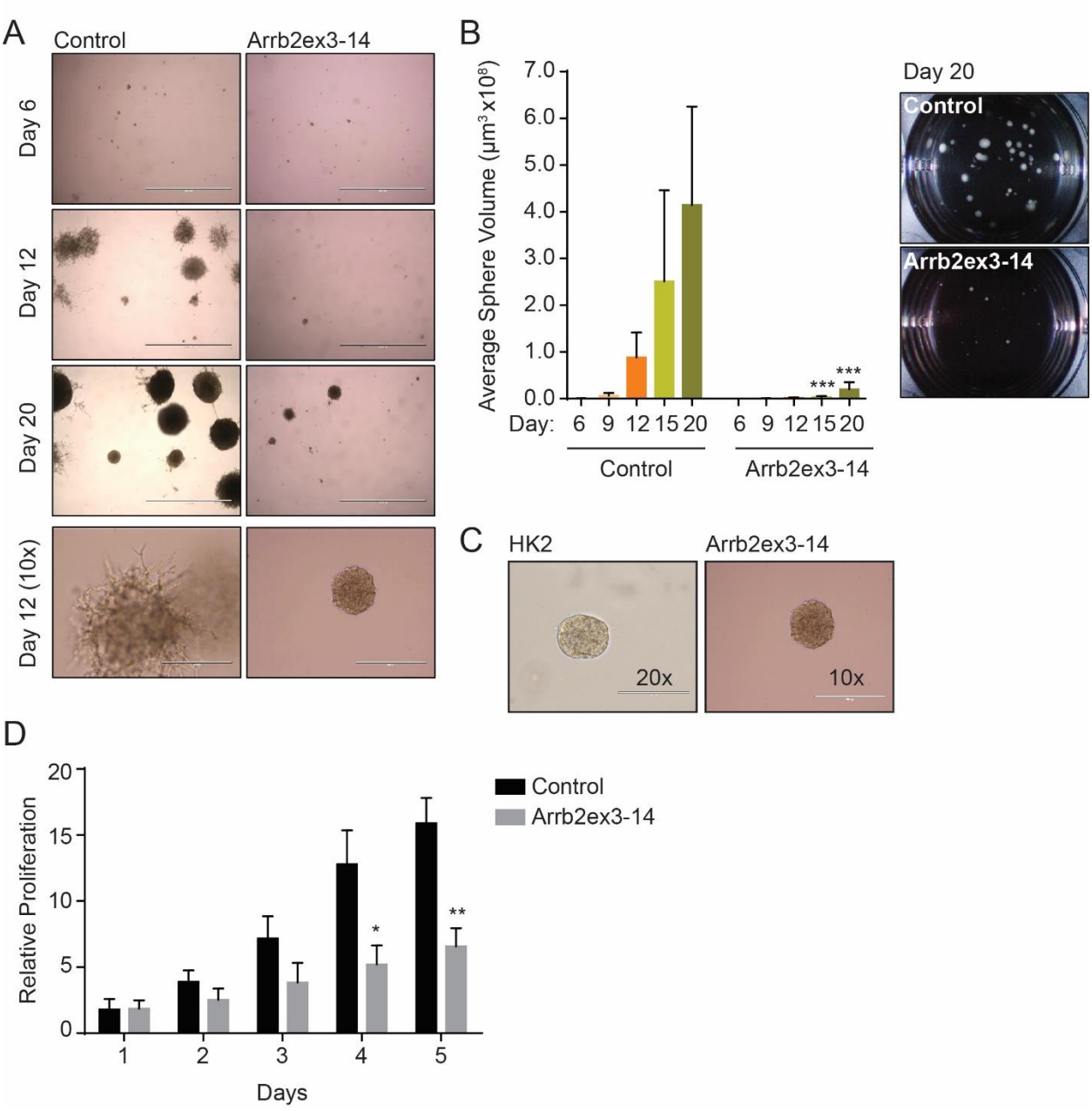

Figure 2-10. βArrestin 2 knockout hinders proliferation. A) 500 control or Arrb2ex3-14 single cells were seeded in a 3D matrigel sandwich; matrigel mixed with plain media in a 1:1 ratio, in 24-well inserts and allowed to grow for 20 days. Media containing serum was added to the top of the matrigel and changed every three days. Initial largest 15 single cells spheres were chosen from each group and traced till end point. Sphere sizes were collected every 3 days till day 15 and at end point day 20. Lower panel; 10x image representation at day 12 to show clear sphere structures from each group. B) Left panel: average volume of the 15 spheres plotted for each time point. Right panel; bird's eye view of the wells at the end point. C) An HK2 sphere at 20x and an Arrb2ex3-14 sphere at 10x magnification by day 12. D) Prestoblue

proliferation assay for control and Arrb2ex3-14 cells over 5 days. Arrb2ex3-14 cells proliferation was measured relative to control cells. Data shown are mean ± SD for three trials, *$P < 0.05$, **$P < 0.001$, ***$P < 0.0001$.

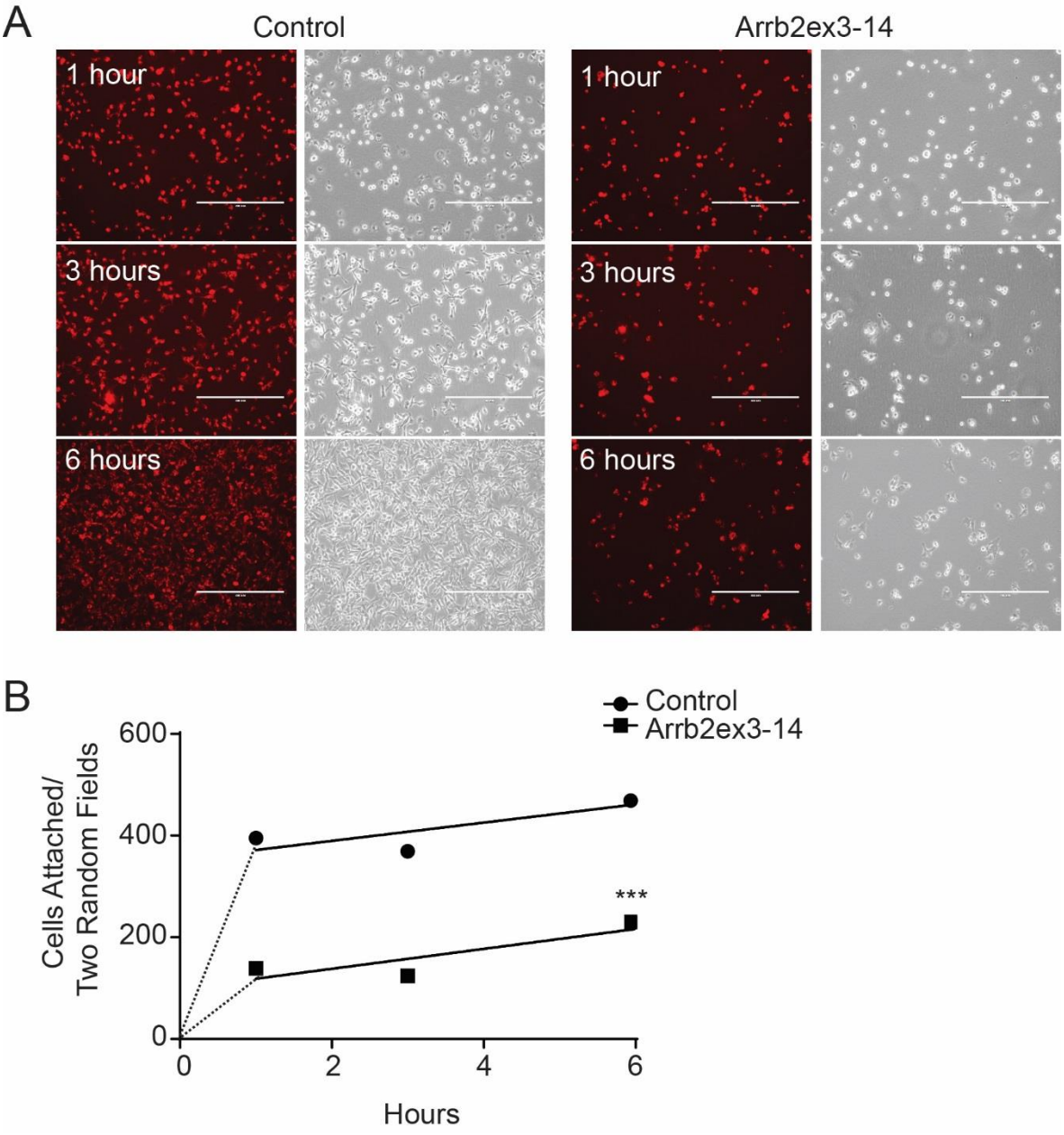

Figure 2-11. βArrestin 2 knockout reduces cell attachment. A) SN12C cells (control and *Arrb2* KO) were labeled with DilC12 and $2.5x10^5$ cells were seeded in 6-well plates. Cells were observed under RFP (red panels) or normal light (phase contrast panels) at 1, 3, and 6 hours after seeding). B) Attached cell number was counted for two random 10x fields per cell line at each time point (right panel graph). ****P*< 0.0001.

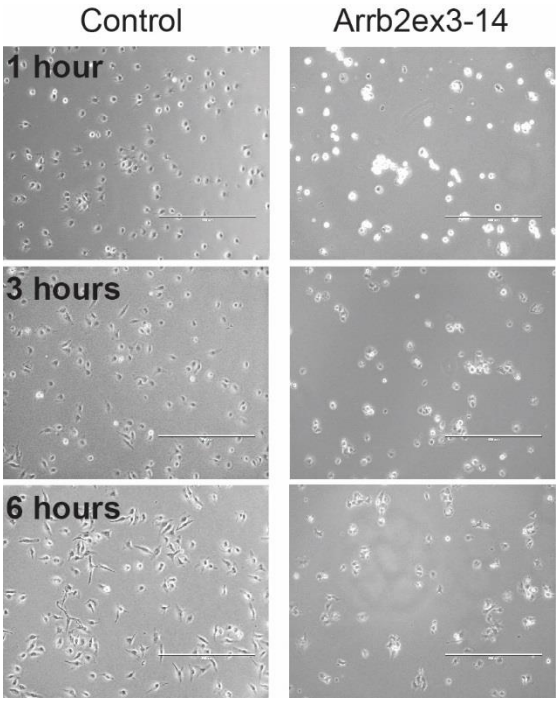

Figure 2-12. βArrestin 2 knockout reduces cell attachment on Fibronectin. 2.5 x 10^5 control and Arrb2ex3-14 cells were seeded on fibronectin coated 6-well plates, and cell attachment was observed under a phase contrast microscope. Images represent cells at 1, 3, and 6 hours after seeding. Cells with white halos are semi attached or floating cells.

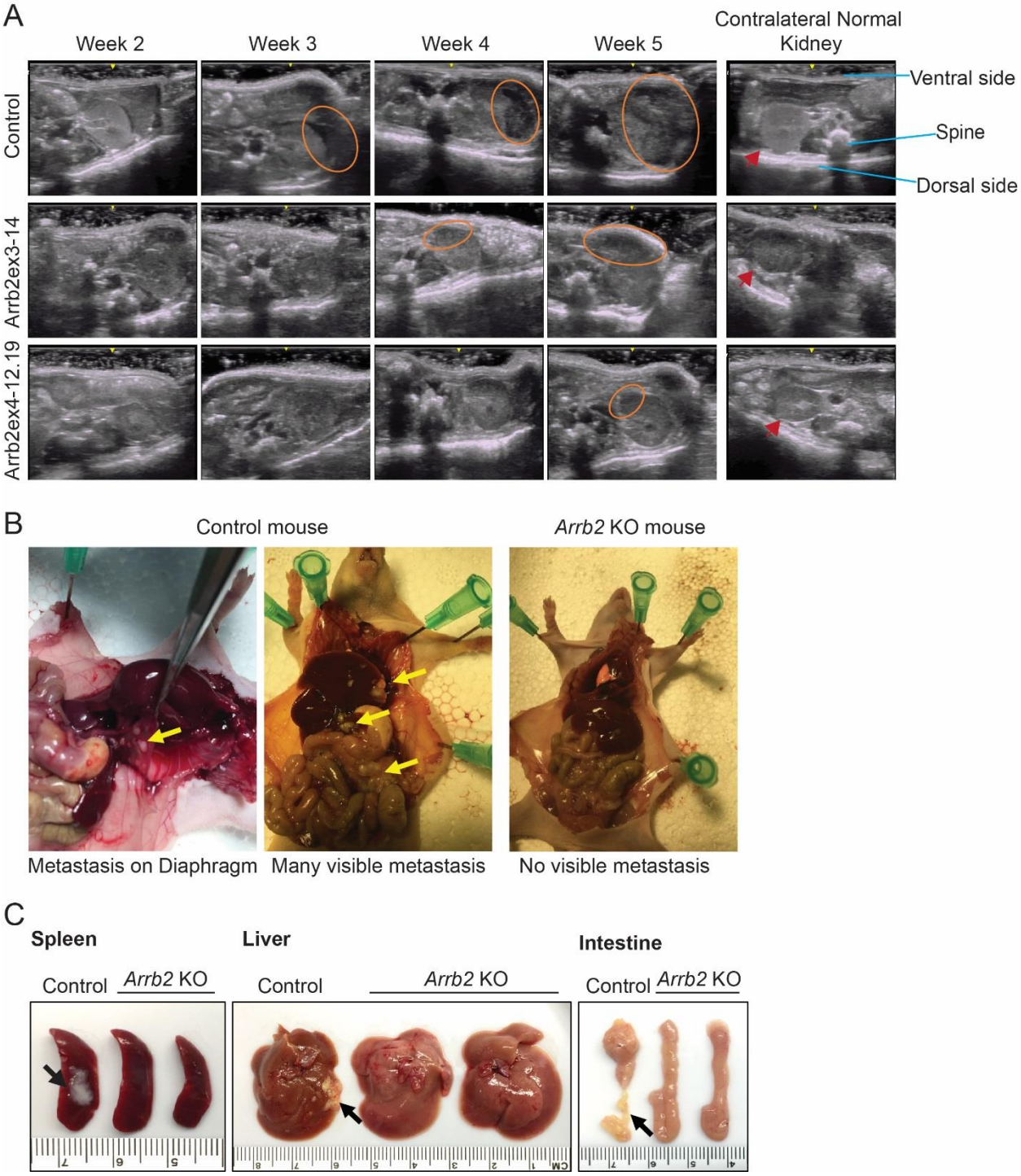

Figure 2-13. Tracking tumor size and metastasis. A) Ultrasound imaging of mice kidneys from week 2 till week 5 after tumor implantation. Tumor growth images here are shown for the same mouse tracked over time, and are representative of the rest of the mice for each group. Orange circles show where the tumor is seen. Circle size indicate observed potential tumor area. An image example of the normal contralateral kidney is also shown for the

same mouse. B) A representation of the overall visible metastasis status at experiment termination for control compared to *Arrb2* KO mice. C) Visible metastasis on spleen, liver, and intestine in control mice (one spleen and one liver are a representation of 5 out of 7 mice with visible metastasis, and one intestine part is a representation of 7 out of 7 mice with visible metastasis) vs. *Arrb2* KO.

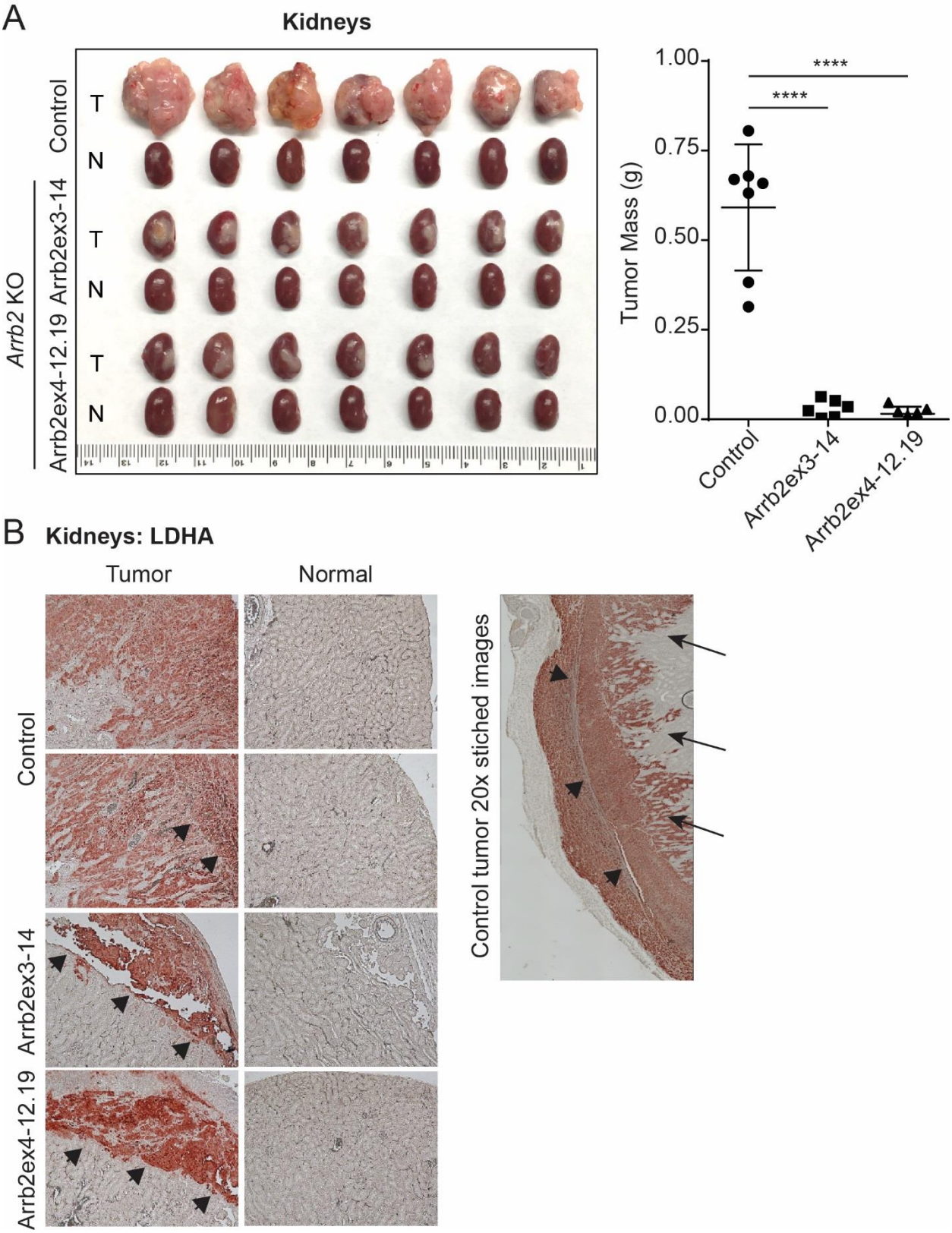

Figure 2-14. βArrestin 2 knockout tumors fail to grow *in vivo*. A) Left panel: Subrenal tumor growth. 1 x 10^6 control, Arrb2ex3-14, or Arrb2ex4-12.19 cells were

embedded in collagen and implanted under the renal capsule of athymic nude mice (n=7 per cell line) and allowed to grow for 5 weeks. (N), contralateral normal kidney. (T), kidney with tumor. Right panel: tumor mass measured by subtracting N kidney mass from T kidney mass. B) Representative anti-human LDHA staining of kidney tissue. Tissues were sectioned at 7 μm thickness. Right panel: stitched image for one representative control tumor sections at 20x magnification. Arrow heads point to the edge of the cortex under the capsule. Arrows point to invading tumor cells into the cortex.

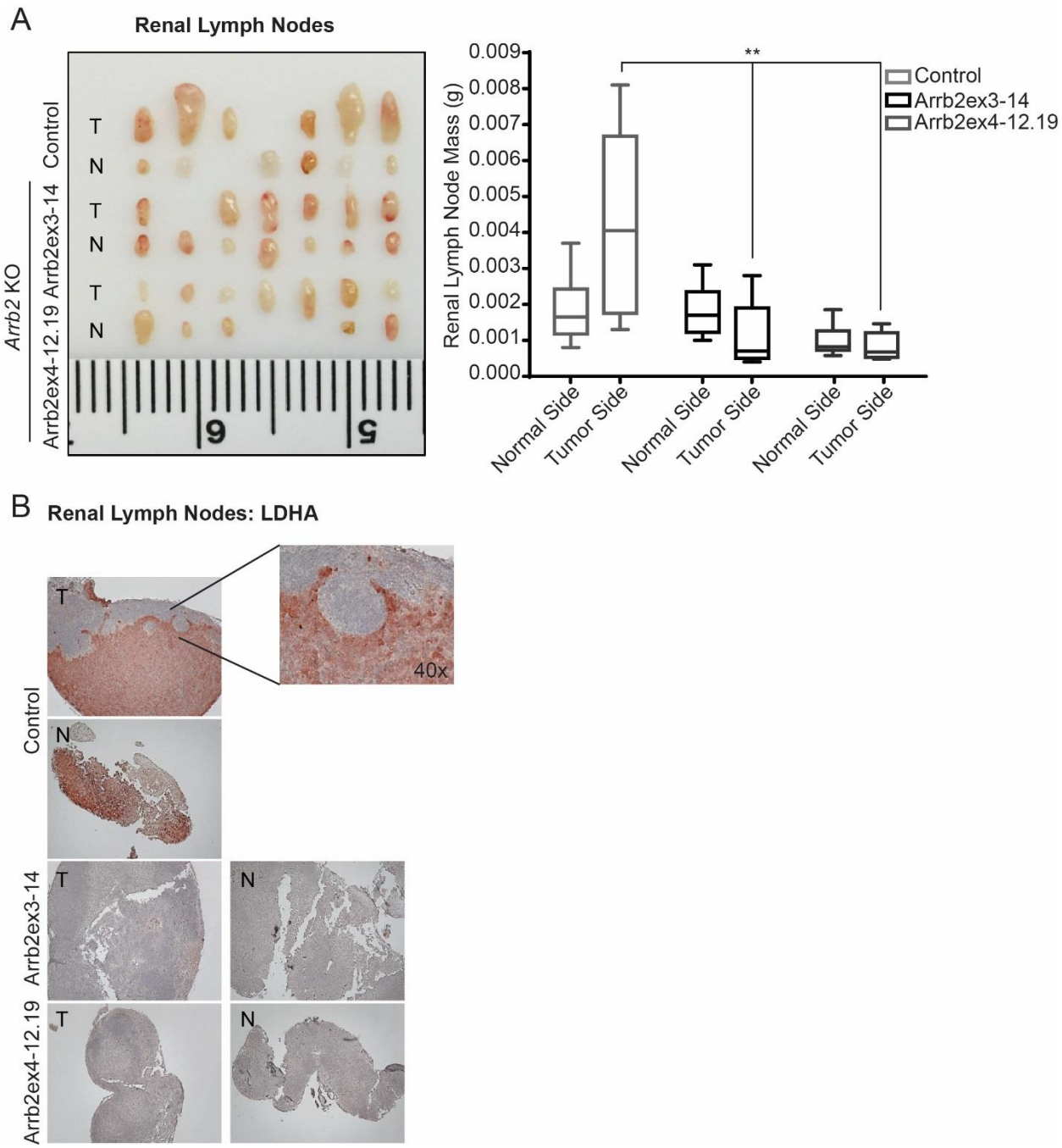

Figure 2-15. βArrestin 2 knockout tumors fail to metastasize to renal lymph nodes. A) Left panel: renal lymph nodes, tumor side (T) and contralateral normal side (N) nodes imaged at experiment endpoint. Right panel: renal lymph nodes of tumor side and normal side weighed (g) for each of the groups. ***P*< 0.001.B) Representative anti-human LDHA staining of the RLNs.

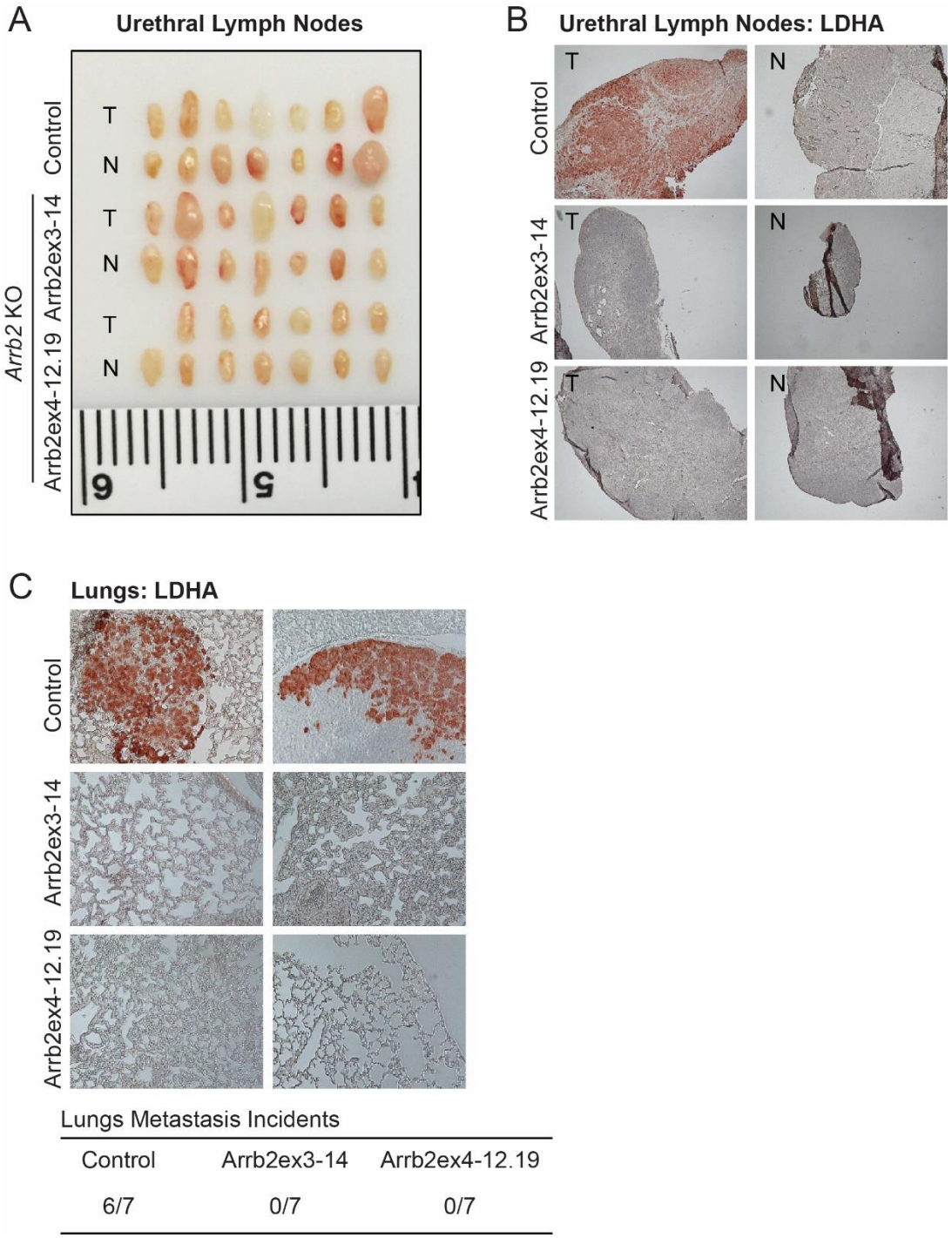

Figure 2-16. βArrestin 2 knockout tumors fail to metastasize to urethral lymph nodes and lungs. A) Adjacent ULNs, tumor side (T) and contralateral normal side (N) nodes imaged at experiment endpoint. B) 10x images representative of anti-human LDHA staining of the ULNs were either from tumor side (T), or normal contralateral side (N). C) Images representing lung tissue sections. Metastasis detected with anti-human LDHA staining. Metastasis was found in 6 out of 7 control mice, and none was detected in the *Arrb2* KO mice.

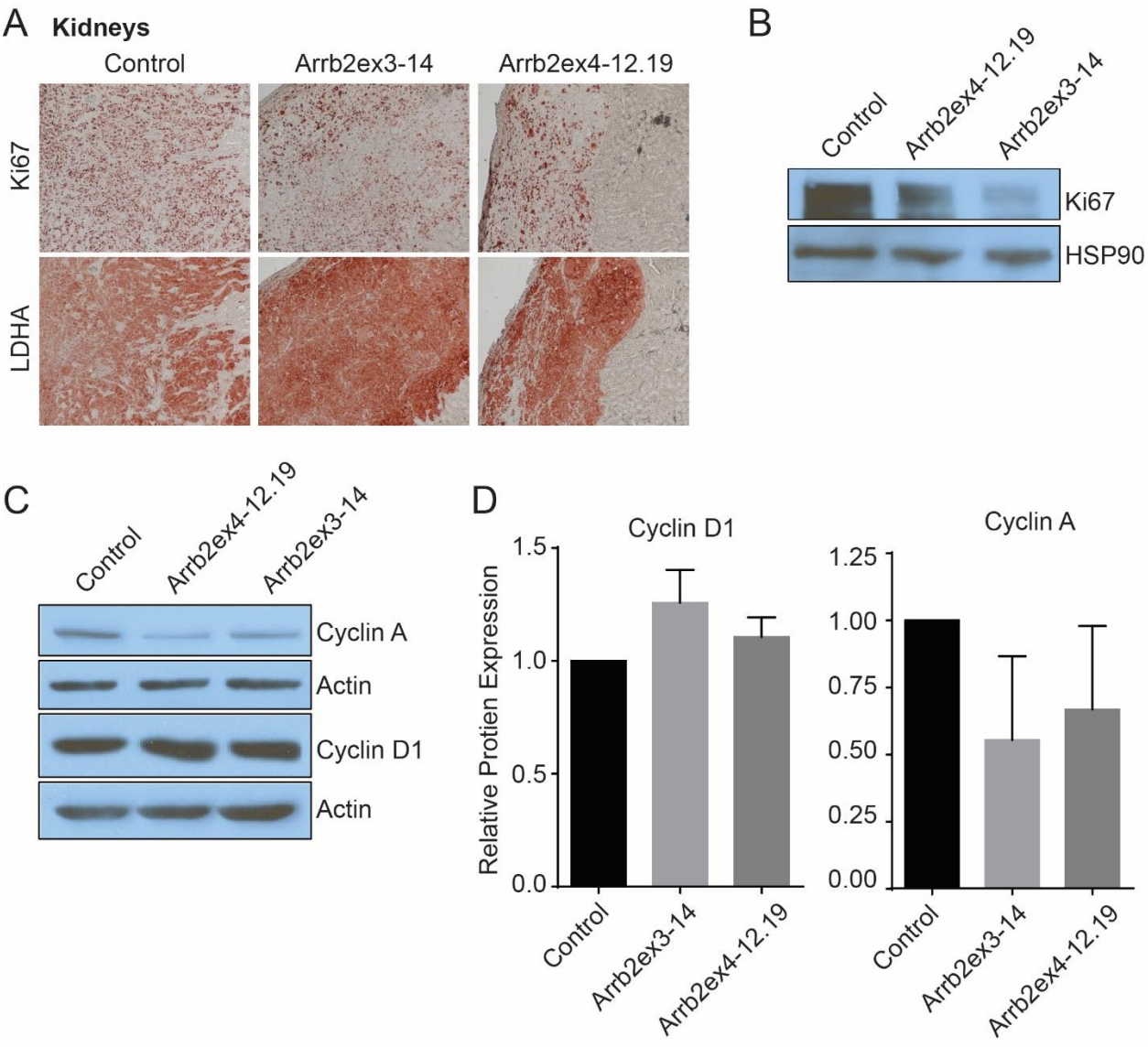

Figure 2-17. Reduced proliferation capacities in knockout cells A) Images representing proliferation marker anti-human Ki67 upper panel and consecutive anti-human LDHA staining of the same tumor area as a reference. B) Protein expression levels of Ki67 in Arrb2ex3-14, Arrb2ex4-12.19, and control. C) Cyclin A and Cyclin D1 protein expression in the cell lines. D) Quantification of Cyclin A and Cyclin D1 protein levels.

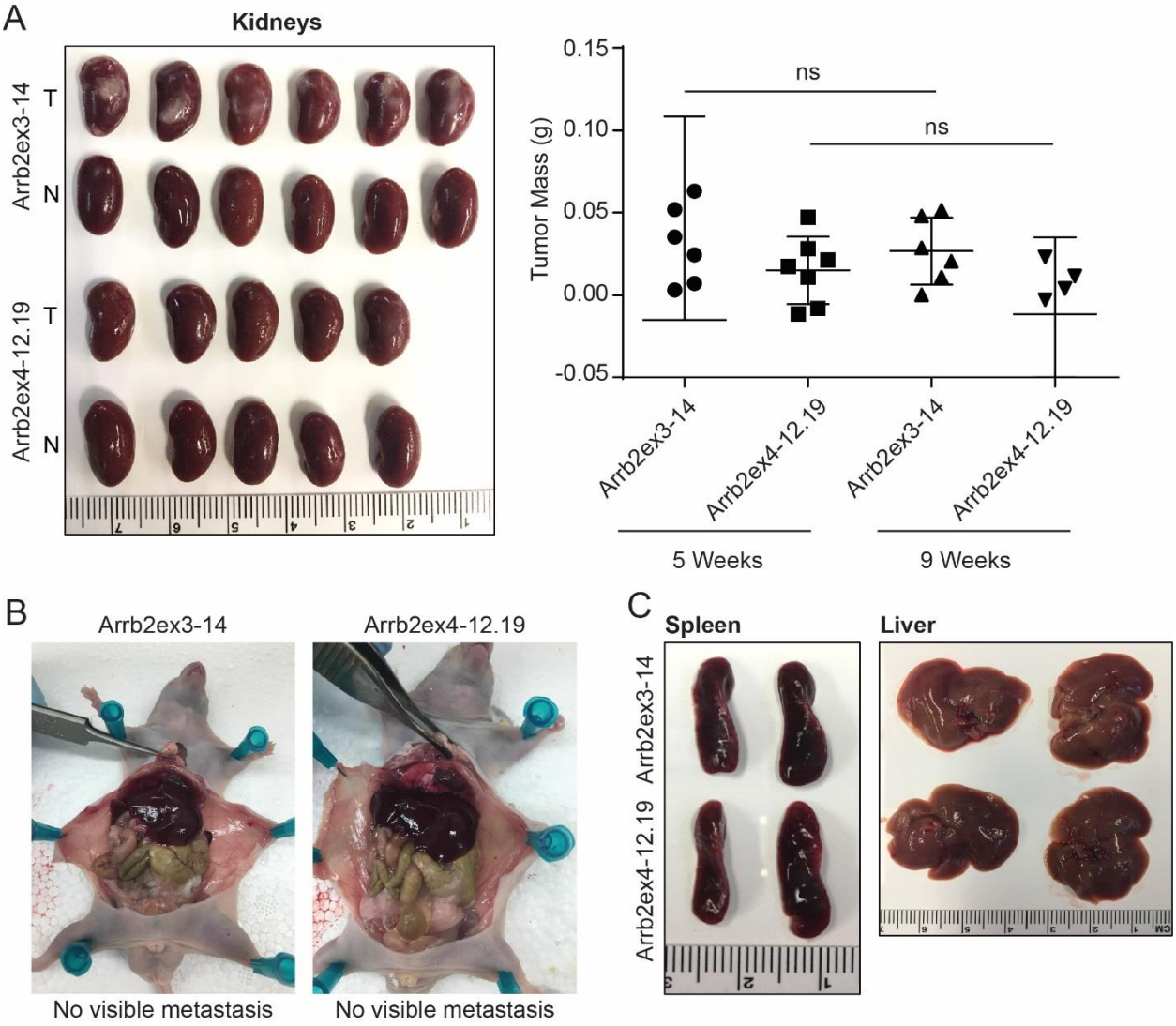

Figure 2-18. *Arrb2* knockout tumor growth over 9 weeks. A) Left panel: Subrenal tumor growth. 1 x 10^6 Arrb2ex3-14, or Arrb2ex4-12.19 cells were embedded in collagen and implanted under the renal capsule of athymic nude mice (n=6 or n=5 respectively) and allowed to grow for 9 weeks. (N), contralateral normal kidney. (T), kidney with tumor. Right panel: tumor mass measured by subtracting N kidney mass from T kidney mass. Outlier negative values were removed from the plot. B) A representation of the overall visible metastasis status at experiment termination for *Arrb2* KO mice. C) No visible metastasis on spleen and liver in *Arrb2* KO mice (two spleens and two livers are a representation of the rest of the mice).

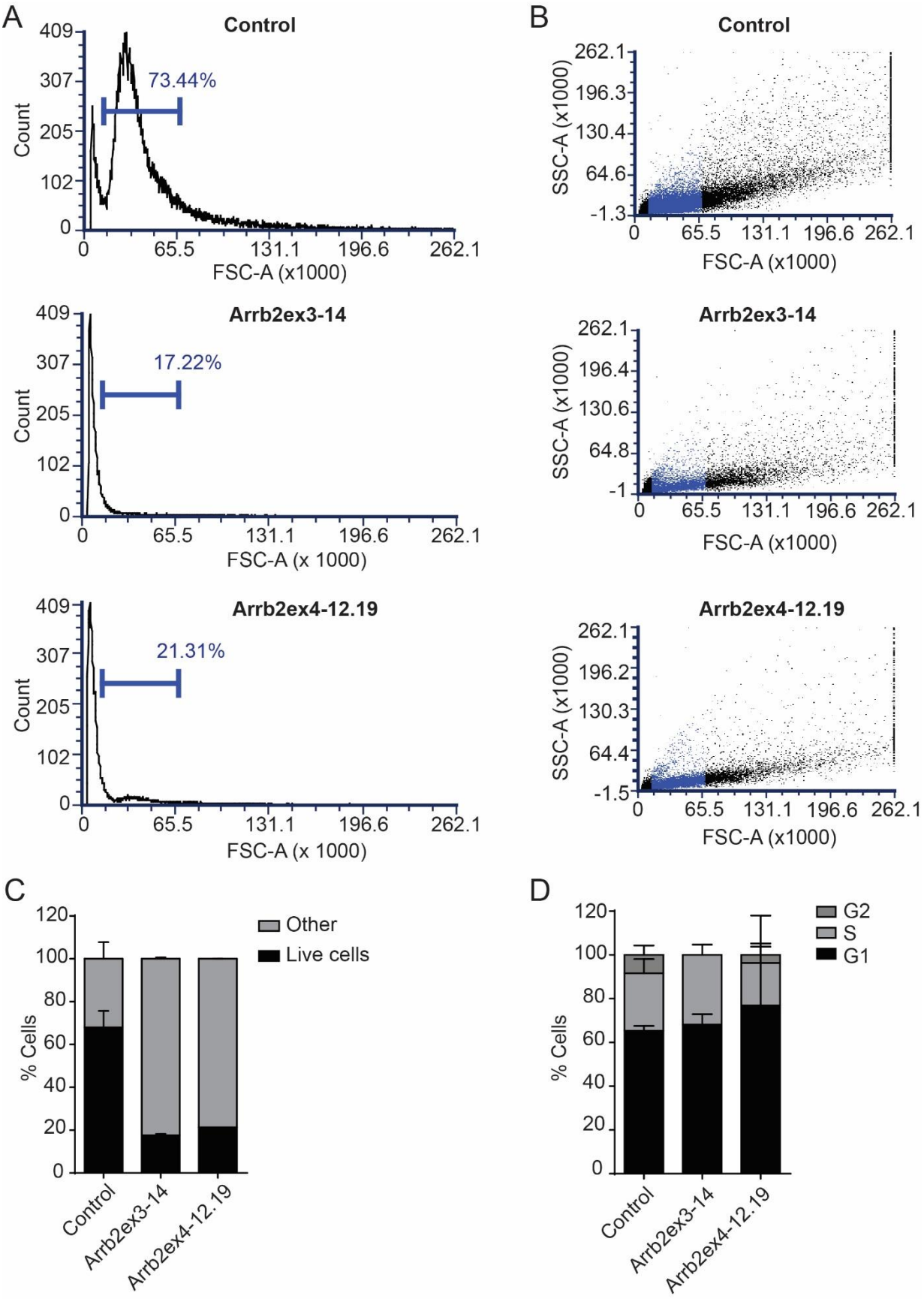
A
Control
409
307
205
102
0
Count
73.44%
0
65.5
131.1
196.6
262.1
FSC-A (x1000)
Arrb2ex3-14
17.22%
FSC-A (x 1000)
Arrb2ex4-12.19
21.31%
B
Control
262.1
196.3
130.4
64.6
-1.3
SSC-A (x1000)
FSC-A (x1000)
Arrb2ex3-14
196.4
130.6
64.8
-1
Arrb2ex4-12.19
196.2
130.3
64.4
-1.5
C
120
100
80
60
40
20
% Cells
Other
Live cells
Control
Arrb2ex3-14
Arrb2ex4-12.19
D
G2
S
G1

Figure 2-19. Cell cycle analysis. 5 x 10^4 cells were counted in the LSRII flow machine and analyzed for cell size and cell cycle status. A) FSC plot for each of the cell lines. Blue bar represents gating for live cells. Percentage of cells counted in the gate is indicated above the bar. B) FSC and SSC dot plots. Blue area represents cells gated in A. C) Bar plot representation of the distribution of live cells compared to other cells in A. D) Distribution of live gated cells in G1, S, and G2.

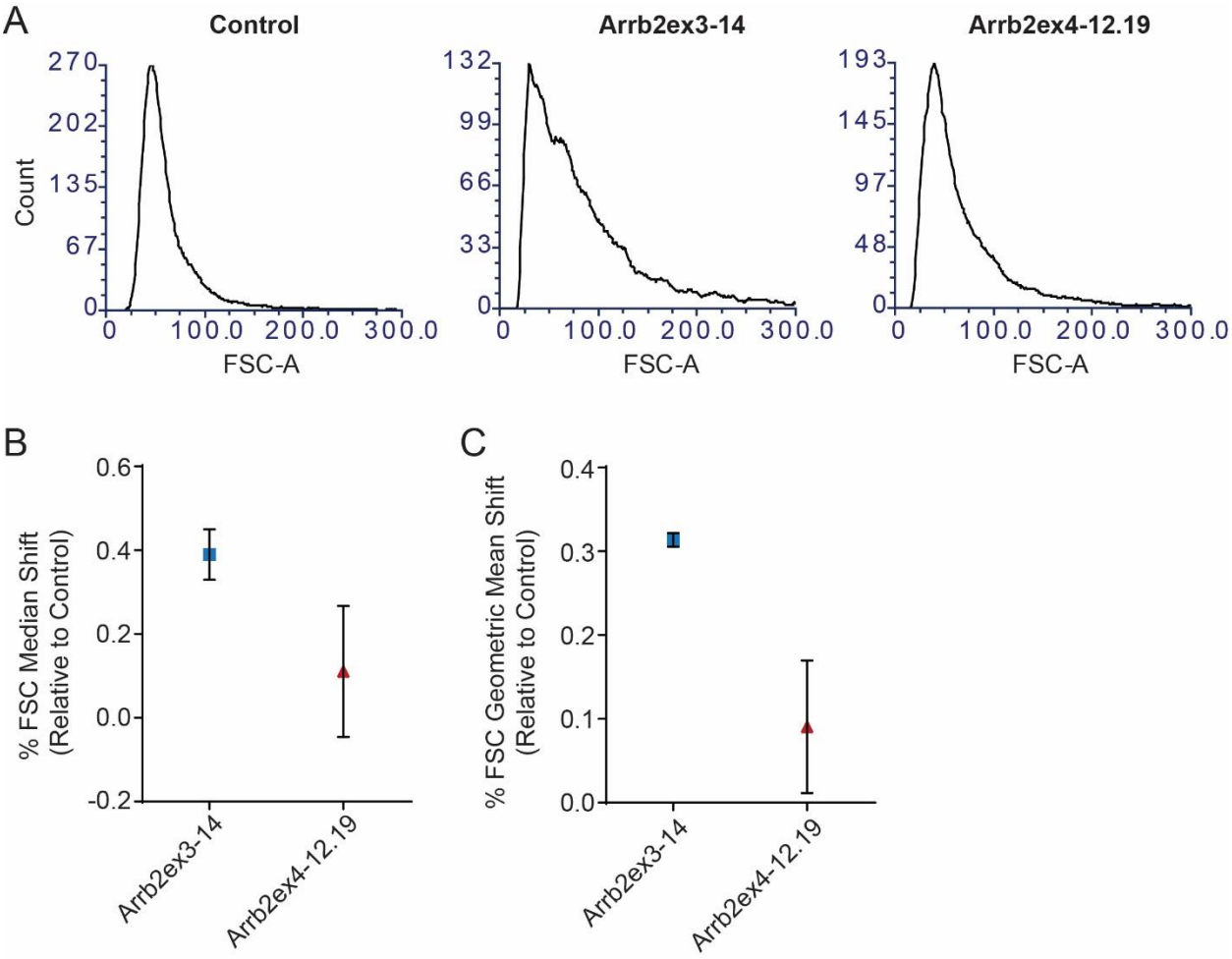

Figure 2-20. Cell size changes of *Arrb2* KO cells compared to control. A) Data shows histograms of FSC of 1 x 10^4 cells counted on the LSR II flow machine before gating for live cells. Histograms are representative of three trials. B and C) Representation of the % shift or difference in the FSC Median or geometric mean, respectively, relative to control cells. Error bars indicate standard deviation.

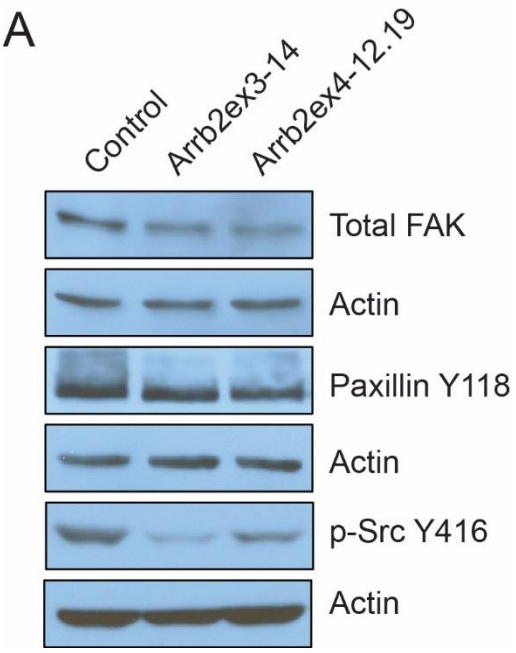

Figure 2-21. Reduced activity of focal adhesion regulatory proteins. A) Measurement of protein levels for total FAK, Paxillin, and p-Src in the cell lines. B) Confocal images (40x) staining for Paxillin (green), phalloidin (red), and DAPI (blue). Arrow heads point on example focal adhesion structures.

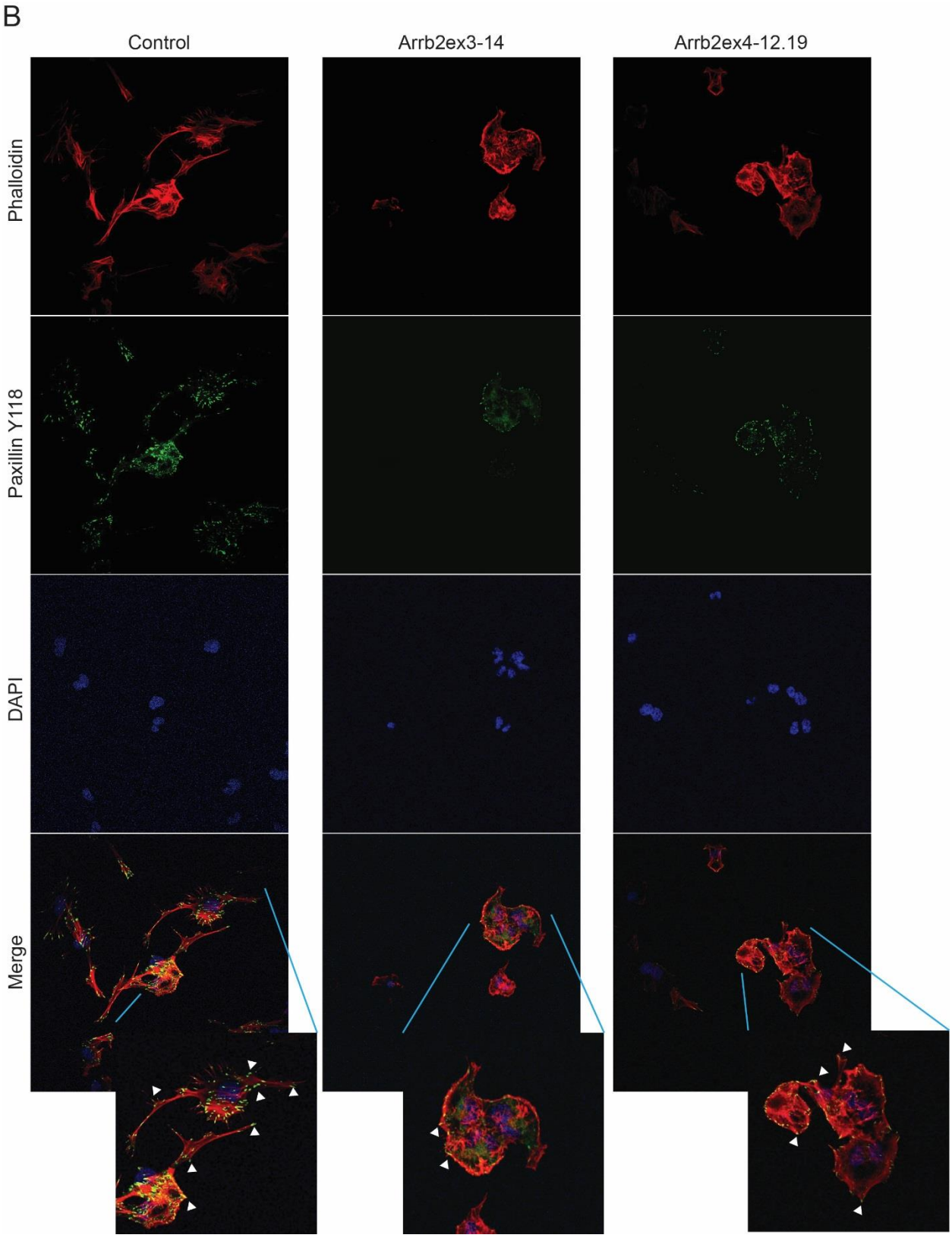

Figure 2-21. Continued

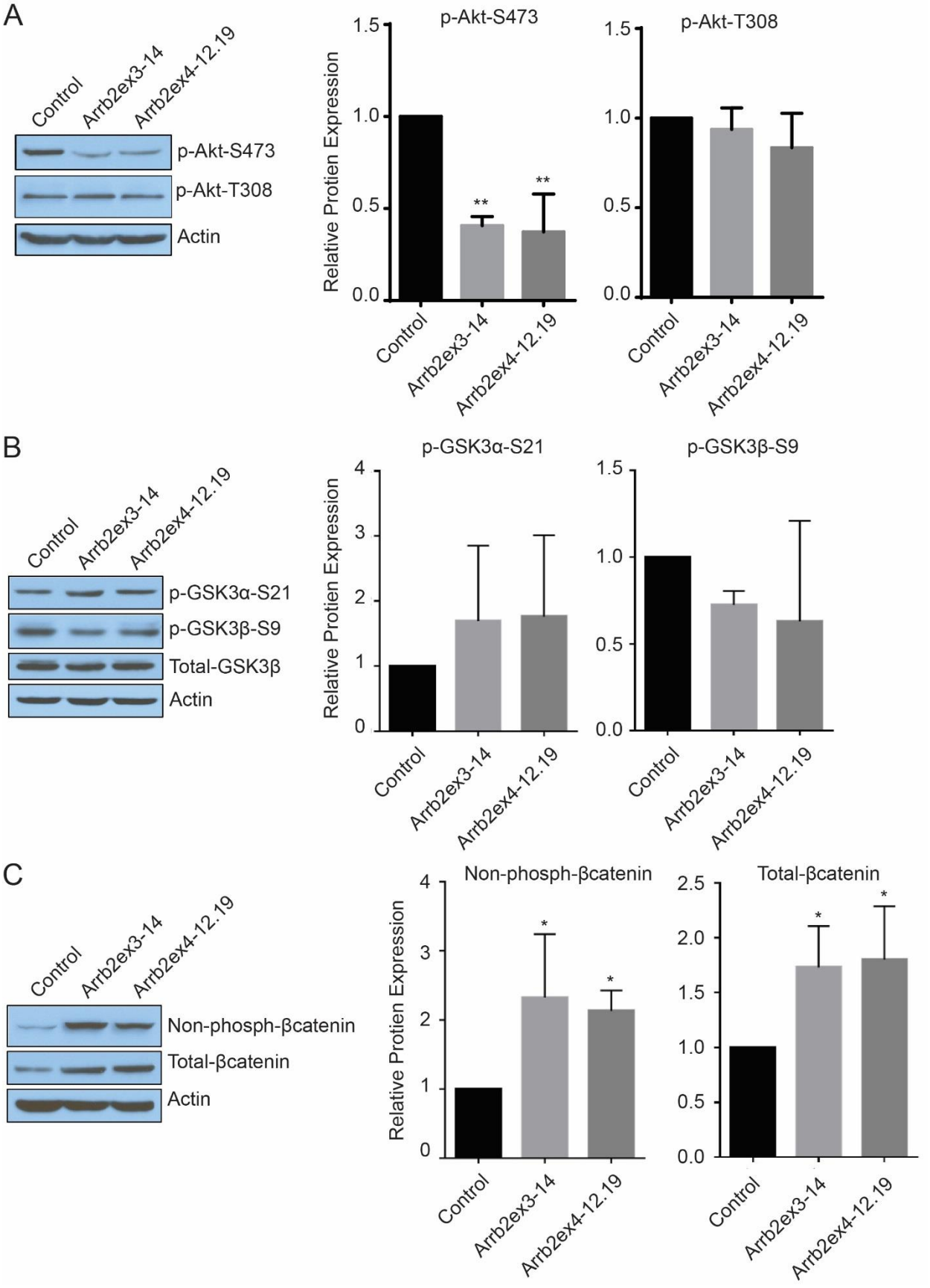
A
Control
Arrb2ex3-14
Arrb2ex4-12.19
p-Akt-S473
p-Akt-T308
Actin
p-Akt-S473
p-Akt-T308
Relative Protien Expression
1.5
1.0
0.5
0.0
**
**
Control
Arrb2ex3-14
Arrb2ex4-12.19
B
Control
Arrb2ex3-14
Arrb2ex4-12.19
p-GSK3α-S21
p-GSK3β-S9
Total-GSK3β
Actin
p-GSK3α-S21
p-GSK3β-S9
Relative Protien Expression
4
3
2
1
0
1.5
1.0
0.5
0.0
Control
Arrb2ex3-14
Arrb2ex4-12.19
C
Control
Arrb2ex3-14
Arrb2ex4-12.19
Non-phosph-βcatenin
Total-βcatenin
Actin
Non-phosph-βcatenin
Total-βcatenin
Relative Protien Expression
4
3
2
1
0
2.5
2.0
1.5
1.0
0.5
0.0
*
*
*
*
Control
Arrb2ex3-14
Arrb2ex4-12.19

Figure 2-22. Examining Akt activity and downstream effectors in *Arrb2* KO cells. A) p-Akt S473 and p-Akt T308 levels and quantification. B) p-GSK3 (α and β) and total GSK3β protein levels and quantifications. C) Active non-phosphorylated βcatenin and total βcatenin levels and quantifications. Data shown are mean ± SD for at least three trials,*$P < 0.05$, **$P < 0.001$, ***$P < 0.0001$.

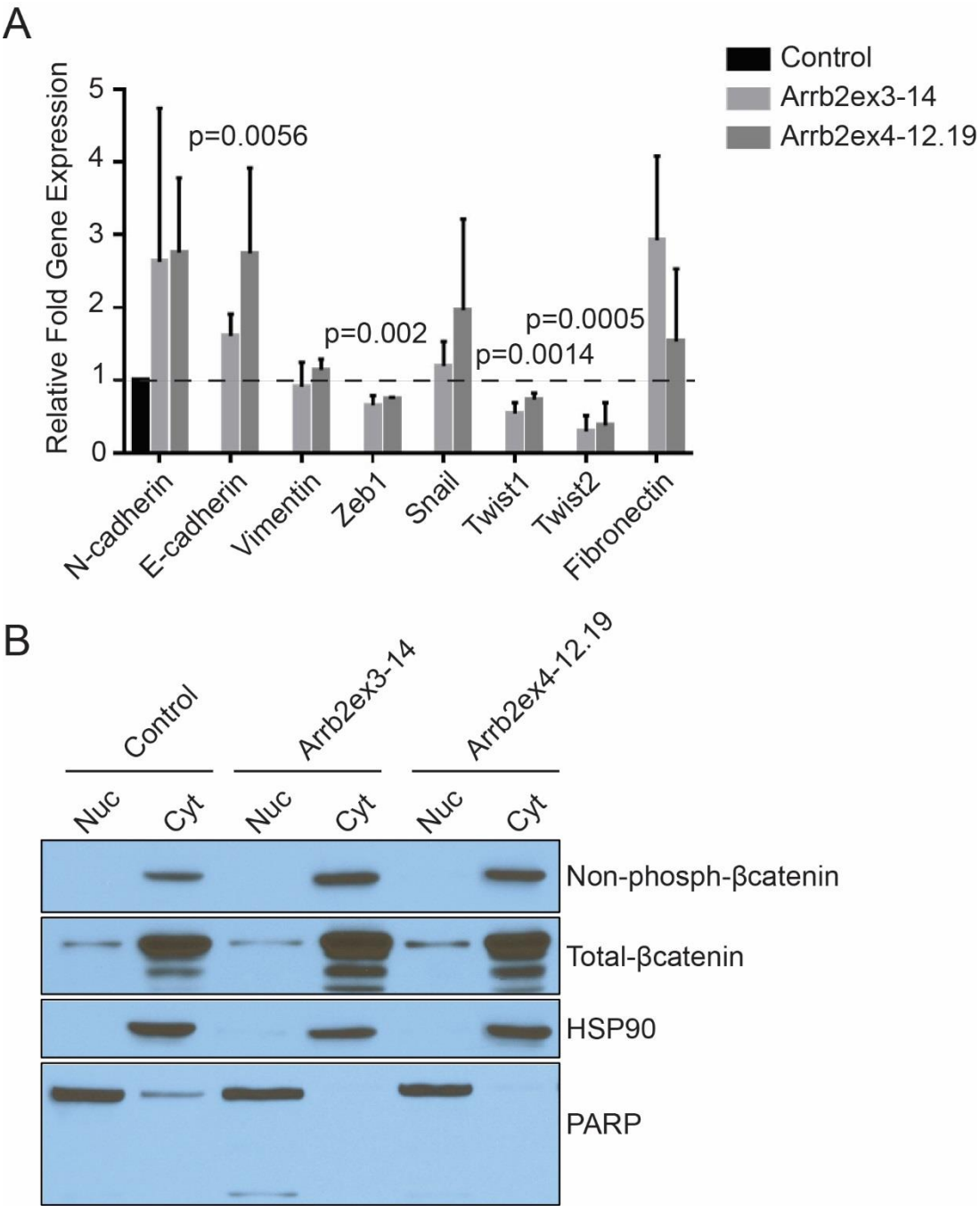

Figure 2-23. Main EMT genes expression levels and βcatenin localization. A) Relative expressions of hallmark EMT genes mRNA in control and *Arrb2* KO cells were measured by real-time PCR. Gene expression is represented as a fold change in mRNA levels relative to control cells (black bar). Significant *P* values are indicated above their respected bars. B) Cytosolic versus nuclear fractions were isolated for each of the cell line and blotted for total and active levels of βcatenin. HSP90 is a marker for the cytosolic fraction, and PARP represents nuclear fraction. C) Confocal imaging (40x) showing localization of

active βcatenin (green), phalloidin (red), and DAPI (blue). Arrows point to example βcatenin localizing at the plasma membrane.

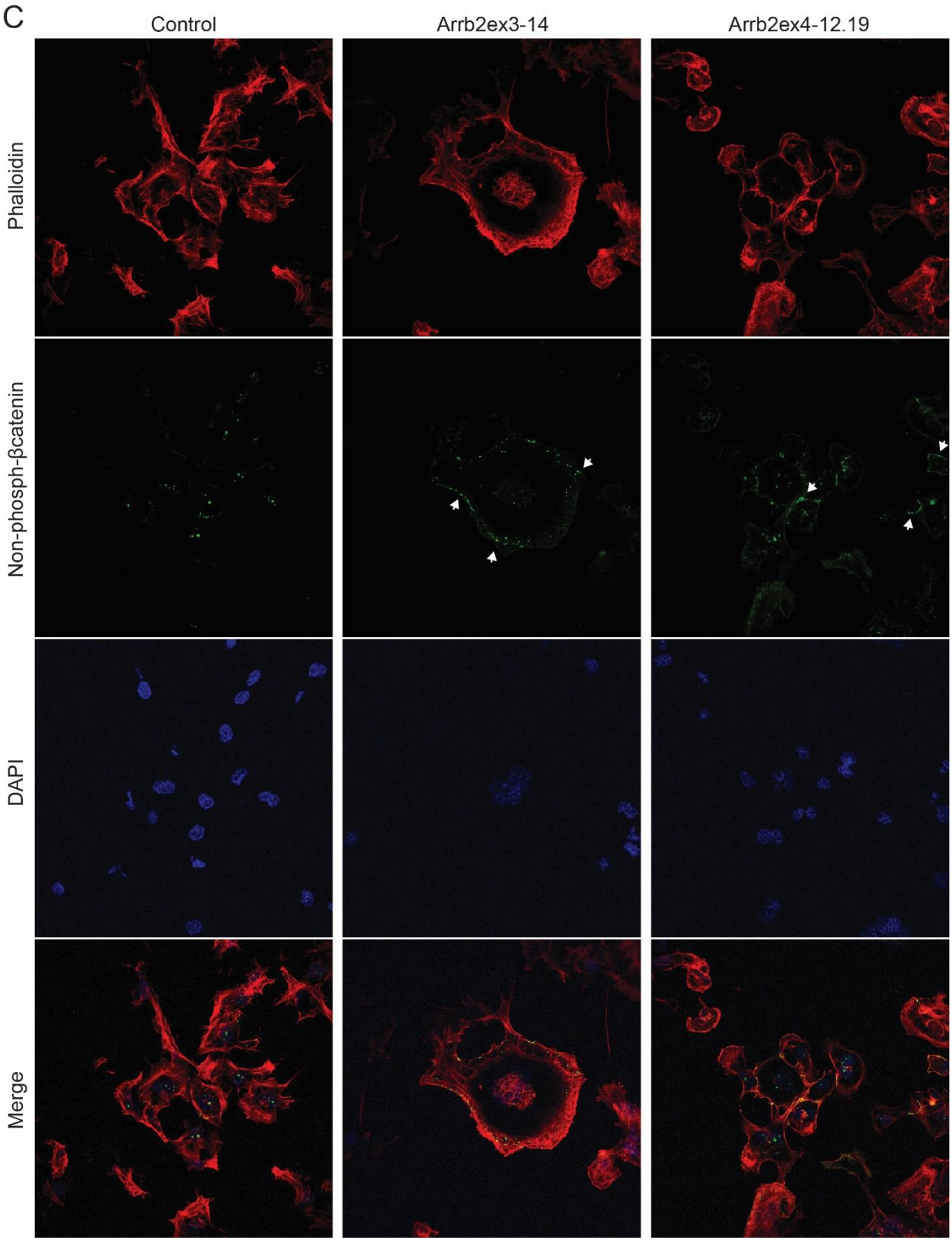

Figure 2-23. Continued

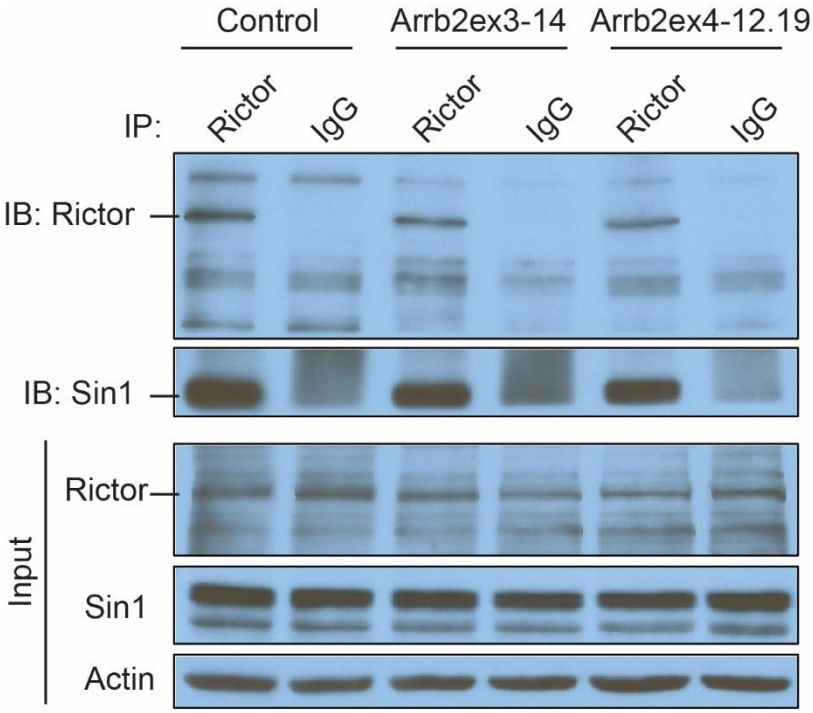

Figure 2-24. No increased Sin1 binding to Rictor in the mTORC2 with *Arrb2* KO. Cells were lysed and immunoprecipitated with anti-Rictor or IgG control isotype. Rictor or Sin1 levels in the protein complex were detected by immunoblotting blotting. An input lysate was immunoblotted as well as a loading control.

CHAPTER 3
DISCUSSION

The mechanisms underlying RCC progression are poorly understood. Ever since 2001, when HIF2 was identified as a major driver for most ccRCC cases, *Vhl* mutations were characterized and as a result, tyrosine receptor kinases targeted therapies such as VEGFR and PDGFR, became popular forms of therapy along with other conventional therapies (172, 173). However, RCC is extremely difficult to describe as a single disease type. RCC is histologically divided between a clear cell RCC or a non-clear cell RCC subtype. Clear cell RCC is majority subtype, comprising >75% of Kidney cancers. On the other hand, non-clear cell RCC is further subdivided into papillary RCC (~15%), chromophobe RCC (3-5%), collecting duct RCC, and some other rare subtypes make up for the rest. Distinguishing the RCC subtype provides a basis for a more effective treatment regimen for patients. However, genetic heterogeneity is very common in RCC even within the same subtype. This makes it difficult to treat patients with advanced or metastatic RCC (146, 173). Nonetheless, advances in biomarker discoveries and personalized genomic sequencing for RCC patients have shown promise for developing more efficacious treatment regimens.

βArrestins have been identified as important mediators of pathophysiological pathways leading to tumor initiation and progression. In this study we note that βArrestin 2 protein is clinically relevant in RCC and is a potential prognostic biomarker. In a number of large scale clinical datasets, such as the TCGA and others of various RCC subtypes, we observed significant upregulation of *Arrb2* but not *Arrb1* mRNA levels compared to normal kidney tissue. Further, *Arrb2* upregulation correlated significantly with the increased stage of the disease in the ccRCC TCGA dataset, was observed to

be associated with the increased metastatic potential in model cell lines used in this study.

The ACHN cell line was recently characterized to better fit the papillary RCC subtype as it was previously known as a possible metastatic ccRCC cell line (174). SN12C is a primary RCC cell line but is of an uncharacterized subtype. Both ACHN and SN12C cells are nccRCC and have a wildtype *Vhl* gene, yet they are shown to be more proliferative, invasive and metastatic, compared to 786O and CAKI-1 which are both ccRCCs. 786O but not CAKI-1 cells have *Vhl* mutations. This further confirms the genomic and mechanistic differences in RCC progression, regardless of histological characterization.

Recently, the importance of βArrestins involvement and regulation of the metastatic cascade, which is defined as the invasive migration of a cancer cell from the primary tumor site and colonizing to a secondary site, is becoming more evident. Here we demonstrate that transient and stable knockdown, as well as knockout of βArrestin 2 activity, greatly hinders SN12C and ACHN cells migration, invasion and metastasis both *in vitro* and *in vivo.* Through characterizing cell morphology, a key indicator in determining the capability for cell motility, we observed the potential invasiveness and highly motility of RCC tumor cells. Typically, highly invasive and motile cells tend to adapt polarized cell morphologies that enable them to invade and migrate through extracellular matrix material and adjacent tissue. Migratory and invasive cells create lamellipodia and invadopodia at its leading edge as it moves along and through extra cellular matrix (163, 175, 176). Many molecular complexes are involved in this multistep and highly regulated cytoskeletal rearrangement process. Here, we observed a

mesenchymal to epithelial morphological switch for the SN12C cell after *Arrb2* KO. KO cells lost their cytoplasmic extensions and focal adhesion formation, and were no longer able to invade through the extracellular matrix, such as matrigel *in vitro*. KO cells also closely resembled epithelial HK2 cell spheres though still larger in size. Key epithelial marker, E-cadherin, significantly increased in gene expression, while mesenchymal driver genes *Twist1*, *Twist2*, and *Zeb1* decreased. Importantly, knockout cells were unable to invade far or at all into the kidney cortex compared to control cells. We believe that the reduced capacities of SN12C *Arrb2* KO cells to invade through kidney tissue had prevented potential metastasis to near or distant organs.

The molecular basis for βArrestins induced EMT and cell invasiveness is diverse and has been observed in several cancer cell types. In ovarian cancer cells for example, EMT results from the scaffolding of βArrestins to endothelin-A receptor (ET_AR) after stimulation by endothelin-1 (ET-1) ligand (177, 178). In addition, downstream EGFR transactivation via the βArrestin-cSrc interaction stimulates Akt activation, and thus increases cell invasiveness independent of MMP9 activity in an ET-1 dose-dependent manner. Alternatively, βArrestin-mediated stabilization of β-catenin is observed to be critical for increased transcriptional activity of genes promoting EMT and thus increase cell invasiveness and metastasis. Here, βArrestin 1 plays a protective role for β-catenin by reducing its degradation through direct binding to intracellular Axin after ET_AR stimulation. This allows tyrosine phosphorylation of β-catenin and increased nuclear interaction with TCF-4 which potentiates prometastasis gene expression (177, 178). Our results suggests, an alternative role for βArrestin 2 where it can promote

increased activity and stability of cytosolic β-catenin, which ultimately leads to the stability of E-cadherin complex and contributes to reduced cell proliferation.

Interestingly, after *Arrb2* KO, we observe a significant delay in cell proliferation further indicating βArrestin 2's role in cancer cell progression. This was attributed to *Arrb2* KO showing a ~2-fold decrease in the rate of proliferation compared to control SN12C cells. In addition, we observe a significant reduction in subrenal *Arrb2* KO tumor size and growth rate even after an extended incubation time, thus further implicating its role in disease progression. It was originally proposed that the role of βArrestins in cell proliferation was through their involvement in regulating the MAPKs and PI3K-Akt pathways. Later, it was shown that functional roles of βArrestins expanded to be involved in pathways controlling cell cycle progression and replication.

In this study we showed *Arrb2* KO had a negative impact on cell proliferation and cell cycle progression. Through monitoring Ki67, a proliferation marker that strictly stains cells only in the active cell cycle state. Cyclin A which is responsible for cell cycle transition mainly during the G2/M checkpoints, the final stage before cell division, was downregulated in the absence of βArrestin 2. In both IHC and western blot analysis, Ki67 levels suggest that βArrestin 2 is a facilitator of tumor cell growth. In addition, we observed no distinct changes in p-Akt-T308 levels, but p-Akt-S473 levels were significantly reduced in KO cells. Therefore the data suggested that, cell proliferation and cytoskeletal rearrangement could be, in part, under the regulation of mTORC2, an upstream complex that is responsible for Akt-S473 phosphorylation and an important complex in Akt-regulated pathways.

Unlike the mTORC1 complex, mTORC2 is insensitive to rapamycin. mTORC2 also contains Sin1 and Rictor subunits that are unique to the complex. Further, there are several ACG family kinases are downstream of and are activated by mTORC2, such as Akt (PKA), SGK, PKC, and PKG, indicating its role in modulating metabolism, cell survival, cell growth, and other downstream oncogenic pathways (170, 179-182). While numerous studies have unraveled the regulation of mTORC1 activity and its downstream effectors, only recently have advances been made to better understand regulatory pathways and functions of mTORC2 activation or inhibition. Recently, Lui *et al*. proposed a PIP_3-dependent activation directly upstream of mTORC2. PIP_3, but not PIP_2, binds to the PH domain of Sin1 protein which then releases Sin1 blockade of mTOR kinase domain (183, 184). In our study, we find that the Sin1-Rictor complex formation was not hindered by *Arrb2* KO, yet p-Akt S473 levels remain depleted. This suggests that during *Arrb2* KO, another molecule stimulating mTORC2 activity is hindered or downregulated. As a result, our data indicate a potential direct or indirect βArrestin 2 regulation of mTORC2 activity. A planar cell polarity protein called Prickle1 has been recently shown by Daulat *et al.* to be a binding partner to Mnk1, and together form a complex specifically with Rictor in the mTORC2 and are necessary for Akt activation (185). The study presents similar cellular structure phenotypes with reduced cell migration, when Prickle1 and Mnk1 activity is depleted, as to our SN12C *Arrb2* KO cells. Sin1 was also a binding partner to purified Prickle1. Previously, DeWire *et al.* demonstrated a physically βArrestin 2-Mnk1 interaction that is important for the protein translation process (186). This leads us to speculate that perhaps in SN12C *Arrb2* KO

cells, Prickle1 and/ or Mnk1 activity is modulated. However, the details of this mechanisms are unclear at this time and require further investigation.

Later discoveries in this study elucidated that the activity of p-Src was altered after *Arrb2* KO. p-Src levels were greatly reduced in KO cells compared to control cells. A βArrestin-Src interaction has been identified previously and in a NSCLC study, βArrestin 1 facilitates Rb dissociation from E2F and promotion cell cycle through Src activity (77). A STRING (Search Tool for the Retrieval of Interacting Genes/Proteins) database for protein-protein interactions predictions (Figure 3-1) offered us clues that could explain the differential proteins activities and localizations profiles that are implicated in both cell structure and proliferation in our study. The analysis suggests that *Arrb2*, Src (vSrc and cSrc), FAK (*Ptk2*), E-cadherin, Cyclin A (*Ccna1* and *Ccna2*), *Twist1*, *Twist2*, *Zeb1*, and βcatenin, which were all impacted by *Arrb2* KO, are very likely to be all linked together through a βArrestin-Src interaction. This analysis could explain the reason behind two major phenotypic changes. In our system, cell morphology goes hand in hand with cell proliferation. Here the most likely biological process in effect according to STRING is the regulation of cell proliferation. As a control, we also performed a STRING analysis only on the proteins regulating EMT and cytoskeletal rearrangement studied here with *Arrb2* and Src (Figure 3-2). Indeed, a very likely biological process, yet not the most likely one, controlled by this group of proteins is cell-cell adhesion, which correlates with our findings.

If we include some specific mTORC2 molecules such as Rictor, Mnk1 (*Mknk1*) and Prickle1 to our list of proteins, we do not observe any close interactions between Mnk1 or Prickle1 with our cluster initially (Figure 3-3). There is still, a suggested Rictor-

Paxillin interaction. However, if we add a secondary level of interactions (Figure 3-4), we then see a possible, yet distant, Mnk1-Cyclin B interaction, but no Prickle1 connections. Cyclin B is another protein that is highly expressed during the G2 phase of the cell cycle (187, 188).

Therefore, we propose that even though there is a hindered mTORC2 activity in *Arrb2* KO cells, the main mechanism implicated is likely through an upstream βArrestin 2 regulation of Src to downstream FAK, βcatenin, and CDK/Cyclin A. mTORC2 can very well be a mechanism involved in the progression of RCC tumor, yet not necessarily through the same pathway as Src. The fact that we identified a modified mTORC2 activity in the background of βArrestin 2 is very important to the field of understanding the regulation of mTORC2. Future studies will be necessary to further explore this relationship.

It is currently unclear whether a specific stimulus or activation of a receptor is inducing the upregulation of βArrestin2 activity in RCC types. One possibility is that common chromosomal gains in RCC, such as chromosome 17 where *Arrb2* gene is located, is the reason for the increased *Arrb2* mRNA expression in metastatic RCC. Despite this, and through the work we have presented, it is apparent βArrestin 2 plays a significant and important role in RCC tumorigenesis in a variety of subtypes. Nevertheless, current attempts to therapeutically target βArrestins to slow cancer progression has yet to show success due to the proteins ubiquitous expression patterns and difficulty probing critical interaction/ligand binding regions (85, 189). In this study, we show clear evidence that βArrestin 2 was only expressed in RCC and not in normal kidney tissue or cells, and has proven to be a key factor in cancer progression. *Arrb2*

KO induced a mesenchymal to epithelial transformation and greatly reduced tumor growth, metastasis and invasion. Our results, provide evidence suggesting βArrestin 2 as a useful prognostic biomarker and potential therapeutic target in the future to combat RCC.

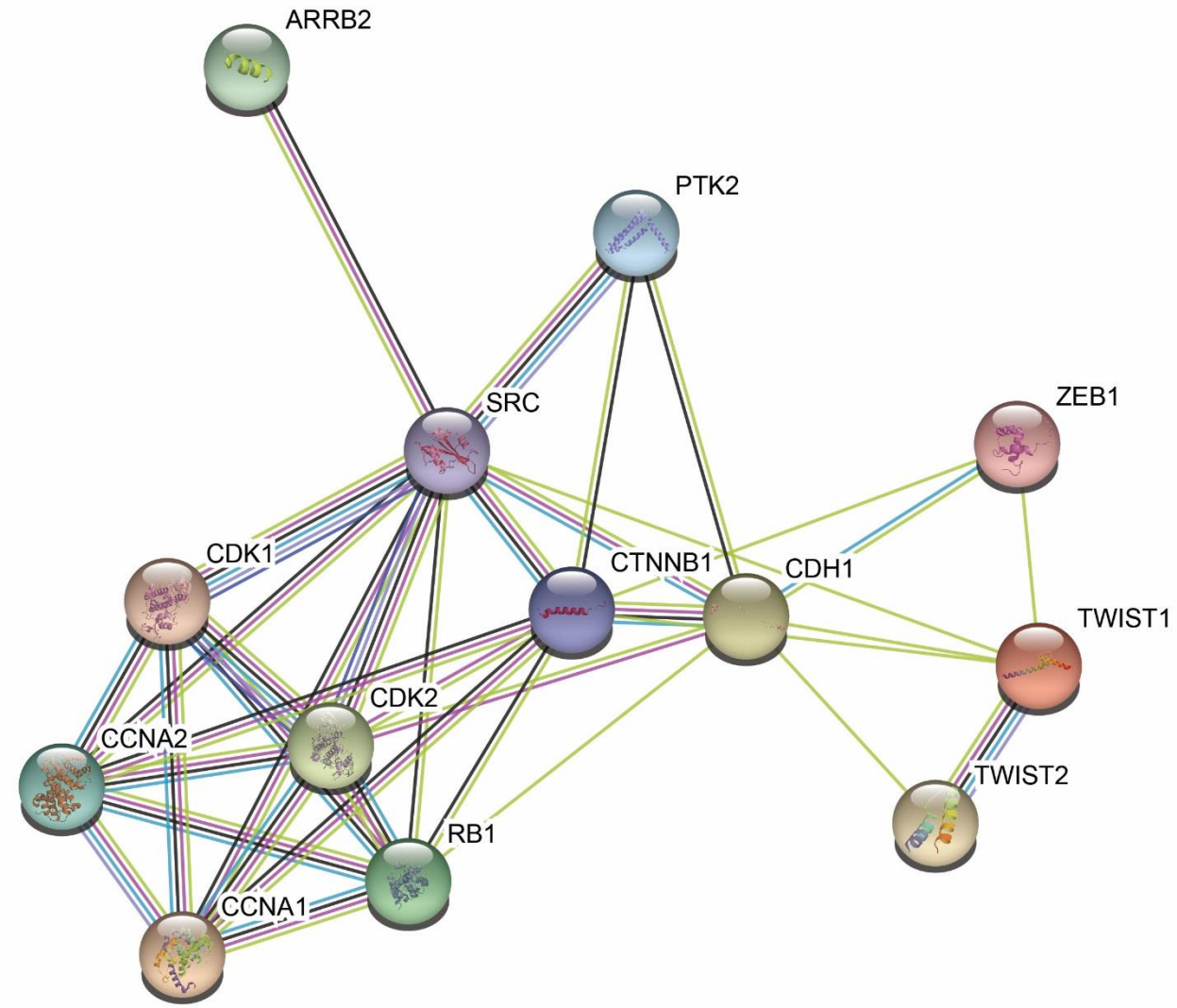

Biological Process (GO)			
pathway ID	*pathway description*	*count in gene set*	*false discovery rate*
GO:0042127	regulation of cell proliferation	10	4.77e-06
GO:0007264	small GTPase mediated signal transduction	8	5.49e-06
GO:0010243	response to organonitrogen compound	8	1.25e-05
GO:0071417	cellular response to organonitrogen compound	7	1.44e-05
GO:0009719	response to endogenous stimulus	9	2.32e-05

Figure 3-1. STRING database predicted protein-protein interactions between βArrestin 2 and the other molecules examined here that have been shown or predicted to be modulated by the *Arrb2* KO. Proteins included are ones examined for both cell morphology and proliferation changes. As shown in the table summary (lower panel), the most likely biological processes these molecules are regulating is the regulation of cell proliferation as it is the top hit. *Arrb2* is connected to this network through Src interactions. Line length reflect on the strength or likelihood of the shared function and/ or binding of two linked proteins. Line colors; light blue: known interactions from curated databases, pink: known interactions experimentally determined, green: predicted

interactions within the gene neighborhood, red: predicted interactions through gene fusions, light green: prediction by textmining, black: prediction by co-expression, and purple: prediction by protein homology.

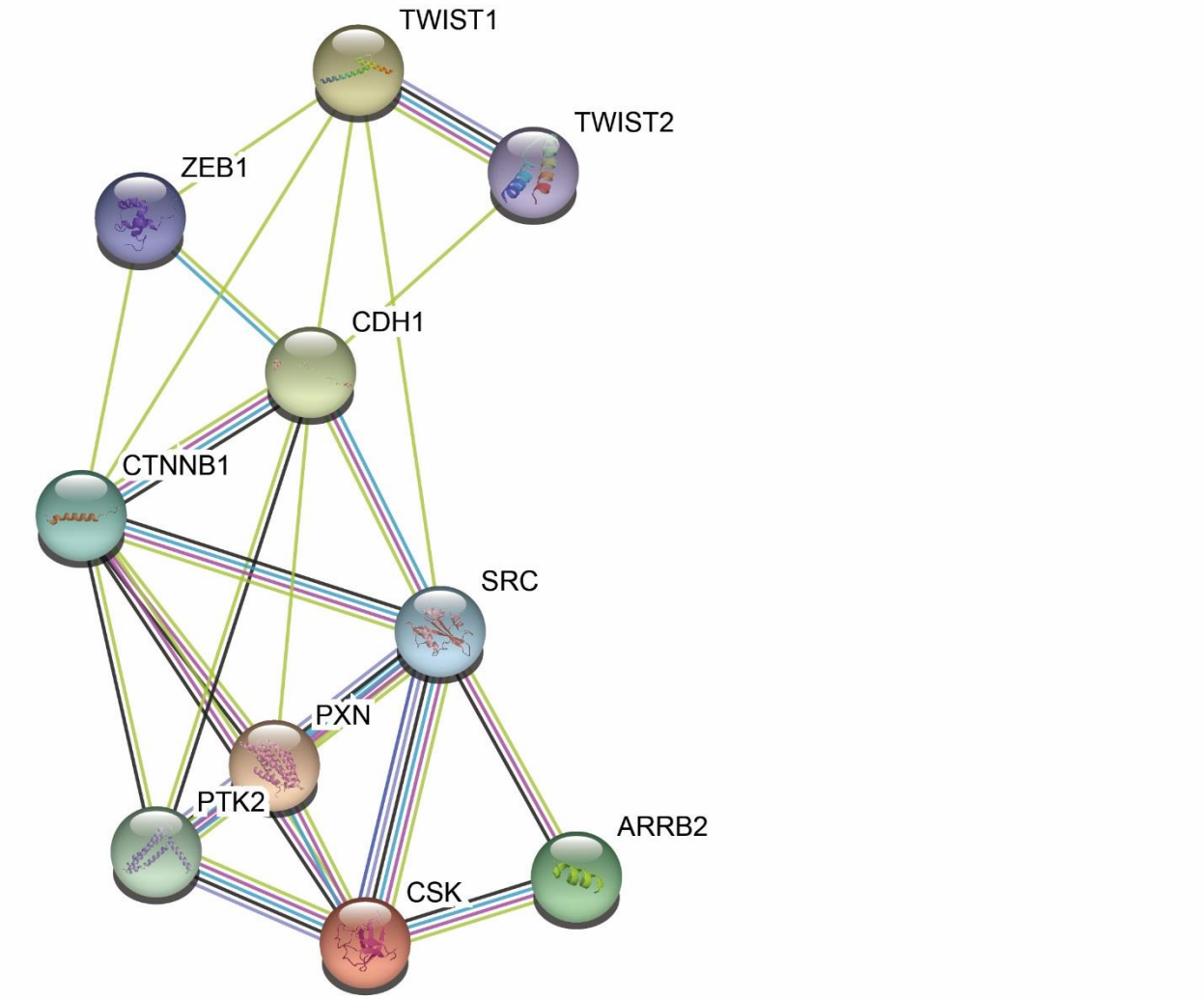

Biological Process (GO)			
pathway ID	*pathway description*	*count in gene set*	*false discovery rate*
GO:0071417	cellular response to organonitrogen compound	7	3.62e-06
GO:0071495	cellular response to endogenous stimulus	8	3.62e-06
GO:0071310	cellular response to organic substance	9	5.46e-06
GO:0022407	regulation of cell-cell adhesion	6	7.4e-06
GO:0007172	signal complex assembly	3	1.08e-05

Figure 3-2. Visualizing protein-protein predicted interactions between βArrestin 2 and molecules examined here that have been shown or predicted to be modulated by the *Arrb2* KO in the context of cell morphology and MET. Shown in the table summary (lower panel), likely biological processes these molecules are regulating are the regulation of cell-cell adhesion and signal complex assembly. *Arrb2* is connected to this network through *Src* (vSrc) interactions. Line length reflect on the strength or likelihood of the shared function and/ or binding of two linked proteins. Line colors; light blue: known interactions from curated databases, pink: known interactions experimentally determined, green: predicted interactions within the gene neighborhood, red: predicted

interactions through gene fusions, light green: prediction by textmining, black: prediction by co-expression, and purple: prediction by protein homology.

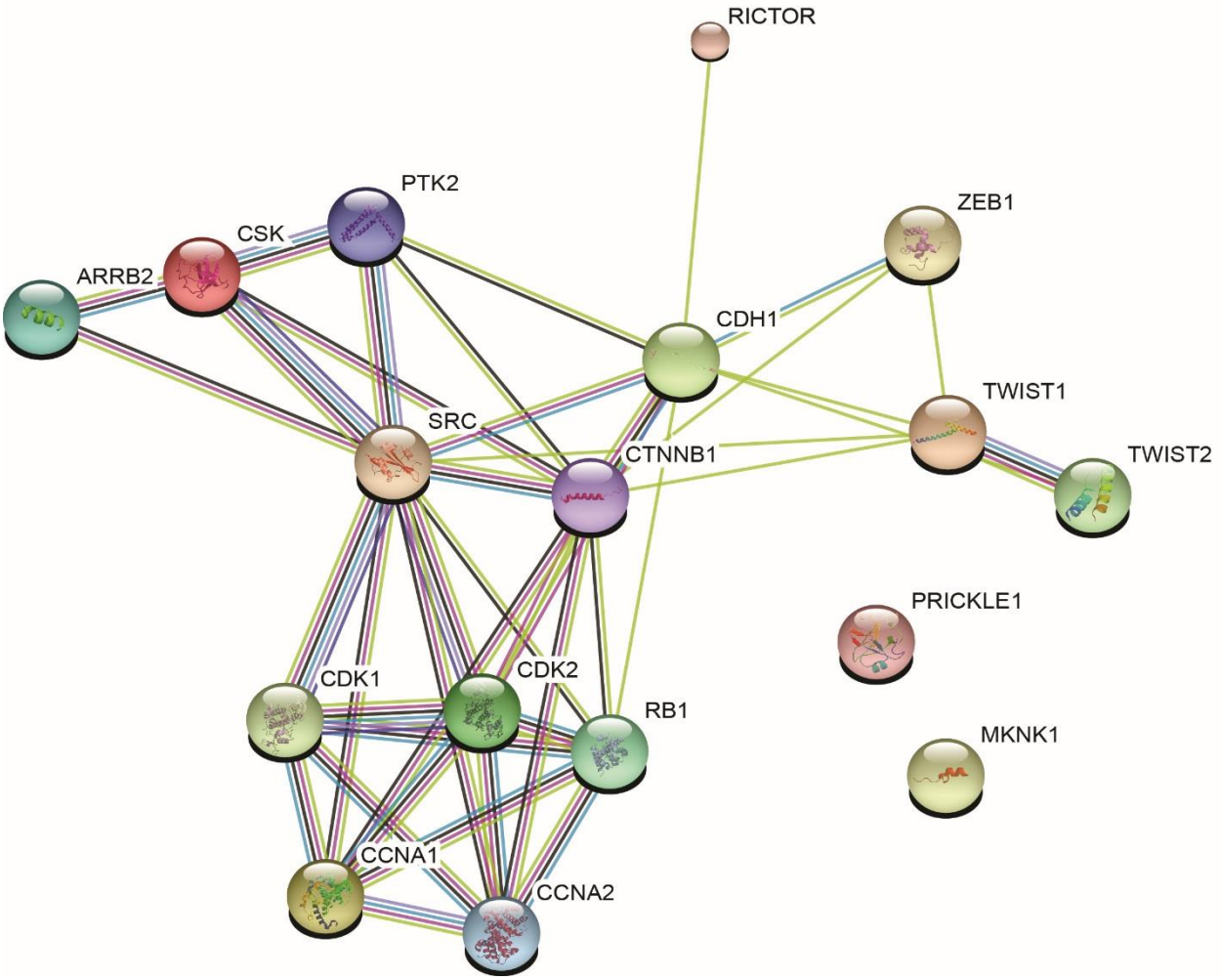

Figure 3-3. Visualizing protein-protein predicted interactions between βArrestin 2 and molecules examined here with the addition of mTORC2 related proteins. Line colors; light blue: known interactions from curated databases, pink: known interactions experimentally determined, green: predicted interactions within the gene neighborhood, red: predicted interactions through gene fusions, light green: prediction by textmining, black: prediction by co-expression, and purple: prediction by protein homology.

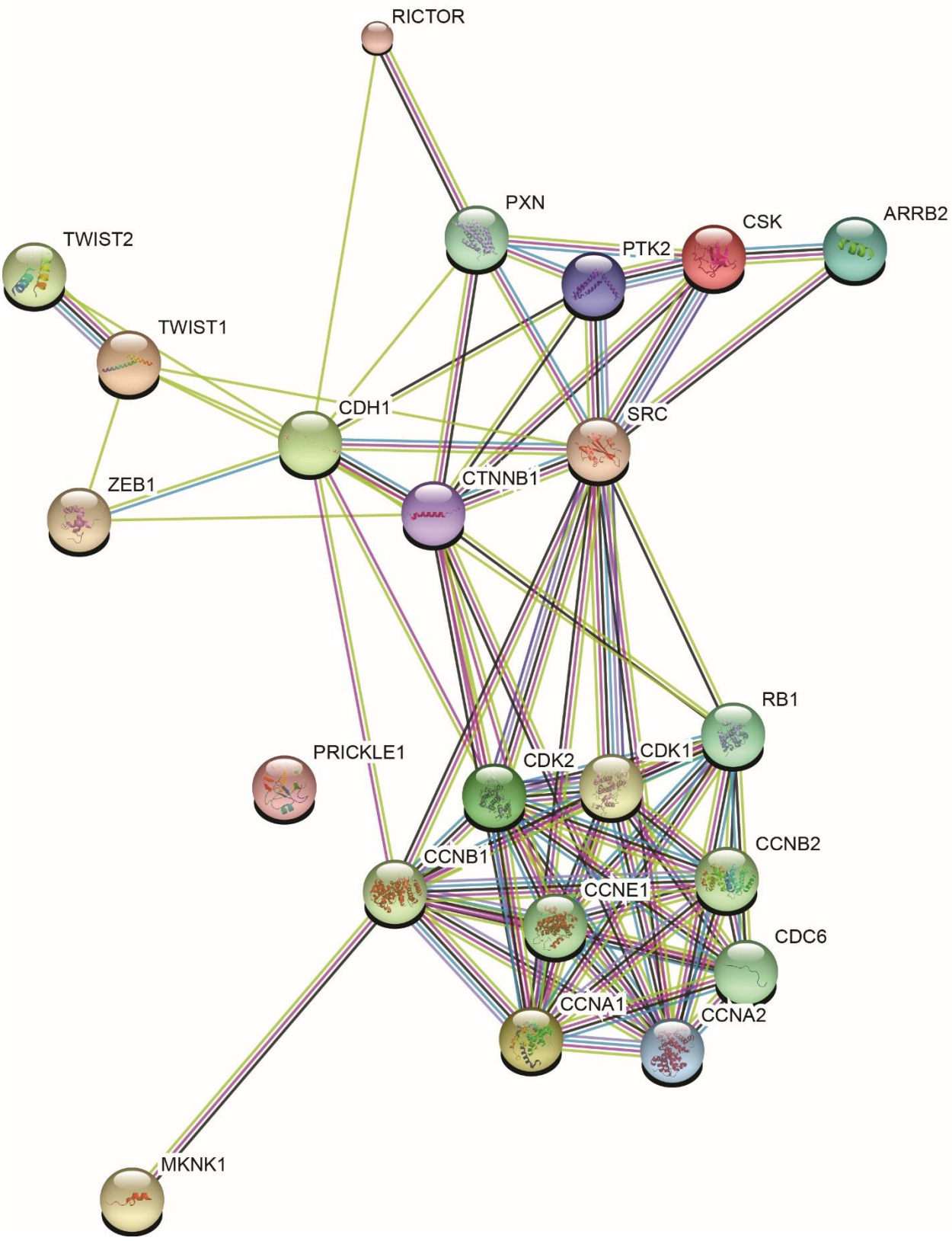
RICTOR
PXN
CSK
ARRB2
TWIST2
PTK2
TWIST1
CDH1
SRC
ZEB1
CTNNB1
RB1
PRICKLE1
CDK2
CDK1
CCNB2
CCNB1
CCNE1
CDC6
CCNA1
CCNA2
MKNK1

Figure 3-4. STRING database predicted interactions between βArrestin 2 and molecules examined here with the addition of mTORC2 related proteins at an additional depth of interactions. Line length reflect on the strength or likelihood of the shared function and/ or binding of two linked proteins. Line colors; light blue: known interactions from curated databases, pink: known interactions experimentally determined, green: predicted interactions within the gene neighborhood, red: predicted interactions through gene fusions, light green: prediction by textmining, black: prediction by co-expression, and purple: prediction by protein homology.

LIST OF REFERENCES

1. Lefkowitz RJ. Historical review: a brief history and personal retrospective of seven-transmembrane receptors. Trends in pharmacological sciences. 2004;25(8):413-22.

2. Pierce KL, Premont RT, Lefkowitz RJ. Seven-transmembrane receptors. Nature reviews Molecular cell biology. 2002;3(9):639-50.

3. Hamm HE. The many faces of G protein signaling. The Journal of biological chemistry. 1998;273(2):669-72.

4. Hepler JR, Gilman AG. G proteins. Trends in biochemical sciences. 1992;17(10):383-7.

5. Neer EJ. Heterotrimeric G proteins: organizers of transmembrane signals. Cell. 1995;80(2):249-57.

6. Luttrell LM. Composition and function of g protein-coupled receptor signalsomes controlling mitogen-activated protein kinase activity. Journal of molecular neuroscience : MN. 2005;26(2-3):253-64.

7. Gesty-Palmer D, Luttrell LM. Refining efficacy: exploiting functional selectivity for drug discovery. Advances in pharmacology. 2011;62:79-107.

8. Luttrell LM. Transmembrane signaling by G protein-coupled receptors. Methods in molecular biology. 2006;332:3-49.

9. Weller M, Virmaux N, Mandel P. Light-stimulated phosphorylation of rhodopsin in the retina: the presence of a protein kinase that is specific for photobleached rhodopsin. Proceedings of the National Academy of Sciences of the United States of America. 1975;72(1):381-5.

10. Benovic JL, Strasser RH, Caron MG, Lefkowitz RJ. Beta-adrenergic receptor kinase: identification of a novel protein kinase that phosphorylates the agonist-occupied form of the receptor. Proceedings of the National Academy of Sciences of the United States of America. 1986;83(9):2797-801.

11. Benovic JL, Mayor F, Jr., Staniszewski C, Lefkowitz RJ, Caron MG. Purification and characterization of the beta-adrenergic receptor kinase. The Journal of biological chemistry. 1987;262(19):9026-32.

12. Premont RT, Gainetdinov RR. Physiological roles of G protein-coupled receptor kinases and arrestins. Annual review of physiology. 2007;69:511-34.

13. Zhan X, Gimenez LE, Gurevich VV, Spiller BW. Crystal structure of arrestin-3 reveals the basis of the difference in receptor binding between two non-visual subtypes. Journal of molecular biology. 2011;406(3):467-78.

14. Xiao K, McClatchy DB, Shukla AK, Zhao Y, Chen M, Shenoy SK, et al. Functional specialization of beta-arrestin interactions revealed by proteomic analysis. Proceedings of the National Academy of Sciences of the United States of America. 2007;104(29):12011-6.

15. Luttrell LM, Lefkowitz RJ. The role of beta-arrestins in the termination and transduction of G-protein-coupled receptor signals. Journal of cell science. 2002;115(Pt 3):455-65.

16. Goodman OB, Jr., Krupnick JG, Santini F, Gurevich VV, Penn RB, Gagnon AW, et al. Beta-arrestin acts as a clathrin adaptor in endocytosis of the beta2-adrenergic receptor. Nature. 1996;383(6599):447-50.

17. Laporte SA, Oakley RH, Zhang J, Holt JA, Ferguson SS, Caron MG, et al. The beta2-adrenergic receptor/betaarrestin complex recruits the clathrin adaptor AP-2 during endocytosis. Proceedings of the National Academy of Sciences of the United States of America. 1999;96(7):3712-7.

18. Wang P, Gao H, Ni Y, Wang B, Wu Y, Ji L, et al. Beta-arrestin 2 functions as a G-protein-coupled receptor-activated regulator of oncoprotein Mdm2. The Journal of biological chemistry. 2003;278(8):6363-70.

19. Ridge KD, Abdulaev NG, Sousa M, Palczewski K. Phototransduction: crystal clear. Trends in biochemical sciences. 2003;28(9):479-87.

20. Gether U, Kobilka BK. G protein-coupled receptors. II. Mechanism of agonist activation. The Journal of biological chemistry. 1998;273(29):17979-82.

21. Stephenson RP. A modification of receptor theory. 1956. British journal of pharmacology. 1997;120(4 Suppl):106-20; discussion 3-5.

22. Kenakin T. Ligand-selective receptor conformations revisited: the promise and the problem. Trends in pharmacological sciences. 2003;24(7):346-54.

23. Kenakin T. Efficacy at G-protein-coupled receptors. Nature reviews Drug discovery. 2002;1(2):103-10.

24. Azzi M, Charest PG, Angers S, Rousseau G, Kohout T, Bouvier M, et al. Beta-arrestin-mediated activation of MAPK by inverse agonists reveals distinct active conformations for G protein-coupled receptors. Proceedings of the National Academy of Sciences of the United States of America. 2003;100(20):11406-11.

25. Reiter E, Ahn S, Shukla AK, Lefkowitz RJ. Molecular mechanism of beta-arrestin-biased agonism at seven-transmembrane receptors. Annual review of pharmacology and toxicology. 2012;52:179-97.

26. Violin JD, Lefkowitz RJ. Beta-arrestin-biased ligands at seven-transmembrane receptors. Trends in pharmacological sciences. 2007;28(8):416-22.

27. Rajagopal S, Rajagopal K, Lefkowitz RJ. Teaching old receptors new tricks: biasing seven-transmembrane receptors. Nature reviews Drug discovery. 2010;9(5):373-86.

28. Rajagopal S, Ahn S, Rominger DH, Gowen-MacDonald W, Lam CM, Dewire SM, et al. Quantifying ligand bias at seven-transmembrane receptors. Molecular pharmacology. 2011;80(3):367-77.

29. Wei H, Ahn S, Shenoy SK, Karnik SS, Hunyady L, Luttrell LM, et al. Independent beta-arrestin 2 and G protein-mediated pathways for angiotensin II activation of extracellular signal-regulated kinases 1 and 2. Proceedings of the National Academy of Sciences of the United States of America. 2003;100(19):10782-7.

30. Gesty-Palmer D, Chen M, Reiter E, Ahn S, Nelson CD, Wang S, et al. Distinct beta-arrestin- and G protein-dependent pathways for parathyroid hormone receptor-stimulated ERK1/2 activation. The Journal of biological chemistry. 2006;281(16):10856-64.

31. Luttrell LM, Ferguson SS, Daaka Y, Miller WE, Maudsley S, Della Rocca GJ, et al. Beta-arrestin-dependent formation of beta2 adrenergic receptor-Src protein kinase complexes. Science. 1999;283(5402):655-61.

32. Luttrell LM, Roudabush FL, Choy EW, Miller WE, Field ME, Pierce KL, et al. Activation and targeting of extracellular signal-regulated kinases by beta-arrestin scaffolds. Proceedings of the National Academy of Sciences of the United States of America. 2001;98(5):2449-54.

33. Kuhn H. Light-regulated binding of rhodopsin kinase and other proteins to cattle photoreceptor membranes. Biochemistry. 1978;17(21):4389-95.

34. Wilden U, Wust E, Weyand I, Kuhn H. Rapid affinity purification of retinal arrestin (48 kDa protein) via its light-dependent binding to phosphorylated rhodopsin. FEBS letters. 1986;207(2):292-5.

35. Murakami A, Yajima T, Sakuma H, McLaren MJ, Inana G. X-arrestin: a new retinal arrestin mapping to the X chromosome. FEBS letters. 1993;334(2):203-9.

36. Smith WC, Gurevich EV, Dugger DR, Vishnivetskiy SA, Shelamer CL, McDowell JH, et al. Cloning and functional characterization of salamander rod and cone arrestins. Investigative ophthalmology & visual science. 2000;41(9):2445-55.

37. Lohse MJ, Benovic JL, Codina J, Caron MG, Lefkowitz RJ. beta-Arrestin: a protein that regulates beta-adrenergic receptor function. Science. 1990;248(4962):1547-50.

38. Attramadal H, Arriza JL, Aoki C, Dawson TM, Codina J, Kwatra MM, et al. Beta-arrestin2, a novel member of the arrestin/beta-arrestin gene family. The Journal of biological chemistry. 1992;267(25):17882-90.

39. Kovacs JJ, Hara MR, Davenport CL, Kim J, Lefkowitz RJ. Arrestin development: emerging roles for beta-arrestins in developmental signaling pathways. Developmental cell. 2009;17(4):443-58.

40. Sterne-Marr R, Gurevich VV, Goldsmith P, Bodine RC, Sanders C, Donoso LA, et al. Polypeptide variants of beta-arrestin and arrestin3. The Journal of biological chemistry. 1993;268(21):15640-8.

41. Hirsch JA, Schubert C, Gurevich VV, Sigler PB. The 2.8 A crystal structure of visual arrestin: a model for arrestin's regulation. Cell. 1999;97(2):257-69.

42. Milano SK, Pace HC, Kim YM, Brenner C, Benovic JL. Scaffolding functions of arrestin-2 revealed by crystal structure and mutagenesis. Biochemistry. 2002;41(10):3321-8.

43. Han M, Gurevich VV, Vishnivetskiy SA, Sigler PB, Schubert C. Crystal structure of beta-arrestin at 1.9 A: possible mechanism of receptor binding and membrane Translocation. Structure. 2001;9(9):869-80.

44. Kern RC, Kang DS, Benovic JL. Arrestin2/clathrin interaction is regulated by key N- and C-terminal regions in arrestin2. Biochemistry. 2009;48(30):7190-200.

45. Lohse MJ, Maiellaro I, Calebiro D. Kinetics and mechanism of G protein-coupled receptor activation. Current opinion in cell biology. 2014;27:87-93.

46. Gurevich VV, Gurevich EV. The molecular acrobatics of arrestin activation. Trends in pharmacological sciences. 2004;25(2):105-11.

47. Gurevich VV, Gurevich EV. The new face of active receptor bound arrestin attracts new partners. Structure. 2003;11(9):1037-42.

48. Kim M, Vishnivetskiy SA, Van Eps N, Alexander NS, Cleghorn WM, Zhan X, et al. Conformation of receptor-bound visual arrestin. Proceedings of the National Academy of Sciences of the United States of America. 2012;109(45):18407-12.

49. Hanson SM, Francis DJ, Vishnivetskiy SA, Kolobova EA, Hubbell WL, Klug CS, et al. Differential interaction of spin-labeled arrestin with inactive and active

phosphorhodopsin. Proceedings of the National Academy of Sciences of the United States of America. 2006;103(13):4900-5.

50. Vishnivetskiy SA, Francis D, Van Eps N, Kim M, Hanson SM, Klug CS, et al. The role of arrestin alpha-helix I in receptor binding. Journal of molecular biology. 2010;395(1):42-54.

51. Lefkowitz RJ, Rajagopal K, Whalen EJ. New roles for beta-arrestins in cell signaling: not just for seven-transmembrane receptors. Molecular cell. 2006;24(5):643-52.

52. McDonald PH, Chow CW, Miller WE, Laporte SA, Field ME, Lin FT, et al. Beta-arrestin 2: a receptor-regulated MAPK scaffold for the activation of JNK3. Science. 2000;290(5496):1574-7.

53. Miller WE, McDonald PH, Cai SF, Field ME, Davis RJ, Lefkowitz RJ. Identification of a motif in the carboxyl terminus of beta -arrestin2 responsible for activation of JNK3. The Journal of biological chemistry. 2001;276(30):27770-7.

54. Gurevich EV, Benovic JL, Gurevich VV. Arrestin2 and arrestin3 are differentially expressed in the rat brain during postnatal development. Neuroscience. 2002;109(3):421-36.

55. Gurevich EV, Benovic JL, Gurevich VV. Arrestin2 expression selectively increases during neural differentiation. Journal of neurochemistry. 2004;91(6):1404-16.

56. Celver J, Vishnivetskiy SA, Chavkin C, Gurevich VV. Conservation of the phosphate-sensitive elements in the arrestin family of proteins. The Journal of biological chemistry. 2002;277(11):9043-8.

57. Kovoor A, Celver J, Abdryashitov RI, Chavkin C, Gurevich VV. Targeted construction of phosphorylation-independent beta-arrestin mutants with constitutive activity in cells. The Journal of biological chemistry. 1999;274(11):6831-4.

58. Vishnivetskiy SA, Paz CL, Schubert C, Hirsch JA, Sigler PB, Gurevich VV. How does arrestin respond to the phosphorylated state of rhodopsin? The Journal of biological chemistry. 1999;274(17):11451-4.

59. Scott MG, Le Rouzic E, Perianin A, Pierotti V, Enslen H, Benichou S, et al. Differential nucleocytoplasmic shuttling of beta-arrestins. Characterization of a leucine-rich nuclear export signal in beta-arrestin2. The Journal of biological chemistry. 2002;277(40):37693-701.

60. Ma L, Pei G. Beta-arrestin signaling and regulation of transcription. Journal of cell science. 2007;120(Pt 2):213-8.

61. Kohout TA, Lin FS, Perry SJ, Conner DA, Lefkowitz RJ. beta-Arrestin 1 and 2 differentially regulate heptahelical receptor signaling and trafficking. Proceedings of the National Academy of Sciences of the United States of America. 2001;98(4):1601-6.

62. Conner DA, Mathier MA, Mortensen RM, Christe M, Vatner SF, Seidman CE, et al. beta-Arrestin1 knockout mice appear normal but demonstrate altered cardiac responses to beta-adrenergic stimulation. Circulation research. 1997;81(6):1021-6.

63. Bohn LM, Lefkowitz RJ, Gainetdinov RR, Peppel K, Caron MG, Lin FT. Enhanced morphine analgesia in mice lacking beta-arrestin 2. Science. 1999;286(5449):2495-8.

64. Hu S, Wang D, Wu J, Jin J, Wei W, Sun W. Involvement of beta-arrestins in cancer progression. Molecular biology reports. 2013;40(2):1065-71.

65. DeFea KA, Vaughn ZD, O'Bryan EM, Nishijima D, Dery O, Bunnett NW. The proliferative and antiapoptotic effects of substance P are facilitated by formation of a beta -arrestin-dependent scaffolding complex. Proceedings of the National Academy of Sciences of the United States of America. 2000;97(20):11086-91.

66. Barnes WG, Reiter E, Violin JD, Ren XR, Milligan G, Lefkowitz RJ. beta-Arrestin 1 and Galphaq/11 coordinately activate RhoA and stress fiber formation following receptor stimulation. The Journal of biological chemistry. 2005;280(9):8041-50.

67. Witherow DS, Garrison TR, Miller WE, Lefkowitz RJ. beta-Arrestin inhibits NF-kappaB activity by means of its interaction with the NF-kappaB inhibitor IkappaBalpha. Proceedings of the National Academy of Sciences of the United States of America. 2004;101(23):8603-7.

68. Gao H, Sun Y, Wu Y, Luan B, Wang Y, Qu B, et al. Identification of beta-arrestin2 as a G protein-coupled receptor-stimulated regulator of NF-kappaB pathways. Molecular cell. 2004;14(3):303-17.

69. Mythreye K, Blobe GC. The type III TGF-beta receptor regulates epithelial and cancer cell migration through beta-arrestin2-mediated activation of Cdc42. Proceedings of the National Academy of Sciences of the United States of America. 2009;106(20):8221-6.

70. Finger EC, Lee NY, You HJ, Blobe GC. Endocytosis of the type III transforming growth factor-beta (TGF-beta) receptor through the clathrin-independent/lipid raft

pathway regulates TGF-beta signaling and receptor down-regulation. The Journal of biological chemistry. 2008;283(50):34808-18.

71. Hanahan D, Weinberg RA. Hallmarks of cancer: the next generation. Cell. 2011;144(5):646-74.

72. Revankar CM, Vines CM, Cimino DF, Prossnitz ER. Arrestins block G protein-coupled receptor-mediated apoptosis. The Journal of biological chemistry. 2004;279(23):24578-84.

73. Yang X, Zhou G, Ren T, Li H, Zhang Y, Yin D, et al. beta-Arrestin prevents cell apoptosis through pro-apoptotic ERK1/2 and p38 MAPKs and anti-apoptotic Akt pathways. Apoptosis : an international journal on programmed cell death. 2012;17(9):1019-26.

74. Povsic TJ, Kohout TA, Lefkowitz RJ. Beta-arrestin1 mediates insulin-like growth factor 1 (IGF-1) activation of phosphatidylinositol 3-kinase (PI3K) and anti-apoptosis. The Journal of biological chemistry. 2003;278(51):51334-9.

75. Buchanan FG, Gorden DL, Matta P, Shi Q, Matrisian LM, DuBois RN. Role of beta-arrestin 1 in the metastatic progression of colorectal cancer. Proceedings of the National Academy of Sciences of the United States of America. 2006;103(5):1492-7.

76. Alvarez CJ, Lodeiro M, Theodoropoulou M, Camina JP, Casanueva FF, Pazos Y. Obestatin stimulates Akt signalling in gastric cancer cells through beta-arrestin-mediated epidermal growth factor receptor transactivation. Endocrine-related cancer. 2009;16(2):599-611.

77. Dasgupta P, Rastogi S, Pillai S, Ordonez-Ercan D, Morris M, Haura E, et al. Nicotine induces cell proliferation by beta-arrestin-mediated activation of Src and Rb-Raf-1 pathways. The Journal of clinical investigation. 2006;116(8):2208-17.

78. Dasgupta P, Rizwani W, Pillai S, Davis R, Banerjee S, Hug K, et al. ARRB1-mediated regulation of E2F target genes in nicotine-induced growth of lung tumors. Journal of the National Cancer Institute. 2011;103(4):317-33.

79. Moussa O, Yordy JS, Abol-Enein H, Sinha D, Bissada NK, Halushka PV, et al. Prognostic and functional significance of thromboxane synthase gene overexpression in invasive bladder cancer. Cancer research. 2005;65(24):11581-7.

80. Moussa O, Ashton AW, Fraig M, Garrett-Mayer E, Ghoneim MA, Halushka PV, et al. Novel role of thromboxane receptors beta isoform in bladder cancer pathogenesis. Cancer research. 2008;68(11):4097-104.

81. Kelley-Hickie LP, Kinsella BT. Homologous desensitization of signalling by the beta (beta) isoform of the human thromboxane A2 receptor. Biochimica et biophysica acta. 2006;1761(9):1114-31.

82. Fereshteh M, Ito T, Kovacs JJ, Zhao C, Kwon HY, Tornini V, et al. beta-Arrestin2 mediates the initiation and progression of myeloid leukemia. Proceedings of the National Academy of Sciences of the United States of America. 2012;109(31):12532-7.

83. Bryja V, Gradl D, Schambony A, Arenas E, Schulte G. Beta-arrestin is a necessary component of Wnt/beta-catenin signaling in vitro and in vivo. Proceedings of the National Academy of Sciences of the United States of America. 2007;104(16):6690-5.

84. Keefe AD, Pai S, Ellington A. Aptamers as therapeutics. Nature reviews Drug discovery. 2010;9(7):537-50.

85. Kotula JW, Sun J, Li M, Pratico ED, Fereshteh MP, Ahrens DP, et al. Targeted disruption of beta-arrestin 2-mediated signaling pathways by aptamer chimeras leads to inhibition of leukemic cell growth. PloS one. 2014;9(4):e93441.

86. Dhanasekaran DN, Reddy EP. JNK signaling in apoptosis. Oncogene. 2008;27(48):6245-51.

87. Choi WS, Klintworth HM, Xia Z. JNK3-mediated apoptotic cell death in primary dopaminergic neurons. Methods in molecular biology. 2011;758:279-92.

88. Guo C, Whitmarsh AJ. The beta-arrestin-2 scaffold protein promotes c-Jun N-terminal kinase-3 activation by binding to its nonconserved N terminus. The Journal of biological chemistry. 2008;283(23):15903-11.

89. Bruchas MR, Macey TA, Lowe JD, Chavkin C. Kappa opioid receptor activation of p38 MAPK is GRK3- and arrestin-dependent in neurons and astrocytes. The Journal of biological chemistry. 2006;281(26):18081-9.

90. Gesty-Palmer D, El Shewy H, Kohout TA, Luttrell LM. beta-Arrestin 2 expression determines the transcriptional response to lysophosphatidic acid stimulation in murine embryo fibroblasts. The Journal of biological chemistry. 2005;280(37):32157-67.

91. Kook S, Gurevich VV, Gurevich EV. Arrestins in apoptosis. Handbook of experimental pharmacology. 2014;219:309-39.

92. Luan B, Zhang Z, Wu Y, Kang J, Pei G. Beta-arrestin2 functions as a phosphorylation-regulated suppressor of UV-induced NF-kappaB activation. The EMBO journal. 2005;24(24):4237-46.

93. Kendall RT, Strungs EG, Rachidi SM, Lee MH, El-Shewy HM, Luttrell DK, et al. The beta-arrestin pathway-selective type 1A angiotensin receptor (AT1A) agonist [Sar1,Ile4,Ile8]angiotensin II regulates a robust G protein-independent signaling network. The Journal of biological chemistry. 2011;286(22):19880-91.

94. Takahashi-Yanaga F. Activator or inhibitor? GSK-3 as a new drug target. Biochemical pharmacology. 2013;86(2):191-9.

95. Sun X, Zhang Y, Wang J, Wei L, Li H, Hanley G, et al. Beta-arrestin 2 modulates resveratrol-induced apoptosis and regulation of Akt/GSK3ss pathways. Biochimica et biophysica acta. 2010;1800(9):912-8.

96. Xu C, Reichert EC, Nakano T, Lohse M, Gardner AA, Revelo MP, et al. Deficiency of phospholipase A2 group 7 decreases intestinal polyposis and colon tumorigenesis in Apc(Min/+) mice. Cancer research. 2013;73(9):2806-16.

97. Crotty TM, Nakano T, Stafforini DM, Topham MK. Diacylglycerol kinase delta modulates Akt phosphorylation through pleckstrin homology domain leucine-rich repeat protein phosphatase 2 (PHLPP2). The Journal of biological chemistry. 2013;288(3):1439-47.

98. Chen M, Pratt CP, Zeeman ME, Schultz N, Taylor BS, O'Neill A, et al. Identification of PHLPP1 as a tumor suppressor reveals the role of feedback activation in PTEN-mutant prostate cancer progression. Cancer cell. 2011;20(2):173-86.

99. Fang S, Jensen JP, Ludwig RL, Vousden KH, Weissman AM. Mdm2 is a RING finger-dependent ubiquitin protein ligase for itself and p53. The Journal of biological chemistry. 2000;275(12):8945-51.

100. Honda R, Yasuda H. Activity of MDM2, a ubiquitin ligase, toward p53 or itself is dependent on the RING finger domain of the ligase. Oncogene. 2000;19(11):1473-6.

101. Oda E, Ohki R, Murasawa H, Nemoto J, Shibue T, Yamashita T, et al. Noxa, a BH3-only member of the Bcl-2 family and candidate mediator of p53-induced apoptosis. Science. 2000;288(5468):1053-8.

102. Villunger A, Michalak EM, Coultas L, Mullauer F, Bock G, Ausserlechner MJ, et al. p53- and drug-induced apoptotic responses mediated by BH3-only proteins puma and noxa. Science. 2003;302(5647):1036-8.

103. Hara MR, Sachs BD, Caron MG, Lefkowitz RJ. Pharmacological blockade of a beta(2)AR-beta-arrestin-1 signaling cascade prevents the accumulation of DNA damage in a behavioral stress model. Cell cycle. 2013;12(2):219-24.

104. Fidler IJ. The pathogenesis of cancer metastasis: the 'seed and soil' hypothesis revisited. Nature reviews Cancer. 2003;3(6):453-8.

105. Weiss L. Metastasis of cancer: a conceptual history from antiquity to the 1990s. Cancer metastasis reviews. 2000;19(3-4):I-XI, 193-383.

106. Talmadge JE, Fidler IJ. AACR centennial series: the biology of cancer metastasis: historical perspective. Cancer research. 2010;70(14):5649-69.

107. DeFea KA. Stop that cell! Beta-arrestin-dependent chemotaxis: a tale of localized actin assembly and receptor desensitization. Annual review of physiology. 2007;69:535-60.

108. Fong AM, Premont RT, Richardson RM, Yu YR, Lefkowitz RJ, Patel DD. Defective lymphocyte chemotaxis in beta-arrestin2- and GRK6-deficient mice. Proceedings of the National Academy of Sciences of the United States of America. 2002;99(11):7478-83.

109. Decaillot FM, Kazmi MA, Lin Y, Ray-Saha S, Sakmar TP, Sachdev P. CXCR7/CXCR4 heterodimer constitutively recruits beta-arrestin to enhance cell migration. The Journal of biological chemistry. 2011;286(37):32188-97.

110. Sun Y, Cheng Z, Ma L, Pei G. Beta-arrestin2 is critically involved in CXCR4-mediated chemotaxis, and this is mediated by its enhancement of p38 MAPK activation. The Journal of biological chemistry. 2002;277(51):49212-9.

111. Anthony DF, Sin YY, Vadrevu S, Advant N, Day JP, Byrne AM, et al. beta-Arrestin 1 inhibits the GTPase-activating protein function of ARHGAP21, promoting activation of RhoA following angiotensin II type 1A receptor stimulation. Molecular and cellular biology. 2011;31(5):1066-75.

112. Ma X, Zhao Y, Daaka Y, Nie Z. Acute activation of beta2-adrenergic receptor regulates focal adhesions through betaArrestin2- and p115RhoGEF protein-mediated activation of RhoA. The Journal of biological chemistry. 2012;287(23):18925-36.

113. Ma X, Espana-Serrano L, Kim WJ, Thayele Purayil H, Nie Z, Daaka Y. betaArrestin1 regulates the guanine nucleotide exchange factor RasGRF2 expression and the small GTPase Rac-mediated formation of membrane protrusion and cell motility. The Journal of biological chemistry. 2014;289(19):13638-50.

114. Cameron RT, Baillie GS. Arrestin regulation of small GTPases. Handbook of experimental pharmacology. 2014;219:375-85.

115. Shenoy SK, Han S, Zhao YL, Hara MR, Oliver T, Cao Y, et al. beta-arrestin1 mediates metastatic growth of breast cancer cells by facilitating HIF-1-dependent VEGF expression. Oncogene. 2012;31(3):282-92.

116. Semenza GL. Vasculogenesis, angiogenesis, and arteriogenesis: mechanisms of blood vessel formation and remodeling. Journal of cellular biochemistry. 2007;102(4):840-7.

117. Zecchini V, Madhu B, Russell R, Pertega-Gomes N, Warren A, Gaude E, et al. Nuclear ARRB1 induces pseudohypoxia and cellular metabolism reprogramming in prostate cancer. The EMBO journal. 2014;33(12):1365-82.

118. Park C, Kim Y, Shim M, Lee Y. Hypoxia enhances ligand-occupied androgen receptor activity. Biochemical and biophysical research communications. 2012;418(2):319-23.

119. Fridman R, Toth M, Chvyrkova I, Meroueh SO, Mobashery S. Cell surface association of matrix metalloproteinase-9 (gelatinase B). Cancer metastasis reviews. 2003;22(2-3):153-66.

120. Egeblad M, Werb Z. New functions for the matrix metalloproteinases in cancer progression. Nature reviews Cancer. 2002;2(3):161-74.

121. Bergers G, Brekken R, McMahon G, Vu TH, Itoh T, Tamaki K, et al. Matrix metalloproteinase-9 triggers the angiogenic switch during carcinogenesis. Nature cell biology. 2000;2(10):737-44.

122. Zou L, Yang R, Chai J, Pei G. Rapid xenograft tumor progression in beta-arrestin1 transgenic mice due to enhanced tumor angiogenesis. FASEB journal : official publication of the Federation of American Societies for Experimental Biology. 2008;22(2):355-64.

123. Lee SU, Ahn KS, Sung MH, Park JW, Ryu HW, Lee HJ, et al. Indacaterol inhibits tumor cell invasiveness and MMP-9 expression by suppressing IKK/NF-kappaB activation. Molecules and cells. 2014;37(8):585-91.

124. Li TT, Alemayehu M, Aziziyeh AI, Pape C, Pampillo M, Postovit LM, et al. Beta-arrestin/Ral signaling regulates lysophosphatidic acid-mediated migration and invasion of human breast tumor cells. Molecular cancer research : MCR. 2009;7(7):1064-77.

125. Moolenaar WH, van Meeteren LA, Giepmans BN. The ins and outs of lysophosphatidic acid signaling. BioEssays : news and reviews in molecular, cellular and developmental biology. 2004;26(8):870-81.

126. Bhattacharya M, Anborgh PH, Babwah AV, Dale LB, Dobransky T, Benovic JL, et al. Beta-arrestins regulate a Ral-GDS Ral effector pathway that mediates cytoskeletal reorganization. Nature cell biology. 2002;4(8):547-55.

127. Zoudilova M, Kumar P, Ge L, Wang P, Bokoch GM, DeFea KA. Beta-arrestin-dependent regulation of the cofilin pathway downstream of protease-activated receptor-2. The Journal of biological chemistry. 2007;282(28):20634-46.

128. Ge L, Shenoy SK, Lefkowitz RJ, DeFea K. Constitutive protease-activated receptor-2-mediated migration of MDA MB-231 breast cancer cells requires both beta-arrestin-1 and -2. The Journal of biological chemistry. 2004;279(53):55419-24.

129. Rosano L, Cianfrocca R, Masi S, Spinella F, Di Castro V, Biroccio A, et al. Beta-arrestin links endothelin A receptor to beta-catenin signaling to induce ovarian cancer cell invasion and metastasis. Proceedings of the National Academy of Sciences of the United States of America. 2009;106(8):2806-11.

130. Rosano L, Spinella F, Di Castro V, Nicotra MR, Dedhar S, de Herreros AG, et al. Endothelin-1 promotes epithelial-to-mesenchymal transition in human ovarian cancer cells. Cancer research. 2005;65(24):11649-57.

131. Rosano L, Cianfrocca R, Tocci P, Spinella F, Di Castro V, Spadaro F, et al. beta-arrestin-1 is a nuclear transcriptional regulator of endothelin-1-induced beta-catenin signaling. Oncogene. 2013;32(42):5066-77.

132. Purayil HT, Zhang Y, Dey A, Gersey Z, Espana-Serrano L, Daaka Y. Arrestin2 modulates androgen receptor activation. Oncogene. 2014.

133. Lakshmikanthan V, Zou L, Kim JI, Michal A, Nie Z, Messias NC, et al. Identification of betaArrestin2 as a corepressor of androgen receptor signaling in prostate cancer. Proceedings of the National Academy of Sciences of the United States of America. 2009;106(23):9379-84.

134. Zhao M, Zhou G, Zhang Y, Chen T, Sun X, Stuart C, et al. beta-arrestin2 inhibits opioid-induced breast cancer cell death through Akt and caspase-8 pathways. Neoplasma. 2009;56(2):108-13.

135. Kim JI, Lakshmikanthan V, Frilot N, Daaka Y. Prostaglandin E2 promotes lung cancer cell migration via EP4-betaArrestin1-c-Src signalsome. Molecular cancer research : MCR. 2010;8(4):569-77.

136. Raghuwanshi SK, Nasser MW, Chen X, Strieter RM, Richardson RM. Depletion of beta-arrestin-2 promotes tumor growth and angiogenesis in a murine model of lung cancer. Journal of immunology. 2008;180(8):5699-706.

137. Vishnivetskiy SA, Gimenez LE, Francis DJ, Hanson SM, Hubbell WL, Klug CS, et al. Few residues within an extensive binding interface drive receptor interaction and determine the specificity of arrestin proteins. The Journal of biological chemistry. 2011;286(27):24288-99.

138. Milano SK, Kim YM, Stefano FP, Benovic JL, Brenner C. Nonvisual arrestin oligomerization and cellular localization are regulated by inositol hexakisphosphate binding. The Journal of biological chemistry. 2006;281(14):9812-23.

139. Luttrell LM, Miller WE. Arrestins as regulators of kinases and phosphatases. Prog Mol Biol Transl Sci. 2013;118:115-47.

140. Jemal A, Murray T, Samuels A, Ghafoor A, Ward E, Thun MJ. Cancer statistics, 2003. CA: a cancer journal for clinicians. 2003;53(1):5-26.

141. Siegel RL, Miller KD, Jemal A. Cancer Statistics, 2017. CA: a cancer journal for clinicians. 2017;67(1):7-30.

142. Eble JN, World Health Organization., International Agency for Research on Cancer. Pathology and genetics of tumours of the urinary system and male genital organs. LyonOxford: IARC Press ;Oxford University Press (distributor); 2004. 359 p. p.

143. America® CTCo. Kidney cancer survival statistics and results: Rising Tide; 2014 [November 2014]. Available from: http://www.cancercenter.com/kidney-cancer/statistics/.

144. Chow WH, Dong LM, Devesa SS. Epidemiology and risk factors for kidney cancer. Nature reviews Urology. 2010;7(5):245-57.

145. Sun M, Lughezzani G, Perrotte P, Karakiewicz PI. Treatment of metastatic renal cell carcinoma. Nature reviews Urology. 2010;7(6):327-38.

146. Santos N, Wenger JB, Havre P, Liu Y, Dagan R, Imanirad I, et al. Combination therapy for renal cell cancer: what are possible options? Oncology. 2011;81(3-4):220-9.

147. Fredriksson R, Lagerstrom MC, Lundin LG, Schioth HB. The G-protein-coupled receptors in the human genome form five main families. Phylogenetic analysis, paralogon groups, and fingerprints. Molecular pharmacology. 2003;63(6):1256-72.

148. Whalen EJ, Rajagopal S, Lefkowitz RJ. Therapeutic potential of beta-arrestin- and G protein-biased agonists. Trends in molecular medicine. 2011;17(3):126-39.

149. Lappano R, Maggiolini M. G protein-coupled receptors: novel targets for drug discovery in cancer. Nature reviews Drug discovery. 2011;10(1):47-60.

150. Kundu N, Ma X, Kochel T, Goloubeva O, Staats P, Thompson K, et al. Prostaglandin E receptor EP4 is a therapeutic target in breast cancer cells with stem-like properties. Breast Cancer Res Treat. 2014;143(1):19-31.

151. Young D, Waitches G, Birchmeier C, Fasano O, Wigler M. Isolation and characterization of a new cellular oncogene encoding a protein with multiple potential transmembrane domains. Cell. 1986;45(5):711-9.

152. Prickett TD, Wei X, Cardenas-Navia I, Teer JK, Lin JC, Walia V, et al. Exon capture analysis of G protein-coupled receptors identifies activating mutations in GRM3 in melanoma. Nat Genet. 2011;43(11):1119-26.

153. Feigin ME. Harnessing the genome for characterization of G-protein coupled receptors in cancer pathogenesis. The FEBS journal. 2013;280(19):4729-38.

154. Lefkowitz RJ, Shenoy SK. Transduction of receptor signals by beta-arrestins. Science. 2005;308(5721):512-7.

155. Wang P, Wu Y, Ge X, Ma L, Pei G. Subcellular localization of beta-arrestins is determined by their intact N domain and the nuclear export signal at the C terminus. The Journal of biological chemistry. 2003;278(13):11648-53.

156. Semenza GL. Hypoxia-inducible factor 1 (HIF-1) pathway. Science's STKE : signal transduction knowledge environment. 2007;2007(407):cm8.

157. Purayil HT, Zhang Y, Dey A, Gersey Z, Espana-Serrano L, Daaka Y. Arrestin2 modulates androgen receptor activation. Oncogene. 2015;34(24):3144-51.

158. Zhang Y, Thayele Purayil H, Black JB, Fetto F, Lynch LD, Masannat JN, et al. Prostaglandin E2 receptor 4 mediates renal cell carcinoma intravasation and metastasis. Cancer Lett. 2017;391:50-8.

159. Wu C. Focal adhesion: a focal point in current cell biology and molecular medicine. Cell Adh Migr. 2007;1(1):13-8.

160. Chen CS, Alonso JL, Ostuni E, Whitesides GM, Ingber DE. Cell shape provides global control of focal adhesion assembly. Biochemical and biophysical research communications. 2003;307(2):355-61.

161. Wang Y, Botvinick EL, Zhao Y, Berns MW, Usami S, Tsien RY, et al. Visualizing the mechanical activation of Src. Nature. 2005;434(7036):1040-5.

162. Cleghorn WM, Branch KM, Kook S, Arnette C, Bulus N, Zent R, et al. Arrestins regulate cell spreading and motility via focal adhesion dynamics. Mol Biol Cell. 2015;26(4):622-35.

163. Mayor R, Etienne-Manneville S. The front and rear of collective cell migration. Nature reviews Molecular cell biology. 2016;17(2):97-109.

164. Etienne-Manneville S, Hall A. Integrin-mediated activation of Cdc42 controls cell polarity in migrating astrocytes through PKCzeta. Cell. 2001;106(4):489-98.

165. Bellis SL, Miller JT, Turner CE. Characterization of tyrosine phosphorylation of paxillin in vitro by focal adhesion kinase. The Journal of biological chemistry. 1995;270(29):17437-41.

166. Wolfenson H, Bershadsky A, Henis YI, Geiger B. Actomyosin-generated tension controls the molecular kinetics of focal adhesions. Journal of cell science. 2011;124(Pt 9):1425-32.

167. Tian X, Liu Z, Niu B, Zhang J, Tan TK, Lee SR, et al. E-cadherin/beta-catenin complex and the epithelial barrier. J Biomed Biotechnol. 2011;2011:567305.

168. Huber AH, Weis WI. The structure of the beta-catenin/E-cadherin complex and the molecular basis of diverse ligand recognition by beta-catenin. Cell. 2001;105(3):391-402.

169. Wang X, Proud CG. mTORC2 is a tyrosine kinase. Cell Res. 2016;26(1):1-2.

170. Sarbassov DD, Guertin DA, Ali SM, Sabatini DM. Phosphorylation and regulation of Akt/PKB by the rictor-mTOR complex. Science. 2005;307(5712):1098-101.

171. Gaidarov I, Krupnick JG, Falck JR, Benovic JL, Keen JH. Arrestin function in G protein-coupled receptor endocytosis requires phosphoinositide binding. The EMBO journal. 1999;18(4):871-81.

172. Gossage L, Eisen T, Maher ER. VHL, the story of a tumour suppressor gene. Nature reviews Cancer. 2015;15(1):55-64.

173. Merza H, Bilusic M. Current Management Strategy for Metastatic Renal Cell Carcinoma and Future Directions. Curr Oncol Rep. 2017;19(4):27.

174. Brodaczewska KK, Szczylik C, Fiedorowicz M, Porta C, Czarnecka AM. Choosing the right cell line for renal cell cancer research. Mol Cancer. 2016;15(1):83.

175. Geiger B, Spatz JP, Bershadsky AD. Environmental sensing through focal adhesions. Nature reviews Molecular cell biology. 2009;10(1):21-33.

176. Sieg DJ, Hauck CR, Ilic D, Klingbeil CK, Schaefer E, Damsky CH, et al. FAK integrates growth-factor and integrin signals to promote cell migration. Nature cell biology. 2000;2(5):249-56.

177. Tocci P, Caprara V, Cianfrocca R, Sestito R, Di Castro V, Bagnato A, et al. Endothelin-1/endothelin A receptor axis activates RhoA GTPase in epithelial ovarian cancer. Life Sci. 2016;159:49-54.

178. Rosano L, Cianfrocca R, Tocci P, Spinella F, Di Castro V, Caprara V, et al. Endothelin A receptor/beta-arrestin signaling to the Wnt pathway renders ovarian cancer cells resistant to chemotherapy. Cancer research. 2014;74(24):7453-64.

179. Jacinto E, Loewith R, Schmidt A, Lin S, Ruegg MA, Hall A, et al. Mammalian TOR complex 2 controls the actin cytoskeleton and is rapamycin insensitive. Nature cell biology. 2004;6(11):1122-8.

180. Saxton RA, Sabatini DM. mTOR Signaling in Growth, Metabolism, and Disease. Cell. 2017;168(6):960-76.

181. Sarbassov DD, Ali SM, Kim DH, Guertin DA, Latek RR, Erdjument-Bromage H, et al. Rictor, a novel binding partner of mTOR, defines a rapamycin-insensitive and raptor-independent pathway that regulates the cytoskeleton. Curr Biol. 2004;14(14):1296-302.

182. Gan X, Wang J, Wang C, Sommer E, Kozasa T, Srinivasula S, et al. PRR5L degradation promotes mTORC2-mediated PKC-delta phosphorylation and cell migration downstream of Galpha12. Nature cell biology. 2012;14(7):686-96.

183. Yuan HX, Guan KL. The SIN1-PH Domain Connects mTORC2 to PI3K. Cancer Discov. 2015;5(11):1127-9.

184. Liu P, Gan W, Chin YR, Ogura K, Guo J, Zhang J, et al. PtdIns(3,4,5)P3-Dependent Activation of the mTORC2 Kinase Complex. Cancer Discov. 2015;5(11):1194-209.

185. Daulat AM, Bertucci F, Audebert S, Serge A, Finetti P, Josselin E, et al. PRICKLE1 Contributes to Cancer Cell Dissemination through Its Interaction with mTORC2. Developmental cell. 2016;37(4):311-25.

186. DeWire SM, Kim J, Whalen EJ, Ahn S, Chen M, Lefkowitz RJ. Beta-arrestin-mediated signaling regulates protein synthesis. The Journal of biological chemistry. 2008;283(16):10611-20.

187. Nigam N, Prasad S, George J, Shukla Y. Lupeol induces p53 and cyclin-B-mediated G2/M arrest and targets apoptosis through activation of caspase in

mouse skin. Biochemical and biophysical research communications. 2009;381(2):253-8.

188. Yuan J, Kramer A, Matthess Y, Yan R, Spankuch B, Gatje R, et al. Stable gene silencing of cyclin B1 in tumor cells increases susceptibility to taxol and leads to growth arrest in vivo. Oncogene. 2006;25(12):1753-62.

189. Kang Y, Zhou XE, Gao X, He Y, Liu W, Ishchenko A, et al. Crystal structure of rhodopsin bound to arrestin by femtosecond X-ray laser. Nature. 2015;523(7562):561-7.

BIOGRAPHICAL SKETCH

Jude Masannat was born in Amman, Jordan in 1990. She attended The Ahhliyah School for Girls from age four till sixteen where she excelled in her IGCSE exams before leaving Amman. In 2006, Jude was awarded a United World Scholarship by the Jordanian committee to be the representative Jordanian student for that year, attending the United World College of the Atlantic (UWC-AC) in Wales, UK. UWC-AC was one of the original founding schools of the International Baccalaureate (IB) program. At the time, Nelson Mandela was the honorary Vice President of the UWC Foundation, while Her Majesty Queen Noor of Jordan is to this time, the honorary President. Jude then served on multiple leadership committees and earned her beach lifeguarding certificate for her community service, while studying higher level Chemistry, Biology, and English (as a first language) subjects, as well as, Economics, Mathematics and Arabic (self-taught). Her interest in research stemmed from her IB Extended Essay requirement project that she completed in Biology. As a UWC student, Jude secured multiple admissions to esteemed colleges and universities in the United States and became a UWC Davis Scholarship awardee. She ultimately chose the University of Florida (UF), in Gainesville, FL as it was one of the top research institutes among her choices.

At UF Jude was an Honor Program student and graduated with *Suma Cum Laude*. She earned a double major Bachelor of Science degree in the Interdisciplinary Studies in Biochemistry and Genetics, and in Microbiology and Cell Science. During her undergraduate time, Jude joined Dr. Jorg Bungert's lab, in the Department of Biochemistry, College of Medicine, as an undergraduate research assistant to work on identifying co-transcription regulators binding the Upstream Stimulatory Factor 1 protein which regulates β-globin gene expression. During her undergraduate career, Jude was

awarded intra and extramural HMMI research awards for her research with Dr. Bungert and Dr. David Botstein at Princeton University. She was also a University Scholar Program awardee for her work. Not only was she focused on becoming a future scientist, Jude was also an Honors Ambassador for the Honors Program, resident assistant for the Housing Department, and a competitive fencer on the UF Fencing Team until her graduation in 2012.

Jude joined the Interdisciplinary Sciences Program (IDP) in Biomedical Sciences at the University of Florida, College of Medicine in 2012 as a Grinter Fellowship recipient. In 2013, she joined Dr. Yehia Daaka's laboratory in the concentration of Physiology and Pharmacology. During her time as a graduate student, he research focused on understanding the role of βArrestin 2 protein in renal cell carcinoma (RCC) progression and the possible mechanisms involved. She completed her work in 2017, and discovered a very crucial role for βArrestin 2 in certain RCCs that was not previously reported.

In addition to her research, Jude was a mentor to undergraduate students, and was a teaching assistant for dental students in the Histology course. Additionally, she was very involved in conferences and presentations at various events. Importantly, Jude served on a number of committees and advisory boards, and was the president of the Organization for Graduate Student Advancement and Professional Development (OGAP) under the Graduate School, and organized a hallmark event for graduate students, the Graduate Student Research Day 2017, along with many other events. Jude was the Alec Courtelis awardee for 2016. After graduation, Jude will be joining the

Department of Head and Neck, and Endocrine Oncology, at Moffitt Cancer Center, Tampa FL, as postdoctoral fellow under the supervision of Dr. Christine Chung.